AN INVESTIGATION OF THE DAMPING RESPONSE AND STRUCTURAL STRENGTH OF A FIBREGLASS AND RUBBER PARTICLE COMPOSITE SLEEPER

A thesis submitted in fulfilment of the requirements for the degree

Master of Engineering in Mechanical Engineering

In the Faculty of Engineering and Technology

Full Name: Abednigo Jabu Mbatha

Highest Qualification: B-TECH: Engineering: Mechanical

Student number: 210038616

Supervisor: Prof Alugongo

Co-Supervisors: Dr O Maube

: Dr NZ Nkomo

Date: 12/09/2022

Table of contents

Declaration

I declare that this thesis is my own work. It is being submitted for the degree M.Eng in Mechanical Engineering at the Vaal University of Technology, Vanderbijlpark, South Africa. It has not been submitted before for any degree or examination at any other University.

Signature of Candidate:

Date: 13/09/2022

Statement 1

This thesis is being submitted in fulfilment of the requirement for the degree of Masters of Engineering: Mechanical Engineering

Signature of Candidate:

Date: 13/09/2022

Statement 2

This thesis is the result of my own independent work/investigation, except where otherwise stated. Other sources are acknowledged by giving explicit references, and a list of references is appended.

Signature of Candidate:

Date: 13/09/2022

Statement 3

I hereby give consent for my thesis, if accepted, to be available for online publication, photocopying, and interlibrary loan and for the title and summary to be made available to outside organisations.

Signature of Candidate:

Date: 13/09/2022

List of Publications

- Published Articles
    i. Mbatha Abednigo Jabu, AA Alugongo, O Maube, NZ Nkomo (2021), "*A Review of The Effectiveness of Different Types of Railway Sleepers*", International Journal of Engineering Trends and Technology 69.10(2021):193-199.

Upcoming Journal Publications

ii. Vibrational effects of hybrid railway sleeper composite containing rubber particles and glass fibre.
iii. Mechanical properties of hybrid rubber particles and glass fibre railway sleeper composite.

Acknowledgement

This research work was supported by the Vaal University of Technology and funded by NRF. The authors wish to thank the Department of Industrial Engineering, Operation Management and Mechanical Engineering at the Vaal University of Technology for facilitating this work.

Abstract

A railway sleeper is a supporting and dampening beam placed underneath the railway track and can be made of different materials. There are four main types of railroad sleeper materials: timber or wooden, steel, concrete and composite material. The railway structural material often suffers from aggressive loading and vibration in the locomotive industry, and the sleepers' current durability and their vibration properties are not sufficiently resilient to vibration. There is a need for a structural material that can withstand significantly higher static and dynamic loads as trains become heavier and faster.

Tyre disposal is a global challenge to the environment, with approximately 1.5 billion tyre waste generated annually. Tyres are non-biodegradable, making their disposal extremely difficult.This study seeks to find a way to recycle the waste tyres in an environmentally friendly manner in accordance with Sustainable Development Goal 11, which focuses on sustainable cities and communities. The study aimed to optimize a hybrid composite sleeper using waste tyres ground into particles, fibreglass reinforcement and polyester resin to enhance the composites' structural strength while increasing the composite sleeper's damping. The specific objectictives were to characterized rubber particles of waste tyres and fabricate a composite railroad sleeper material using waste rubber particles, glass fibre, and polyester resin..Thereafter , evaluate the mechanical properties of the composite sleeper under loading conditions and damped vibration properties .Lastly , determine the optimal composite sleeper .

The rubber particles were characterized through sieving, moisture analysis and SEM. Thereafter, the composite was fabricated following the full experimental design. After that composite was fabricated using the hand lay-up method where the rubber volume fraction of 5, 10, 15 and 20% were varied, and fibreglass volume fractions of 5, 6, 7 and 8 % were obtained. The UTM (universal testing machine) was used to carry out mechanical tests, which included tensile strength, compression strength and flexural strength. Then Leeb hardness was carried out, and the damping properties of composites were determined using a shaker table. Minitab software was used for the optimisation of the composite mix

The ANOVA test showed the model's accuracy in predicting tensile strength, compression strength, flexural strength, and vibrational damping, as shown by R^2 values of 60.69%, 86.60%, 60.05% and 81.41 %, respectively. However, the model was not reliable for hardness which had an R^2 value of 37.87%.

The optimisation model indicated that rubber particles of size 150 µm with 7.48% volume fraction of rubber particles and fibreglass volume fraction of 8% are optimum. The corresponding mechanical properties responses for the optimum are tensile strength of 13.3851 MPa, the compression strength of 36.0272 MPa, the flexural strength of 36.5865 MPa and Leeb hardness of 647.7510. The damping properties of composite gave a value of 0.1416. Thereafter, optimum results were validated experimentally, and the model was shown to represent the data accurately. The fabricated composite could help to absorb aggressive forces caused by heavily loaded trains. At the same time, maintain the composite's mechanical strength and eliminate pollution caused by tyres in our environment.

Further investigation is required into the impact of using a variety of rubber particle sizes 75 m on the vibrational damping and mechanical characteristics of the composite railway sleeper. Studying the impacts of various synthetic and natural rubber kinds on composite characteristics is also necessary.

List of figures

List of tables

Nomenclature

Symbol	Description	Units
A	Area	m^2
B	Breadth	mm
b	Width of specimen	mm
d	Average thickness	mm
d	Diameter	µm
g	Gravity acceleration	m/s^2
L	Length of span	mm
F	Breaking load	N
P	Pressure	Kpa
R	Flexural strength	MPa
T	Temperature	^0C

Abbreviations

AOAC	Association of Official Analytical Chemists
ASTM	American Society for Testing and materials
ATM	Advanced materials technology
CCD	Charge Coupled device
Cka	Carbon K alpha
EDS	Electronic Data Capture
ISO	International Organization for Standardization
Oka	Oxygen K alpha
SABS	South African Bureau of Standards
SEM	Scanning Electron Microscope
UTM	Universal Testing Machine
VUT	Vaal University of Technology

CHAPTER 1: INTRODUCTION

1.1 Background of the study

A Railway sleeper is an essential structural material of the railway track system (Meesit et al., 2017). A supporting and dampening beam placed underneath the railway track and can be made of different materials is called railway sleeper (Taherinezhad et al., 2013). There are four main types of railroad sleeper materials used: timber or wooden, steel, concrete and composite materials. Concrete and steel sleepers were widely used in the late 1990s due to their durability over wooden sleepers (Lichtberger 2005). However, the vibration with concrete and steel sleepers in the railway track system causes several problems such as concrete failure, rail fasteners failure, flexural cracking and rail seat abrasion. Kaewunruen and Remennikov (2011) implemented several approaches to solve the vibration problem in the railway sleepers industry by introducing ballasts in the rail way's structural material to improve the track system's damping (Sakdirat Kaewunruen and Remennikov 2011). Ballasts used in railway sleepers improve the damping of the railway track system. However, the ballasts deteriorate with time as they are excited by the vibration from trains passing over them (Sakdirat Kaewunruen and Remennikov 2011).

Furthermore, severe abrasion can result in rail tipping, loss of clip toe load, and widening gauge size. All these faults can ultimately result in train derailment (Richard R', 2012). The chipping loss of concrete material in railway sleeper lands under the rail seat, which can lead to the concrete sleeper's premature failure (Kernes *et al.* 2011).

Carrascal (2007) and Connolly (2015) introduced an innovative method of using railway sleeper pads which are mounted underneath the structural material of the railway to improve the damping of the railway track system. Yet, this composite sleeper pad material tends to loosen and slowly detach from the railway structure when heavily loaded trains are in motion. This is due to the vibration within the railway track system. Meesit (2017) introduced an innovative method of using waste tyre rubber particles with cement to make railway sleepers. This method was successful due to the ability of rubber material to absorb the vibration in the railway line (Meesit *et al.*, 2017). However, when the waste tyre rubber particles are mixed with concrete, the compression strength of the sleeper is reduced significantly (Sakdirat Kaewunruen and Remennikov, 2011; Meesit et al., 2017).

Abu-jdayil (2016) developed a composite material which consisted of polyester resin with rubber particles embedded within as the dampening medium. Abu-jdayil (2016) reported that on the one hand, as the rubber volume fraction in the composite increased, the damping also increased, but on the other hand, the compressive strength of the composite decreased. However, Abu-jdayil et al. (2016) only used polyester resin and rubber particles in the composite material. This study will focus on using polyester resin, waste tyre rubber particles and fibreglass to increase the sleeper's damping without adversely affecting its compressive strength. The choice of material was influenced by the ability of rubber particles to absorb vibration without any compromise on the structural integrity of the composite material.

The current study seeks to fabricate a composite material using waste tyre rubber particles to increase resilience to shock loads in railway sleepers and handle the mechanical forces present. The railway sleeper mechanical and vibrational properties will be analysed.

1.2 Problem statement

Railway structural material often suffers from aggressive loading and vibration in the locomotive industry (Meesit *et al*., 2017). Researchers have used several approaches to address this problem, such as introducing composite sleepers to improve the damping in the railway track system. Ballasts were also introduced into the structural material of the railway to improve the damping of the structural material (Sakdirat Kaewunruen and Remennikov 2011). However, as the ballasts deteriorate due to the vibration of the track system, they tend to form voids and air pockets between the ballasts and sleepers; this phenomenon could cause cracking of the railway sleeper.

Furthermore, railway sleeper pads are mounted underneath structural material to improve the damping properties of the railway track system (Carrascal *et al.*, 2007; Connolly *et al.*, 2015). However, this component can loosen easily and come off from the railway's main structure when the train is in motion (Kernes *et al*. 2011). The sleepers' current durability and their vibration properties are not sufficiently resilient to vibration. This phenomenon can lead to premature failures, such as cracking the mid-span of the sleeper and also on the rail seat due to impact loading (Alex M Remennikov and Kaewunruen 2008). There is a need for a structural material that can withstand significantly higher static and dynamic loads as trains become heavier and faster.

Meesit (2017) fabricated a composite material using rubber particles with concrete. This composite had improved damping properties compared to traditional wooden sleepers and concrete sleepers. However, the reduction of compression strength in the composite was noticed. Silica fume was added to the composite to counteract this reduction in compressional strength. However, the compressional strength was still lower than expected to ensure the durability of the sleeper material. Abu-jdayil *et al.* (2017) fabricated a composite sleeper using polyester resin with rubber particles.

However, a reduction of ultimate strength was noticed due to the low hydrophobicity of rubber towards resin and weak bonding between rubber particles (Abu-jdayil, Mourad, and Hussain 2016).

Waste tyre disposal is a global environmental challenge, with approximately 1.5 billion tyre waste generated annually (Mohajerani et al. 2020). Tyres are non-biodegradable, making their disposal extremely difficult; hence this study also seeks to find a way to recycle the waste tyres in an environmentally friendly manner following the Sustainable Development Goal 11 (SDG), which focuses on sustainable cities and communities. The current research intends to fabricate a composite using these waste tyres ground into particles due to their ability to absorb vibration. The fabricated composite will use polyester resin and fibreglass reinforcement to give the composite good mechanical strength properties.

1.3 Purpose of the study

To fabricate a railway sleeper composite material consisting of waste tyre rubber particles, glass fibre and polyester resin to enhance damping and structural properties. The fabricated composite sleeper material is expected to have high structural strength properties compared to the existing sleepers made from wood, steel, and concrete. The higher strength properties will give it greater durability and improved absorption of vibrational forces. Higher absorption of vibrational forces will reduce the possibilities of crack failure and increase the stability of the railway way track to heavily laden trains.

1.4 Significance of the study

The railway industry often makes use of concrete and timber sleepers. The service life of concrete sleepers is normally less than 60 years due to high vibration and aggressive load (static and dynamic) on the railway track system. Hence this study fabricates a railway sleeper that will be durable and last much longer than the traditional sleepers. The fabricated railway sleeper is lighter and has better mechanical properties than the concrete and timber sleepers. The use of waste tyres in the fabrication of sleepers provides an environmentally friendly and sustainable method of disposal of waste tyres. Burning tyres, the preferred disposal method, harms our environment and health, causing diseases such as cancer (Malahova et al 2019). Furthermore, traditionally employed methods of disposal of tyres cause soil, air, and water pollution.

1.5 Main objective

To fabricate a composite railway sleeper material from waste tyre rubber particles, glass fibre and polyester resin for enhanced vibrational damping and increased structural strength in railroad sleepers.

1.5.1 Specific objectives

i) To characterize the physical properties of the waste tyre rubber particles.
ii) To fabricate a hybrid composite from waste tyre particles, fibreglass and polyester resin.
iii) To evaluate the mechanical properties of the composite sleeper under loading conditions.
iv) To evaluate the damping vibrational properties of the composite sleeper.
v) To determine the optimal composite sleeper design concerning damping properties and structural strength.

1.6 Scope of the Study

Only recycled rubber particles from tyres will be used in this study, and the rubber particles will be used to fabricate the composite sleeper.

1.7 Thesis outline

This thesis consists of five chapters. Chapter 1 gives an introduction and background and articulates the study's problem statement. After that, the study's purpose, importance and objectives are outlined. Chapter 2 reviews the study's literature by giving overview of railway sleepers, stating railway components in depth and narrowing it down to composites sleepers. After that, it reviews different types of railway sleepers and methods used to prevent sleepers' failure.

Chapter 3 describes the experimental methodology. This includes the characterization of rubber particle materials and fabrication of the composites. After that, mechanical and vibration tests were carried out on the fabricated composites. Chapter 4 gives characterization properties of raw material, mechanical properties and vibration properties of the fabricated composites. The last section of the chapter covers the optimizations and applications of the developed composite railway sleeper.

Chapter 5 concludes the thesis by giving key insight and limitations of the study. Thereafter, recommends future work.

CHAPTER 2: LITERATURE REVIEW

2.1 Overview of the railway structure

A railway is a track system where trains run for transportation. The railway track system consists of ballasts, sleepers, rail and sleeper pads. The components of the track system and different types of railway sleepers are discussed in depth and then narrowed down to composites sleepers.

Several different technologies have been developed for railway sleepers. Figure 2.1 shows the general layout of a railway track system with the main components highlighted. The beam that is placed underneath is called a sleeper. The railway sleeper is a crucial component in the structure of a railway track system. Sleepers are used on the railway track and can be defined as beams placed between the railway track and ballast supports (Taherihezehad *et al.,* 2013). The main function of railway sleepers is to maintain the rail gauge and distribute and transfer the transported rail load to ballast or other support components. Furthermore, sleepers play an important role in resisting longitudinal, lateral movement of the railway track system and resisting abrading actions of the bearing plates (Burrow *et al.*, 2007; BS EN 13230-1, 2009).

Figure 2.1 - Main components of a railway track system (Taherihezehad *et al.* 2013)

Granular stones on the bed of the railway track are called ballasts. The primary tasks of the ballasts are to provide a constant flexible vertical support (Esveld *et al.* 2001). In addition, the ballasts assist in the track levelling and line enhancing constructability to fix the track in position longitudinally and laterally (Esveld *et al.* 2001).

The sleeper pads increase the track system's elasticity. However, these sleeper pads tend to loosen easily and come off from the main structure due to the high vibration of the track system when fully loaded or high-speed trains are on track (Kernes *et al*. 2011).

Several different types of sleepers are used in the railway industry. The types of railway sleepers in everyday use are timber, steel, composite and concrete sleepers (Lichtberger *et al.* 2005). The timber sleeper has been widely used over centuries as it met the quality requirement at the time. However, with recent developments in train technology, the railway track has to be able to sustain trains that move at faster speeds. Thus, the demands on sleeper material properties have increased. Timber sleepers are not suited to high-speed trains that carry an ever-increasing payload (Manalo *et al*. 2010).

The concrete sleeper was introduced to meet the needs of recent developments in train technology. However, the concrete sleeper has a significant flaw in that rail abrasion tends to occur, resulting in a mode of failure. Rail abrasion is a loss of concrete material due to high vibration caused by heavily loaded trains (Kernes *et al.*, 2011). Rail seat failure can fail rail changing mechanisms as well as rail track gauge widening, potentially causing train derailment (Richard *et al.* 2012)

Several innovative methods have been used to eliminate vibrations in railway tracks, such as installing rail and sleeper pads underneath the rail and sleeper, respectively, to increase the damping of the track system (Carrascal *et al.*: 2007; Connolly *et al.*, 2015). However, finding a sustainable way to eliminate the vibration in the railway industry is still a major challenge.

The idea of incorporating rubber particles in concrete has been explored to enhance the damping characteristics of concrete sleepers. Concrete containing rubber particles has been shown to improve the ability of the composite concrete sleeper, to absorb the vibration energy (Meesit *et al*. 2017). It has been revealed that the amount and size of rubber particles play a vital role in the damping property of concrete (Meesit *et al*., 2017). However, the sleeper fabricated using concrete and waste rubber particles have poor ductility despite good compressional strength. Furthermore, concrete sleepers in whatever form tend to crack when heavily loaded trains are travelling at higher speeds. This often occurs as ballasts deteriorate and become nucleolus sites for forming voids and pockets between the sleepers and ballasts. In addition, the high vibration in the track system leads to micro-cracks forming on the concrete sleeper, ultimately leading to a failure (Kaewunruen *et al.* 2011). It has been observed that cracking of railway sleepers often occurs in the mid-span and also in rail seats because of impact loading (Remennikov *et al.* 2008).

Railroad transportation is in demand due to its economic significance for passengers and goods; hence, the development of railway tracks resilient to vibration is needed. The railway track system should handle the dynamic and static load necessary for a railway structure. This study is expected to improve the damping property and comply with railway sleepers' railway standards (IRS:T 59-2021).

2.2 Components of railway track

The railway way structure consists of ballasts, railway pads, rails and sleepers. The components of the railway structure are discussed in depth in subsequent subheadings.

2.2.2 Rails

Rails are an important transportation system for a lot of countries around the world. Railway lines have been a critical promoter of social growth and the economy around the world. They have been constructed using local materials to suit construction, lifetime design, and maintenance (Kaewunruen *et al*., 2018). The wheel-rail contact is an open system contact that is exposed to various external factors, including temperature, humidity, water, and even leaves. All these environmental conditions affect wheel-rail wear (Zhu *et al*., 2019).

2.2.3 Railway pads

The railway sleeper and sleeper pads are installed underneath the railway to increase the track system's damping (Carrascal *et al*., 2007; Connolly e*t al.,* 2015). Yet, these railway pads tend to wear easily and come off from the main structure tack system due to numerous factors such as climate change and looseness of the fastening system (Kernes *et al*. 2011).

2.2.4 Types of railway sleepers

Several types of railway sleepers are used in the railway industry: concrete sleepers, timber sleepers, composite sleepers and steel sleepers. Table 2.1 summarises the properties of the different types of railway sleepers.

Table 2.1 – Known railway sleepers, failure and functionality

Type of railway sleepers	Life Span in years	Measures to minimise failure	Causes of Failure	References
Composite sleeper	greater than 60	Silica fume, reinforcement	Weak bond	(Meesit et al., 2017)
Steel sleeper	less than 50	Avoid moist places, slag ballast, high salinity, zinc can be put on as coating and corrosive materials	Corrosion and Fatigue failure	(Ferdous, et al 2014;Herbandez et al 2007; Langman et al 1983)
Concrete sleeper	less than 50	To add fly ash, gout reinforcement multilayer abrasion resistant, steel fibre, add silica fume, epoxy coating, and metallic aggregate in the railway region to concrete sleeper	Cracking Impact loading	(Wahid et al 2014;Bakhareu et al 1997)
Timber sleeper	less than 20	Place End plates and impregnation with timber synthetic chemicals and natural treatment	Split end share loading and trans, fungal attack and termite attack	(Ferdous et al 2014; Conners et al 2008)

2.2.4.1 Concrete sleepers

Concrete sleepers can gauge holding characteristics and deliver better line than timber sleepers. Concrete sleepers tend to be heavy, expensive, and incapable of providing service life beyond 50 years (Ferdous *et al.*, 2015). Furthermore, costs for producing and maintaining pre-stressed concrete sleepers are considerably elevated. Their initial costs are about twice that of hardwood timber sleepers (Kaewunruen *et al.*, 2014). Concrete sleepers have high resistance to compression; however, they present weakness when it comes to tension. Due to this characteristic, mono-block concrete sleepers use the technique of pre-stressing to withstand the dynamic loads arising from the train's passage (Papaelias *et al.*, 2018).

Concrete sleepers have higher compression strength when compared with other sleepers and hold a better line. Figure 2.2 shows the failure mode of concrete sleepers through cracking at mid-span and at the end of the upper side of the sleeper. Concrete sleepers are expected to resist the high amount of loads and harsh environments. The heavier loads can result in early damage to concrete sleepers, generally in the form of cracks (Van Dyk *et al.,* 2012).

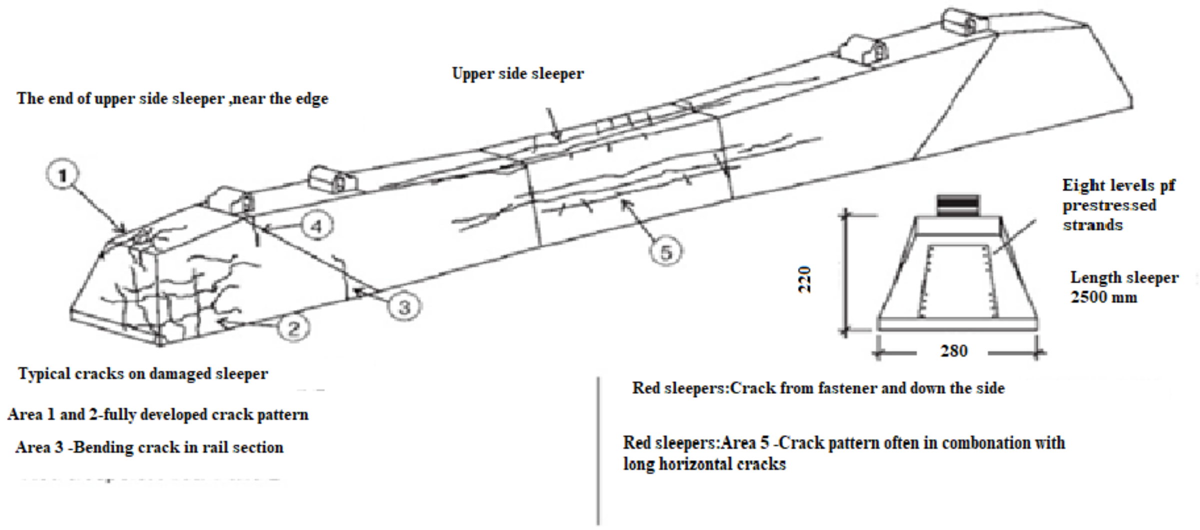

Figure 2.2 - Failure crack pattern of concrete sleeper (Thun *et al.*, 2008)

The concrete sleeper failure can be classified into three categories: rail fastener failure, rail seal abrasion and flexural cracking (Lutch 2009). The cracking occurs on the mid-span and the rail seat because of impact loading (Remennikov *et al.* 2008). Due to the higher stiffness or low ductility of the concrete sleeper could result in rapid deterioration leading to global failure due to flexural cracks (Manalo *et al.* 2010).

Rail seat abrasion is the loss of concrete under the rail seat, and this factor can decrease the service life of the concrete sleeper. It has been observed that when heavier and faster trains travel, the ballast deteriorates progressively, forming voids and pockets between ballasts and sleepers. Since the structure of the track system is subjected to a vibration environment, this could lead to the concrete sleepers cracking and suffering structural damage (Sakdirat *et al.*, 2011). Figure 2.3 shows a rail seat abrasion that could result in rail tipping, loss of clip toe load and widening of the gauge.

Figure 2.3 - Rail seat abrasion (Richard *et al*. 2012).

Severe abrasion can result in rail tipping, loss of clip toe load and widening the gauge out of spec, increasing the potentiality of a train derailment. (Richard et al., 2012)

Table 2.2 - Mechanical properties of concrete sleepers

Properties	Strength parameters	Reference
Compression strength	61.20 MPa	(Meesit *et al*., 2017)
Tensile Strength	6.50 MPa	(Van Dyk *et al.*, 2012)
Concrete modulus of elasticity	47.70 GPa	(Van Dyk *et al.*, 2012)

Damping ratio	0.022	(Meesit *et al.,* 2017)
Deflection	550 mm	(Sadeghi, *et al* 2012)

The concrete sleeper has life span of 50 years and greater compression strength of 61.20 MPa (Ferdous *et al.,* 2015).Even though ,concerete sleeper has higher compression strength when compared with timber sleeper and composite sleeper ,tensile strength of concrete sleeper is low giving strength of 6.50 MPa. The concrete sleeper has a damping ratio ranging from 0.1 to 2.0% depending on the level of pre-stressing and the support conditions (Remennikov *et al.* 2006). This low damping ratio indicates the low tolerance of concrete sleepers to impact forces (Kaewunruen *et al.* 2008).

The average damping ratio of concrete is 0.02146% at 28 days. However, concrete sleepers incorporating silica fume have an improved damping ratio of 21.76 when 10% of cement is replaced with silica fume (Meesit *et al*. 2017). This phenomenon can be attributed to the large interface surface area between silica fume and cement matric, which dissipates vibration energy efficiently (Chung *et al.* 2000). Concrete sleepers containing rubber particles have a higher damping ratio in comparison to concrete incorporating silica fumes of 0.04128 and 0.04038 at 7 and 28 days respectively (Meesit *et al*. 2017). The increasing age of concrete results in a slight reduction in its damping properties due to limited movement of inner molecules within the cement as the hydration reaction of cement progresses (Lin *et al.* 2010).

Material damping depends on hysteretic energy loss as a material (structural element) deforms during vibration. Adding more rubber particles led to increasing damping with incremental amounts of rubber particles. Adding an incremental amount of fibreglass increased the damping ability of the material at all rubber particle percentages. Studies by Zheng *et al.* (2008), Najim *et al.* (2012), and Skripkiūnas *et al.* (2009) stated that rubber particle volume fraction and particle size have a direct influence on the vibrational damping properties of composite material. The authors noted that increasing rubber particles' volume fraction regardless of particle size increased damping. However, this analogy only held true up to 20% beyond this threshold. The vibrational damping decreased due to poor stress transfer and insufficient resin in the composite.

Meesit et al. (2017) study stated that concrete's average vibrational damping ratio is 0.02146 at 28 days. However, concrete sleepers containing rubber particles have higher vibrational damping ratios than concrete incorporating silica fumes with damping values of 0.04128 and 0.04038 at 7 and 28 days, respectively. The increasing age of concrete results in a slight reduction in its damping properties due to limited movement of inner molecules within the cement as the hydration reaction of cement progresses (Lin *et al.* 2010). The current study has an optimum damping value of 0.1416, which is significantly greater than that of concrete, as stated above.

A study by Katarne *et al.* (2021) reported that composites' damping properties depend not only on the material but also on the load frequency since the viscoelasticity and the defect behaviour depend on the frequency. In addition, the damping properties depend on the temperature. This phenomenon is a significant factor in the current study due to the viscoelasticity effect of rubber particles. As forces and temperature act on the composite, the viscoelasticity of rubber particles is altered, improving vibration damping. However, there is a need for further study into the effect of viscoelasticity effects of the rubber particles in composites on vibrational damping.

A study by Poddaeva *et al.* (2021) reported that the damping ability of the rubber particles materials allows it to absorb energy in an irreversible process during its cyclic deformation because rubber can shrink and expand when the load is applied. Composite made of rubber particle materials has better stress dissipative properties, resulting in improved vibrational damping. A study by Gupta *et al.* (2021) aligns with the current study indicating that the coarse rubber particles provide better vibration damping than fine ones.

The addition of rubber particles increases the compressive volumetric strain. It improves the energy dissipation efficiency, which can help reduce the track dilation and minimize the energy transmitted to underlying layers or the track's surroundings. However, including rubber in the mixtures increases axial deformation and reduces the resilient and shear modulus. Therefore, a proper rubber content should be selected with caution to optimize the energy dissipation efficiency while also considering vibration damping (Indraratna *et al.* 2022). The hybrid composite fabricated in this study using rubber particles could help to dissipate energy while maintaining acceptable vibrational damping.

Introducing rubber particles and vibrational damping can also reduce noise as trains run over the railway sleeper (Quan *et al.,* 2022). Using rubber particles in a composite sleeper will help reduce noise levels. This is especially important as trains travel at higher speeds carrying ever heavier loads with technological advancements. Furthermore, it is essential to control the noise level of trains which go through populated areas.

2.2.4.2 Timber sleepers

Timber sleepers have an excellent history of reliable performance and are effective in the railway industry (Zarembski *et al.* 1993). Furthermore, timber sleepers are simple to assemble, easy to replace, easy to work with, easy to handle, and can be fitted in almost all railway track systems (Manalo *et al*. 2010). However, the main disadvantage of timber sleepers is that they are susceptible to mechanical and biological degradation, and fungal decay is a significant problem that causes failure in timber sleepers (Hagaman *et al.* 1991).

Due to the timber sleeper's outlined shortcomings, several alternatives, such as the concrete and steel sleepers (Meesit *et al*. 2017). Figure 2.4 shows timber sleepers' most common failure mode due to fungal decay.

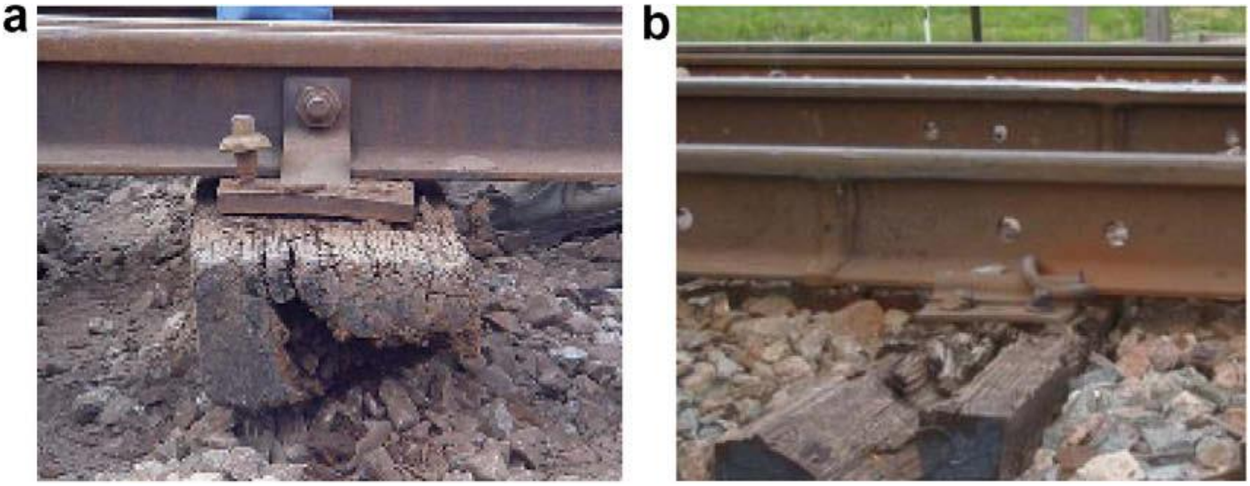

Figure 2.4 - Fungal decay (a), (b) and slitting end) (Manalo *et al.* 2010)

Figure 2.4 (a) shows a timber sleeper that fails because of fungal decay (Hagaman *et al.* 1991). Figure 2.4(b) shows a splitting end of the timber sleeper, which fails the sleeper under transverse shear loadings. Mostly in rainy seasons, timber sleepers absorb moisture and make fungus active in timber sleepers, which can affect the reliability of railway structures by spreading from one sleeper to another through non-nutritional surfaces (Singh *et al.* 1999). Once termites condemn the timber sleeper, they accept all cellulose materials and permanently damage the timber (Eldridge *et al.* 2005).

Splitting at the end of a timber sleeper can be averted or minimised by using an end plate mounted in the last part of the wooden sleeper, as indicated in Figure 2.5 (Bakhareu *et al.* 1997; Ellis *et al.* 2001). This technic has limitations, such as the splitting width and length must be smaller than 20mm and 250 mm, respectively.

Figure 2.5 - End plate splitting (Mbatha *et al.* 2021)

There are two types of timber sleepers' hardwood and softwood. Hardwood is the most common timber sleeper in railway lines in the railway industry, and its advantages over the softwood timber sleeper are its greatest durability and strength. Nevertheless, hardwood timber has become more expensive over the years. Furthermore, its availability is dropping yet no longer has the same quality as before (Manalo *et al.* 2011).

A screw spike is principally used to maintain the baseplates that attach rails to sleepers and avoid lateral and vertical movements between them. A hardwood timber sleeper has a screw spike resistance of 40 kN (Kaewunruen *et al.*, 2013). Table 2.3 shows the mechanical properties of hardwood and softwood sleepers. The mechanical properties of hardwood timber possess higher strength when compared with wet timber, as shown in Table 2.3.

Table 2.3 - Properties of hardwood timber sleeper (Hamzah *et al.* 2008)

Grade	**Tension parallel to grain (MPa)**	**Compression parallel to grain (MPa)**	**Compression perpendicular to the grain (MPa)**	**Shear parallel to grain (MPa)**	**Modulus of elasticity (MPa)**	**Modulus of rapture (MPa)**
Softwood	16.55	68.80	9.53	12.90	18,400	121
Hard wood	20.00	76.00	9.79	15.00	20,100	142

Softwood timber is from gymnosperm trees such as evergreen trees and conifers, often called softwoods. Softwood sleeper timber has poor resistance to gauge spreading and spike hole enlargement compared with hardwood sleepers. Furthermore, it tends to spike hole enlargement and gauge spreading (Ghorban *et al.*, 2013).

Hardwood timber possesses greater resistance to fungal decay compared with softwood sleepers. Softwood offers less resistance to gauge spreading, end splitting and spike hole enlargement than hardwood sleepers. Furthermore, softwood timbers are less effective in transmitting loads to the ballast section than hardwood sleepers (Wolf *et al.*, 2014). Table 2.4 shows the properties of oak.

Table 2.4 - Properties of oak (softwood) (Manalo *et al.* 2015).

Properties of timber	**Oak**
Density (kg/m^3)	1096.00
Modulus of elasticity (GPa)	8.40
Modulus of rapture (MPa)	57.90
Shear strength (MPa)	5.00
Rail seat compression (MPa)	4.60
Screw withdrawal (kN)	22.20

The mechanical properties of oak are low compared to hardwood timber, as shown in Table 2.4. A softwood timber sleeper has a screw spike resistance of 22.2 kN. Moreover, hardwood timber has a better capability of transmitting the load to the ballast than softwood sleepers; therefore, softwood sleeper timber and hardwood timber should not be mixed on the railway line (Manalo *et al.* 2010). The maximum deflection produced by all kinds of timber sleepers is 20 mm, assuming that the sleepers maintained their elastic behaviour (Hamzah *et al.* 2008).

Australian railway maintenance requires approximately 2.5 million pieces of timber sleeper per year to do their care on the railway system (Ellis *et al.* 2001). The United States of America use 14 0000 timber sleepers for replacement and maintenance per year. This maintenance accounts for about 2% of the timber sleepers installed on railway lines in the country, out of the 700 million timber sleepers for replacement and maintenance (Control *et al.* 2017). German is in demand of 11 million timber sleepers for maintenance and replacement per year (Control *et al*. 2017). The Australian railway industry uses 25-35% of its annual budget to maintain its railway structure (Ferreira *et al.*, 2003). Replacement of the timber sleeper is very costly, and the United States of America railway industry uses more than 1 billion US dollars annually to replace railway sleepers (Merl *et al.* 2003). To lower the replacement costs, fabricating a composite sleeper comparable to a timber sleeper's strength is necessary.

The vibration of timber sleepers has not been studied in depth. However, timber sleepers can absorb any vibration and impact energy produced before transmitting the rest of the loading to the ballast and then to the ground (Hamzah *et al.* 2008)**.**

The railway structure usually is exposed to the effects of moisture from rain, snow, frost, dew and hail. It has been reported that moisture absorption significantly adds to the degradation of timber sleepers and reduces the sleeper's mechanical properties (Gerhards *et al.* 1982). Railways that use timber sleepers allow trains to travel at a speed of less than 100 km/hr (Hamzah *et al.* 2008). Recent developments in train technology require railway tracks that can sustain trains that move at faster speeds; thus, the demands on sleeper material properties have increased. Timber sleepers are not suited to high-speed trains that carry an ever-increasing payload (Manalo *et al*. 2010).

2.2.4.3 Steel sleepers

Steel sleepers are considered to have superior strength when compared with concrete and timber sleepers (Davalos *et al.* 1998). Steel sleepers are easier to work with than timber and concrete sleepers due to their low density. The service life of steel timber is approximately 50 years (Manalo *et al*. 2010). Figure 2.6 shows a traditional steel sleeper layout.

Figure 2.6 - Steel sleeper (Muthukannan *et al.* 2019)

The steel sleeper can only accommodate lightly loaded trains and is not suitable for trains travelling at speeds less than 160km/hr (Mohammad *et al.*, 2017). Steel sleepers are expensive and not widely used due to their susceptibility to corrosion (Qiao *et al.* 1998). Furthermore, fatigue cracking in the fastening holes of steel sleepers is also a significant challenge (Esveld *et al.* 2001).

2.2.4.3.1 Y-shaped steel sleeper

The Y-shaped steel sleeper shown in Figure 2.7 was designed and developed to substitute for the traditional steel sleeper (Control *et al.* 2017).

Figure 2.7 - Y shaped steel sleeper (Miura *et al.* 1998)

Figure 2.7 shows that a Y steel sleeper is shaped like a Y in its level arrangement. Y steel sleeper possesses much greater resistance to cross-movement compared to other sleepers due to its design of the Y-fork. The fork contains a large number of ballasts. This makes the y-shaped steel sleeper have greater resistance to cross movement. However, it is impossible to pull or adjust the y steel sleeper in the ballast by a simple laying device.

Furthermore, because of the y shape, the laying of sleepers should follow strict guidelines (Miur*a et al*. 1998). Another problem with steel sleepers is fatigue cracking in the fastening holes caused by moving trains (Sharma *et al.*, 2017; Ellis *et al.*, 2001). The Y-shaped steel sleeper possesses much greater resistance to cross-movement than other sleepers due to its y-fork design.

Table 2.5 - Mechanical properties of steel and y-shaped steel sleeper

Mechanical properties	**Steel Sleeper**	**References**
Tensile strength (MPa)	580	(ASTM et al. A220)
Compression strength (MPa)	875	(Razumakov *et al*. 2016)

Hardness Vickers	331	(Razumakov *et al*. 2016)
Deflection (mm)	500	(Sadeghi, *et al* 2012)
Young modulus GPa	172	(ASTM *et al.* A220)

The Y-fork contains many ballasts, which makes the y-steel sleeper have greater resistance to cross movement. Furthermore, because of the Y-shape, sleepers should follow strict guidelines (Miura *et al.* 1998).

2.2.4.4 Composite sleepers

Composites consist of fibre, matrix and filler, and it has been observed that development and innovative methods have shown that polymer materials combined with fibre composites could enhance both mechanical and physical properties of railway sleepers (Dechojarassri *et al.* 2005). In the subsequent subsections, natural fibre, synthetic fibre, filler and type of composite and its properties will be discussed.

2.2.4.4.1 Reinforcement Fibres

Fibres are used widely in the reinforcement of composite materials. These fibres can be either synthetic or natural**.** Fibres are used to give strength to composite materials (Oksman *et al.*, 2001; Weyenberg *et al.*, 2006; Joffe *et al*., 2011). Synthetic fibres such as glass, carbon and nylon are used to manufacture composite sleepers. The subsequent subsections will review the different types of fibres used in railway sleeper composites.

2.2.4.4.1.1 Natural Fibres

It has been proven that natural fibre composites have good mechanical properties and electrical resistance. Furthermore, natural fibres have good thermal and acoustic insulation properties and higher cracking resistance (Ramnath *et al.*, 2014; Sanjay *et al.*, 2015; Deng *et al.*, 2016). The mechanical properties of hemp, flax, jute and sisal fibres are excellent, making them suitable for composite manufacture. Figure 2.8 presents the broad classification of natural fibres. It has been found that natural fibre composites have specific mechanical properties that are comparable to those of glass fibre reinforced composites.

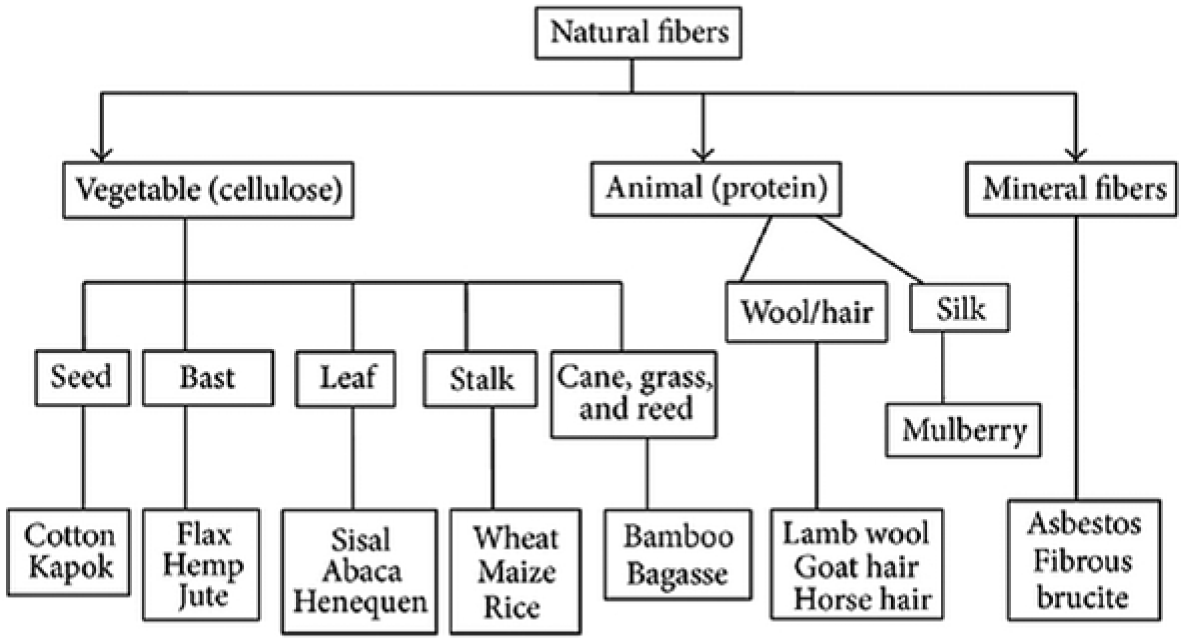

Figure 2.8 - Classification of natural fibres (Sanjay *et al.* 2015)

Natural fibres are classified into three categories vegetable, animal and mineral fibres. Vegetable fibres are seed, bast, leaf, stalk, cane, grass and reed. Animal fibres are classified into two categories wool and silk. Lastly, mineral fibres include asbestos and fibrous brucite. Table 2.6 shows the mechanical properties of different types of natural fibres. Natural fibres provide numerous advantages over synthetic fibres in strengthening composites due to their bio-degradability and eco-friendly behaviour and can be thus efficiently employed for different applications. Furthermore, natural fibres possess less explored characteristics, such as the electric resistance, thermal conductivity and acoustic insulation properties of plant-based composites (Sanjay *et al*., 2018).

Table 2.6 - The Comparison of tensile of natural and synthetic fibres (Sanjay *et al*. 2015)

Fibres	Tensile strength (MPa)	Young's Modulus(GPa)	Elongation at break(%)	Density (g/cm^3)
Abaca	400	12.00	3.00-10.00	1.50
Bagasse	350	22.00	5.80	0.89
Bamboo	290	17.00	-	1.25
Banana	529-914	27.00-32.00	5.90	1.35
Coir	220	6.00	15-25	1.25
Cotton	400	12.00	3.00-10.00	1.51
Curaua	500-1150	11.80	3.70-4.30	1.40

Flax	800-1500	60.00-80.00	1.20-1.60	1.40
Hemp	550-900	70.00	1.60	1.48
Jute	410-780	26.50	1.90	1.48
Kenaf	930	53.00	1.60	-
Pineapple	413-1627	60.00-82.00	14.50	1.44
Ramie	500	44.00	2.00	1.50
Sisal	610-720	9.00-24.00	2.00-3.00	1.34
E-glass	2400	73.00	3.00	2.55
S glass	4580	85	4.60	2.50
Aramid	300	124	2.50	1.40
Hs Carbon	2550	200	1.30	1.82
Carbon(std PAN-based)	4000	230-240	1.40-1.80	1.40

Natural fibres in polymer composites have several shortcomings, including excessive water absorption and poor thermal characteristics. Electric resistance, thermal conductivity, and acoustic insulation capabilities of plant-based composites are some of the least investigated elements. Future research and development should focus on developing environmentally friendly materials with appropriate qualities (Sanjay *et al.*, 2018).

2.2.4.4.1.2 Synthetic fibres

Synthetic fibres have been used in the manufacture of composite railway sleepers. Figure 2.9 shows the broad classification of synthetic reinforcement fibres. Synthetic fibres are artificial fibres, with the majority of them being created from petroleum-based basic materials known as petro-chemicals. Synthetic fibres are made up of a tiny unit or monomer that is a repeating unit. Nylon, acrylics, polyurethane, and polypropylene are some of them. Every year, millions of tons of these fibres are manufactured worldwide (McIntyre *et a*l. 2005).

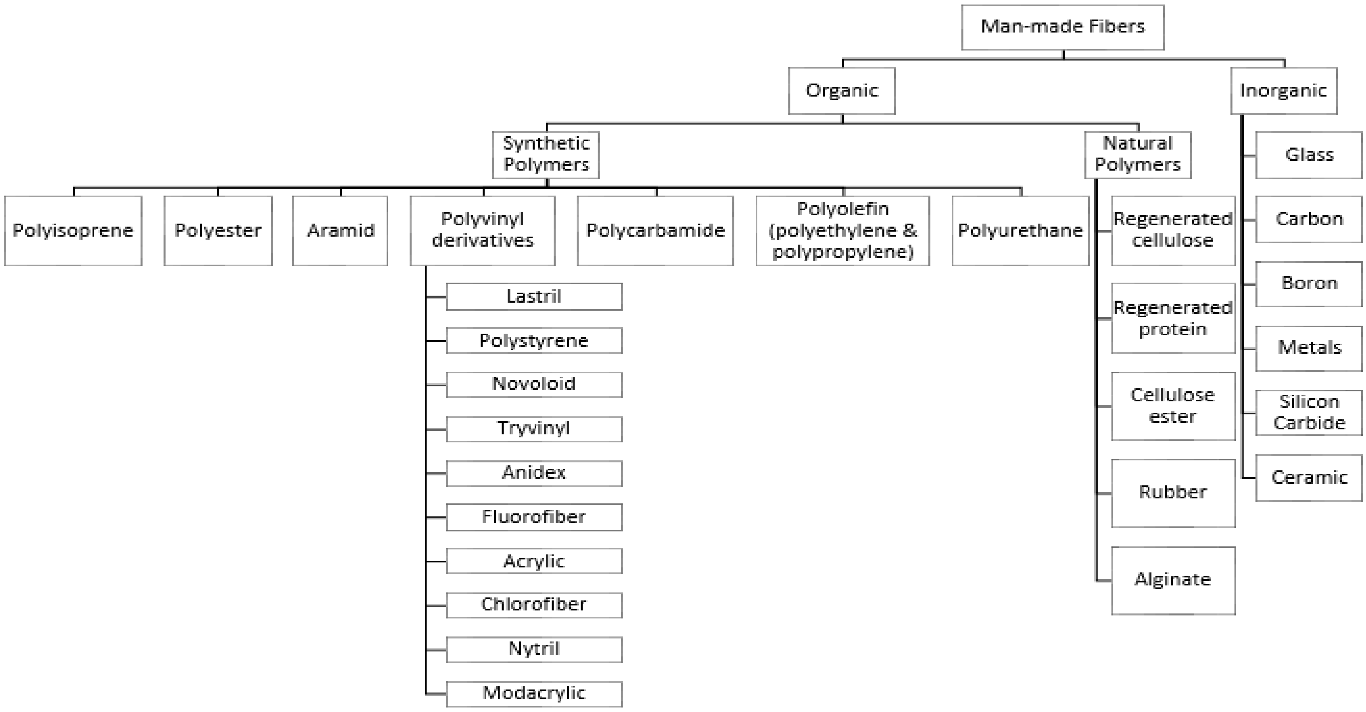

Figure 2.9 - Classification of synthetic fibre (Satheeshkumar *et al.* 2014)

2.2.4.4.1.2.1 Organic Fibres

Organic Polymers fibres can be used as a reinforcement in composite materials (Joffe *et a*l. 2011)**.** Fibres, synthetic such as nylon and polyester or natural such as wool and cotton, are some of the most strongly oriented organic polymers. There are two types of applications for conventional organic fibres. Industrial products such as ropes, motor vehicle tyres, drive belts, and conveyor belts employ woven, knitted, and felted materials. Recently, however, several innovative organic fibres with specialist physical features have surfaced in the patent literature, which are far superior to traditional organic fibre (Schenk *et al.* 1975).

2.2.4.4.1.2.2 Inorganic fibres

Inorganic fibres also find use in the reinforcement of composite materials. These inorganic fibres include glass, carbon, boron, metals and silicon carbide. Some of these concrete fibres can improve and change the properties of concrete. Glass, carbon, and steel fibres are some of the most frequent used inorganic fibres in concrete. It was observed that steel fibre in the composite sleeper increase cracking resistance, improve energy absorption capacity and improves the sleeper bending strength (Parvez *et al.* 2017). Table 2.7 shows the mechanical properties of some synthetic fibres.

The mechanical properties of E glass fibre reinforced composites exceeded those of composites with natural fibres. This is due to inherent fibreglass properties, which have superior mechanical properties. E glass is a continuous fibre which allows better transmission of stresses which is not interrupted due to the size of the fibre (Series *et al.* 2019). It is easier to achieve the required length with synthetic fibres than with natural fibres.

2.2.4.4.2 Composite filler materials

Composites can be reinforced with filler materials to increase the quality and properties of the components based on the requirements and applications (Jani *et al.,* 2016). There are two types of filler materials, either natural or synthetic fillers. Natural fillers consist of wood, rice husk, wood chips, wheal straw and palm kernel shells (Zaaba *et al.,* 2019). Synthetic fillers consist of glass, ceramics, metals, rubber, and other novel materials that can be used as fillers in composites (Geetha *et al.*, 2020). Natural fillers have the advantages of low density, low cost, and biodegradability. However, the main disadvantages of natural fillers in composites are the poor compatibility between filler and matrix and the relatively high moisture sorption (Panigrahi *et al.* 2007). Rubber particles have various possible end uses as filler materials due to their strong elasticity behaviour, as indicated in a study by Norvez *et al.* (2016).In this current study, rubber particles will be used as filler materials due to their elasticity behaviour which leads to reduced vibration.

2.2.4.4.3 Types of composite Sleepers

Different types of composite sleepers are in use on the railway line. Composite made of recycled plastic, Urethane foam and fibreglasses, a composite made of tyre particles crumb, scrap waste sleeper and many more are discussed in the following subheading below.

2.2.4.4.3.1 Polycarbonate and polyethene plastic with fibreglass composite sleeper

Composite sleepers are made of recycled polycarbonate and polyethene plastics with glass fibre reinforcement. Plastic sleepers reinforced with fibres have a greater strength-to-weight ratio than timber. Furthermore, these composite sleepers are more durable and have a longer service life (Jacob *et al.* 2004). However, the damping of impact loads, sound absorption and lateral stability properties of the sleeper from waste plastics is similar to timber sleeper.

Figure 2.10 - Polycarbonate and polyethene plastic with fibreglass composite sleeper (Jain *et al.*, 2016; Manalo *et al.*, 2010).

The Polycarbonate and polyethene plastic with fibreglass composite sleeper is expected to have significantly greater weather resistance than lumber, cheaper primary material usage due to the utilization of scrap plastic, and superior acoustic dampening capabilities than metal and concrete (Fraunhofer *et al*. 2010). The mechanical properties of the railway sleepers made of recycled plastic that was developed in the United States of America (Jain *et al.*, 2016; Manalo *et al.*, 2010). The Rail waste project in Germany has been extruding alternative railway sleepers made from mixed plastic wastes, glass fibre wastes, and auxiliary agents with a thermoplastic polymer matrix since 2008.

Some challenges associated with using recycled plastic sleepers include low stiffness, low strength and resistance ability to hold screws and formation of voids in the sleeper. Furthermore, these sleepers have insufficient lateral resistance and permanent deformation due to creep and temperature variations (Manalo, *et al.*, 2015). The compression strength of plastic sleeper is 29.68 MPa and flexural strength is 3.20 MPa .The plastic sleeper also posses low tensile strength of 3.34 MPa (Lim et al. 2021).

When gaps emerge during manufacturing a plastic sleeper, it becomes difficult to transfer pressure from one area to another, resulting in stress concentration and, eventually, localised failure before the sleeper's intended life. Furthermore, the composite sleeper may be prone to permanent deformation due to creep under sustained stresses (Sullivan *et al.*, 2003). The amount and duration of stress and the temperature at which the load is applied determine the creep rate. Creep causes stress relaxation, which causes the fastening system to loosen, especially in the curve track, causing gauge holding to suffer (Nosker *et al.* 1998).

2.2.4.4.2 Urethane foam and fibreglass composite

Composite sleepers made of foam urethane resin and fibreglass can be machined and fastened using conventional woodworking tools, as shown in Figure 2.11 (Control *et al.* 2017). This sleeper has greater compression strength and gives better resistance to the removal of screw spikes compared to a timber sleeper. Furthermore, the sleeper shows stiffness similar to timber sleepers (Control *et al.*, 2017). However, this kind of sleeper gained limited space in the railway industry due to its high cost (Qiao *et al.* 1998).

Figure 2.11 - Urethane foam and glass fibre (Koller *et al.* 2009)

In 1978, the Japanese company Sekisui Chemical Co. Ltd. created ESLON Neo Lumber FFU (Fibre Reinforced Foamed Urethane), a synthetic wood made of thermosetting stiff urethane resin foam reinforced with long glass fibres for the construction of railway sleepers. FFU is a composite with mechanical properties that fall between wood and plastic. Furthermore, it has both benefits and, unlike typical wooden sleepers, does not require using environmentally destructive chemicals (Wahid *et al.* 2014). Table 2.7 shows the mechanical properties of the urethane foam and glass fibre sleeper. The primary qualities of the composites are their light weight, good resistance to water absorption, heat and corrosion, ease of drilling, and a design life of more than 50 years. An analysis of the acoustic and dynamic properties of an FFU turnout sleeper revealed that it performs similarly to a timber sleeper (Kaewunruen *et al.,* 2013).

Table 2.7 - Properties of urethane foam and glass fibre and strength parameters (Koller *et al.* 2009)

Properties of urethane foam and glass fibre	**Strength parameters**
Density, (kg/m^3)	670-820
Modulus of Elasticity, (MPa)	8100
Modulus of Rupture, (MPa)	142
Rail-Seat Compression, (MPa)	58
Screw Pullout Force, (kN)	65
Electrical Impedance (wet), (Ω)	140x10^6
Impact bending strength, (MPa)	41

This sleeper has been put in about 925 km of track (roughly 1.5 million sleepers) to date, with its principal applications in turnouts, open steel girder constructions, and tunnels (Koller *et al.* 2009). Sekisui FFU sleepers have been placed in Germany, Austria, and, most recently, Australia, in addition to Japan. Their suitability is currently being researched for a long-span rail bridge in Chongqing, China (Liu *et al.* 2012).

2.2.4.4.4 Waste tyre composites with polyester resin

Abu-jdayil, Mourad and Hussain (2016) discovered that mixing waste tyre rubber particles with polyester resin in specific mix proportions reduces the composite's mechanical strength. Too much rubber volume fraction in the composite materials leads to a reduction in mechanical strength due to the low interfacial bond strength of the rubber particles to the polyester matrix (Meesit *et al.*, 2017; Abu-jdayil *et al.*, 2016)

A study by Abu-jdayil, Mourad and Hussain (2016) used rubber particles of 0.8 mm and 2 mm, as shown in Table 2.8. The author used varying rubber volume fractions between 5% and 40 % in the composite.

The author concluded that larger rubber particle sizes reduce the modulus of elasticity and, ultimately, the composite strength, as shown in Table 2.8. This analogy could be attributed to the poor dispersion of large rubber particles in the resin resulting in weak interfacial bonds (Abu-jdayil, Mourad, and Hussain 2016). However, due to their greater surface area, the smaller rubber particles gave the composite higher mechanical strength due to their excellent bond with the polyester resin.

Table 2.8 - Rubber particle volume fraction and ultimate composite tensile strength (Mourad *et al*. 2016)

Rubber Particle volume fraction (vol %)	Maximum tensile strength 0.8 mm size σ_u (MPa)	Maximum tensile strength 2 mm σ_u (Mpa)	Modulus of elasticity (MPa) 0.8 mm	Modulus of elasticity (MPa) 2 mm size
0	37.60	37.60	1030.00	1030.00
5	22.80	8.30	833.60	762.20
10	20.00	7.30	730.20	800.70
15	16.00	5.90	593.10	496.60
20	11.80	7.60	461.80	384.50
25	10.40	3.60	339.30	306.00
30	8.10	5.35	301.00	271.70
35	5.65	1.75	203.80	93.40
40	4.35	1.25	157.60	63.80

The study by Mourad *et al.* (2016), as shown in Table 2.8, indicates that the ultimate tensile strength of 0.8 mm rubber particles is higher than 2 mm. The trend suggests that when the volume fraction of rubber particles increases, the maximum tensile strength decreases. The increasing volume fraction of rubber particles results in poor dispersal and decreases the composite strength, as shown in Table 2.8. The modulus of elasticity decreases when rubber particles increase. The trend indicates that when rubber particles' volume fraction is increased, the modulus of elasticity decreases.

Railway sleepers are exposed to different weathering conditions, such as ultraviolet (UV) radiation. The energy that is generated by the sun is sufficient to break the molecular bond of a railway structure. The lignin of the timber can be affected by (UV) Radiation (Ridout *et al.*, 2013). In fibre-reinforced polymer composite, the matrix is often considered the weak component as it undergoes chemical degradation and physical damage during exposure to harsh environments and stress applications (Chin *et al.* 1997).

2.2.4.4.5 Recycled plastic bottles and fibreglass Sleeper

TieTek LLC, in Houston, Texas, created a composite railway sleeper out of recycled plastic bottles and bags, scrapped vehicle tyres, waste fiberglass, and structural mineral fillers, as shown in Figure 2.12. It was made out of 85% recycled materials and was designed to replace traditional timber sleepers; after 17 years, it had been put in over 2 million locations worldwide. The advantages of this sleeper included less noise and vibration, more lateral stability, and a longer lifespan (40 years).

Figure 2.12 - Recycled plastic bottles and fibreglass Sleeper (Vantuono *et al.* 2010)

Recycled plastic bottles and fibreglass Sleeper has numerous advantages over timber sleeper, such as good rail seat abrasion resistance, spike pull and moisture résistance. Furthermore, it also has insect and fungal resistance and low electrical conductivity (Loui *et al.*, 2013). TieTek discontinued production in early 2010 due to various quality control difficulties (Vantuono *et al.* 2010). These difficulties include the limited strength and stiffness of recycled plastic sleepers, which have been cited as significant roadblocks to their broad use on railway track.

Table 2.9 - Recycled plastic bottles and fibreglass Sleeper (Loui *et al.* 2013)

Properties of composite sleeper	Strength parameters
Density, (kg/m^3)	1153
Modulus of Elasticity, (MPa)	greater than 1724
Modulus of Rupture, (MPa)	greater than 18.60
Compressive MOE, (MPa)	269.00
Rail-Seat Compression, (MPa)	16.50
Screw Pullout Force, (kN)	35.60
Thermal Expansion,($cm/cm/^0C$)	$1.35x10^{-4}$
Electrical Impedance (wet), (Ω)	$500x10^6$
Flammability	205.00

Most alternative sleeper technologies were created to replace current wood sleepers; however, their strength and rigidity are less than wooden sleepers. Hardwood timber sleepers have a modulus of rupture of 65 MPa, but recycled plastic sleepers have a modulus of rupture of approximately 20 MPa. Another reason for their limited adoption in the market is the expensive cost of most composite sleepers.

2.2.4.4.7 Industrial plastic waste Sleeper

Under the brand name 'EcoTrax,' 'Axion,' a US green technology business, currently produces composite sleepers manufactured from 100% recycled consumer plastic such as plastic coffee cups, bags, milk jugs, laundry detergent bottles and industrial plastic waste (Ferdous *et al*. 2021). The Polywood Plastic Composite Company invented this production process in 1994, and Axion took over the company's processing function in 2007 (Louie *et al.*, 2013). Industrial waste sleepers shown in Figure 2.13 have been manufactured for several uses since their inception, including switches, road crossings, bridges, and passenger and heavy load tracks.

Figure 2.13 - Industrial plastic waste sleeper (Ferdous *et al*. 2021)

The properties of the axion Eco Trax sleeper are shown in table Table 2.10. This sleeper is susceptible to biological degradations, insects, and moisture than standard timber sleepers, has a longer life expectancy (50 years), and is more resistant to plate wear (Yu *et al*. 2011). The sleeper technology is now available in Europe, Australia, New Zealand, Canada and Southeast Asia (Kondrashchenko *et al.,* 2019).

Table 2.10 - Properties of Industrial plastic waste sleeper (Yu *et al*. 2011)

Properties of composite sleeper	Strength parameters
Density, (kg/m^3)	849-897
Modulus of Elasticity, (MPa)	1724
Modulus of Rupture, (MPa)	20.60
Compressive MOE, (MPa)	176.50
Rail-Seat Compression, (MPa)	20.60
Screw Pullout Force, (kN)	31.60
Thermal Expansion,(cm/cm/^{0}C)	0.74X10^{-4}

2.2.4.4.10 Polypropylene Sleeper

For an underground railway line and narrow gauge railway track in sugar plantations, a South African company produced a composite sleeper built from recycled polypropylene and high- and low-density polyethene components in 2004, as shown in Figure 2.14. When utilized in underground mines where strong pH variations, high water levels, and humidity pose challenges to traditional sleeper materials, it is said to have a longer service life than lumber and concrete sleepers.

Figure 2.14 - Underground sleeper (Wang *et al.* 2019)

Tufflex Plastic recently installed sleepers in underground lines at AngloGold Ashanti and Gold Fields mines in Africa, and their in-service performance is currently being studied (Wang *et al.*, 2019).

2.2.4.4.11 Natural rubber composite Sleeper

In 2005, a group of Thai researchers were inspired by using natural rubber in rubber-asphalt mixtures for road surfaces, bridge bearings, plates for vibration absorbers, and blocks for seismic protection of tall buildings to produce railway sleepers, as shown in Figure 2.15. They used an ebonite technique to improve the natural rubber's mechanical qualities by increasing the rubber's cross-link density. The modified natural rubber had a higher compressive modulus and hardness than the TieTek composites made from scrap rubber/tyres, which they used as a benchmark (Dechojarassri *et al.* 2005).

Figure 2.15 - Natural rubber composite Sleeper (Dechojarassri *et al.* 2005).

According to Erp *et al.* (2015), the cost of a composite sleeper is about 5 to 10 times that of a regular timber sleeper. Due to their insufficient capacity for holding rail fastenings, some composite sleeper technologies struggle to maintain rail track gauges. However, the modified compound of natural rubber composite sleeper was reported to have a very rigid and inelastic performance in holding the spike for the fastening system (Pattamaprom *et al.* 2005).

2.2.4.4.12 Recycled plastic Sleeper

The Dutch company KLP (Kunststof Lankhorst Product) developed 100% polyethylene recycled plastic sleepers reinforced with steel bar under the brand name KLP (Kunststof Lankhorst Product) for the main track, switch, and bridge applications when the use of toxic creosote oil to preserve timber sleepers was banned (transoms). KLP sleepers have been deployed in more than 20 turnout situations in the Netherlands and Germany since they were initially developed in 2006 (Ferdous *et al.*, 2021). The French recently erected 1 km of rail track to evaluate the railway's performance Figure 2.16.

Figure 2.16 - Recycle plastic Sleeper (Ferdous *et al*. 2021)

The manufacturer optimized the volume of materials for its primary track product, which uses 35% less plastic than a solid rectangular sleeper in the typical shape. This is a good approach for reducing sleeper manufacturing and transportation costs. Table 2.11 shows the properties of recycled plastic sleepers. The advantages of this plastic sleeper include a long life (50 years), durability, ease of installation, and environmental friendliness. It is believed to have higher lateral resistance due to its revolutionary design.

Table 2.11 - Recycle plastic sleeper (Siahkouhi *et al*. 2021)

Properties of composite sleeper	Strength parameters
Density, (kg/m^3)	870
Modulus of Elasticity, (MPa)	800
Poisson's ratio	0.4

These plastic railway sleepers help to reduce vibration and noise significantly. Because of the plastic's ductility combined with the steel's strength, the plastic sleepers provide good damping capabilities and optimum stiffness.

2.2.4.4.13 Wood Core Sleeper

Southwest RV and Marine, a Texas-based US firm, produced a plastic composite wood-core sleeper in 2011. Its fundamental design concept consists of a polyethene-based plastic mixture that protects it from insect assault, moisture, and UV degradation and rectangular reinforcement. Inside is a wooden beam that carries the loads Figure 2.17 (Das *et al.* 2018).

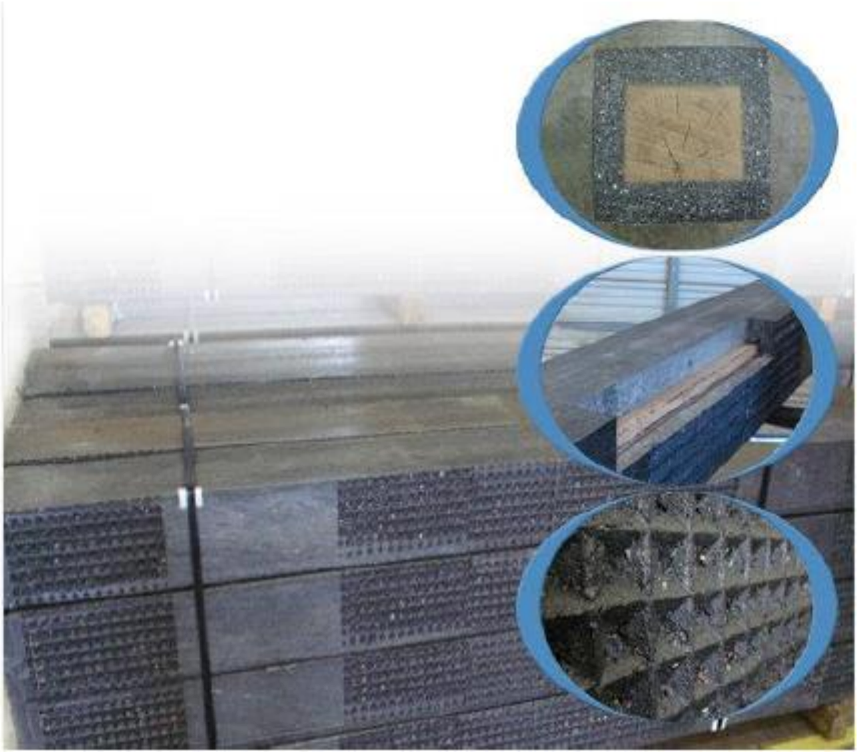

Figure 2.17 - Wood Core Sleeper (Das *et al.* 2018)

A wood core sleeper is a timber sleeper laminated with plastic materials to avoid termite attach and excessive water absorption. Table 2.12 shows the mechanical properties of the wood core sleeper.

Table 2.12 - Properties of wood core sleeper (Das *et al*. 2018)

Properties of composite sleeper	Strength parameters
Density, (kg/m^3)	993
Modulus of Elasticity, (MPa)	1517
Modulus of Rupture, (MPa)	17.20
Compressive MOE, (MPa)	241
Rail-Seat Compression, (MPa)	15.20
Thermal Expansion,(cm/cm/^{0}C)	0.2X10^{-4}

The properties of wood core are comparable with the properties of plastic and timber sleepers. The rail seat compression is 15.2 MPa comparable with a recycled plastic sleeper.

2.2.4.13 Glue Laminated Sandwich Sleeper

The sandwich beam is produced by attaching layers of the fibre-reinforced sandwich together in a horizontal and edges (straight). A study by Thiru *et al*. (2012) evaluated the behaviour of glue-laminated sandwich beams as a replacement for standard timber sleepers in turnout applications. The novel sandwich beam concept Figure 2.18 outperformed most current composite railway sleepers in terms of mechanical qualities and is equivalent to existing timber turnout sleepers. This sleeper has enough resistance to keep the screw in place, which is one of the most common issues with existing plastic composite products.

Figure 2.18 - Glue Laminated Sandwich Sleeper (Thiru *et al*. 2012**)**

Table 2.13 - Properties glue Laminated Sandwich Sleeper (Thiru *et al*. 2012**)**

Properties of composite sleeper	**Strength parameters**
Modulus of Elasticity, (MPa)	5190
Modulus of Rupture, (MPa)	103
Screw Pullout Force, (kN)	63.80

2.2.4.14 Malleable railway Sleeper

IntegriCo Composites Inc. developed a unique processing technology for producing composite sleepers from landfill-bound 100 percent recycled plastic materials, as shown in Figure 2.19 and manufactures several types of sleepers based on the application. Class I, Commuter, Industrial, and Mining are the different types of railroad applications. This product has good moisture, insect, plate-cut, and acidic environment resistance and a long projected life lifetime (50 years). IntegriCo has installed over 1 million composite sleepers in North America since 2005 and is now expanding into Mexico, Canada, and India (Wahid *et al.,* 2014).

Figure 2.19 - Malleable railway Sleeper (Thiru *et al*. 2012**)**

IntegriCo Company has installed over 1 million malleable composite sleepers in North America in railway lines since 2005 and is now expanding all over the country.

Table 2.14 - Properties of Malleable railway Sleeper (Thiru *et al*. 2012**)**

Properties of composite sleeper	**Strength parameters**
Density, (kg/m^3)	1121
Modulus of Elasticity, (MPa)	1655
Modulus of Rupture, (MPa)	18.60
Compressive MOE, (MPa)	262
Rail-Seat Compression, (MPa)	15.90
Screw Pullout Force, (kN)	73.40
Thermal Expansion,($cm/cm/^0C$)	$1.26X10^{-4}$

2.2.4.15 Hybrid Concrete Sleeper

Because geo polymer concrete employs an industrial by-product called fly ash, it is currently regarded as an alternative environmentally friendly railway sleeper. Since 2002, Rocla, Australia's premier concrete sleeper manufacturer, has been producing geo polymer pre-stressed concrete sleepers for mainline rail tracks (Gourley *et al. 2*005). Uehara *et al.* (2010) developed a geo polymer concrete sleeper in 2010 and put it through a series of tests, with the results stratifying the Japanese standard they employed, JIS E 1202. For an industrial trial, Jiménez (Wahid *et al*., 2014) produced alkali-activated fly ash mono-block pre-stressed concrete sleepers, and the testing findings met the Spanish and European requirements codes.

Figure 2.20 - Hybrid Concrete Sleeper (Uehara *et al.* 2010)

Uehara *et al.* (2010) looked into the feasibility of a geo polymer concrete-filled pultruded composite sleeper, as shown in Figure 2.20. The author's findings were promising compared to timber and existing composite sleepers. The durability of an eco-friendly pre-stressed concrete sleeper manufactured from steel slags was recently tested through field inspection in 2014, and it is said to be a viable alternative to traditional pre-stressed concrete sleepers with the added benefit of low environmental impact (Hwang *et al.* 2015). Table 2.15 shows the mechanical properties of a hybrid concrete sleeper. Depending on the prescribed performance targets, different hybrid structural systems have been proposed in the literature (Li *et al.*, 2018).

Table 2.15 - Hybrid concrete sleeper (Khennane et al. 2013)

Properties of composite sleeper	**Strength parameters**
Tensile strength (MPa)	24
Flexural strength (MPa)	22
Compressive strength (MPa)	171

Hybrid buildings are made up of a mix of materials chosen for their inherent properties, such as strength, durability, cost, and aesthetics (Li *et al.,* 2018).

2.2.5 Ballasts

The railway ballast has been adopted in constructing low to medium-speed tracks that handle speeds of less than 250 km/hr (Esveld *et al.* 2001). Ballasts are essential in maintaining the railway track in proper vertical and horizontal alignment. Track geometry weakening or misalignment can be corrected and restored quickly and economically with ballasts *(* Kaewunruen *et al.,* 2012). The tasks of ballast can be divided into two main categories. The primary tasks of the ballasts are to provide a constant flexible vertical support; to assist in the correction of the track level and line to enhance constructability to fix the track in position longitudinally and laterally, and to the maintainability of the railway network (Esveld *et al.* 2001).

The secondary tasks of ballasts are to permit surface water to drain quickly, to prevent the growth of plants on the railway track, to damper noise levels and to reduce the likelihood of any fouling material on the track. Furthermore, the ballasts offer electrical insulation of one rail from the other and moderately influence the development of frost heave in cold climates and movement due to climate uncertainties (Papaelias *et al.* 2018).

2.3 Recycling of waste tyres

The number of vehicles on the roads is increasing yearly; scrap tyres are increasing by approximately one billion tyres per year (Li *et al.* 2014). Small vehicles normally go through a set of tyres every two years. Hence, there is a great number of waste tyres generated. The waste tyres are normally incinerated or dumped in landfills (Nadal *et al.* 2016).

Tyre combustion produces black smoke, which mostly contains two hazardous gases: sulfide of hydrogen and carbon. When one ton of coal is burned, it produces sulphur dioxide, 270 kg of soot, and 450 kg of poisonous gas (Malahova *et al.*, 2019). Furthermore, smoke released from combustion harms human organisms and our environment and contains toxic gases such as carbon monoxide, nitrogen oxides and volatile oxide (Vilcane *et al.,* 2019). The increase in the number of vehicles is a threat to our environment; hence recycling, the waste tyre is necessary to minimize air pollution. A study by Samsuri *et al.* (2010) states that disposable waste tyres require expensive and specialized machines to avoid environmental pollution. However, finding alternative use of waste types can be more economical.

Due to rubber particles having high elasticity due to low young modulus and high yield strain, as shown in a study by Norvez *et al.* (2016), they have several potential ends uses. The waste can be used as a chair, plant holder, rolling storage, decor tire swing, table and garden stairs. Furthermore, waste tyres can be us as playground climbers, rope courses, fillers, swings and sandal soles. In this current study, waste rubber tyres will be utilised as fillers to minimize the vibration of a composite sleeper.

A Study by Samsuri *et al.* (2010) states that rubber has characteristics of reducing vibration and damping properties. Furthermore, a study by Laidoudi *et al.* (2008) says that rubber particles have a better grip when wet and resist gas and water permeability. This could help the sleepers fabricated using rubber particles to maintain their mechanical properties. A study by the state that reinforced scrap rubber particles offers acceptable physical and mechanical properties to the composites. These properties could assist composites with this material to maintain its mechanical properties (Polgar *et al*. 2018).

Using scrap rubber as a filler in composites, concrete mixtures, and other matrices have become a fascinating subject for academics to explore. This interest is due to waste rubber-based goods having a lot of potentials to benefit various fields with minimal environment impact. Rubber waste recycling has proven beneficial in various applications, and the research is still ongoing. According to researchers, waste rubber might also be used as a reinforcing element in a polymer matrix or a rubber matrix. The composites with waste rubber reinforcement have acceptable mechanical and physical characteristics. Recycling discarded rubber into a new, sustainable material has had numerous sound effects, and research and studies in this sector are growing (Polgar *et al.* 2018).

2.4 Characterization of raw materials

The characterization of the raw materials is explained in the following subheading, which includes scanning electron microscope, sieve analysis and moisture absorption.

2.4.1 Scanning electron microscope (SEM)

The scanning electron microscope (SEM) is one of the most flexible equipments for examining and analyzing the morphology of microstructures and chemical composition characterizations. To comprehend the fundamentals of electron microscopy, one must first understand the basic concepts of light optics. The unaided eye can distinguish objects with a visual angle of around 1/60°, equal to a resolution of 0.1 mm (at a viewing distance of 25 cm). By widening the viewing angle with an optical lens, optical microscopy has a resolution limit of 2,000. Light microscopy has played an essential role in scientific research and continues to do so. Since the discovery in the 1890s that a magnetic field may deflect electrons in multiple experiments, electron microscopy has grown in popularity.

The acquisition of signals produced by electron beam and specimen interactions is required for image generation in the SEM. These encounters can be both positive and negative. Elastic and inelastic interactions are the two significant kinds of methods used (Zhou et al. 2007).

2.4.2 Particles size analysis

There are different methods of particle size analysis such as direct microscopy or optical microscopy, sieving method, sedimentation method, conductivity or coulter counter method and laser particle size analysis. This test method is generally used to determine the grade of materials being used as aggregates or recommended for use as aggregates. The findings are used to determine if the particle size distribution complies with applicable specification criteria and to give data for controlling the production of various aggregate products and combinations. The information could also help establish correlations between porosity and packing.

Sieve analysis is one of the most fundamental tests for determining the particle size of all powdered and granular materials. In the sugar refining industry, as well as many other sectors, sieve analyses are of paramount importance (Carpenter *et al.* 1950).

2.4.3 Moisture absorption

The water absorption test is used to determine the rate at which a composite material absorbs water by measuring the increase in size and weight of a specimen as a function of the time when the specimen is submerged in water. The ability of such specimens to absorb water is proportional to their permeability. Higher permeability can result in the initiation of a chemical reaction that could easily destroy the material, whereas low permeability can aid resistance to water, chloride ions, sulfate ions, alkali ions, and other harmful substances that could cause a chemical attack and reduce the durability of the material (Zong *et al*. 2014).

2.5 Fabrication process

Fabricating composite components can be done in a variety of ways. The materials, the part design, and the end-use or application all influence the fabrication process. There are different fabrication processes, namely hand lay-up, compression moulding, pultrusion, vacuum bagging, injection moulding, centrifugal casting, resin transfer moulding, spray lay-up, Filament Winding, and. braiding. Moulding is a technique for shaping resin and reinforcement. Before and during cure, a mould tool is necessary to shape the unformed resin/fibre combination. Hand layup is the most basic thermoset composite production method, which entails laying dry fabric layers, or "plies," or prepreg plies, by hand onto a tool to make a laminate stack. After the layup is finished, the resin is applied to the dry plies (e.g., by resin infusion).

There are several ways for curing available. The most basic method is allowing the cure to occur at ambient temperature. However, curing can be accelerated by using heat (usually from an oven) and pressure (through a vacuum). To cure conditions that need the use of an autoclave, many high-performance thermoset parts require heat and high consolidation pressure. Autoclaves are often costly to purchase and run, and manufacturers use autoclaves to cure a large number of items at the same time.

Computer systems monitor and control the autoclave's temperature, pressure, vacuum, and inert atmosphere, allowing for unattended and remote monitoring of the curing process and maximizing efficiency. The use of an electron beam (E-beam) as a curing method for thin laminates has been investigated. In E-beam curing, the composite layup is exposed to a stream of electrons that emit ionizing radiation, prompting radiation-sensitive resins to polymerize and crosslink. In a similar way, X-ray and microwave curing technologies work. UV curing is a fourth option that includes using UV light to activate a photo initiator added to a thermoset resin, which, once activated, initiates a crosslinking reaction. Light permeable resin and reinforcements are required for UV curing (Nagavally *et al.*, 2016).

In this study hand, the lay-up method will be used to fabricate composites due to its simplicity and lower cost.

2.6 Mechanical test of material

The mechanical tests explanation will be discussed in the following sub headings. The tests include tensile, compression, hardness and flexural strength testing and vibrational analyses.

2.6.1 Tensile testing

The tensile test is useful for determining a material's mechanical properties. The most extensively used test method is the tensile test. This test is used to determine material parameters. This test reveals basic material properties such as Poisson's ratio, elastic modulus, and toughness, which can be used to explain stress-strain curves (Sakthive *et al.,* 2013). Figure 2.21 shows how composite specimens are cut according to the ASTM D-638. The tensile strength of various hybrid composite plates can be determined using the Universal Testing Machine (UTM).

Figure 2.21 - Tensile specimen testing (Sakthive *et al.* 2013)

2.6.2 Compression testing

One of the quality control measures is the compressive strength test, which specifies the quantity or capacity of maximum load the material can bear before fracture. The test item, which can be of cubic, prism, and any other geometric shapes, is placed between two plates of the press and compressed. The test is carried out with the help of an Instron Universal Testing Machine (Ruzaidi *et al.,* 2013).

2.6.3 Flexural testing

The flexural test is used to determine the materials' flexural strength and/or flexural modulus (Oladele *et al.,* 2014). A flexural test involves placing the material horizontally on two supports and applying a force from the top until the material fails. The flexural strength of a material is defined as the greatest force recorded. The flexural test is significant because it addresses all three types of stresses: tensile, compressive, and shear. For any designer, the findings of this test are equally essential. As shown in Figure 2.22 (a), specimens were cut according to the ASTM D-790-10, and the flexural strength of various hybrid composite plates was determined using the Universal Testing Machine (UTM).

(a)

(b)

Figure 2.22 - Specimens for a flexural test (Oladele *et al.* 2014)

2.6.4 Hardness testing

The depth of perforation of an indentor is used to determine the hardness of material using Barcol hardness. According to the American Society for Testing and Materials, the hardness of all hybrid composite plates can be measured using a Barcol hardness tester following ASTM D 2583, a standard for testing materials.

2.6.5 Vibration testing

Vibration testing is used to evaluate product limits and tolerances. Every product is susceptible to vibration stresses, which might cause it to break or fail. Microprocessors and circuit boards are little items, while bridges and skyscrapers are examples of large constructions. There are different types of vibration testing, namely free vibrations, forced vibrations and damped Vibrations.TMR-211-01, a multi-recorder frequency processing library, was used to conduct the vibration test. The TMR-211 serves as the control centre for multiple input/output signals, collecting data, and supplying power. Furthermore, installing the frequency analysis program TMR-211-01 allows for real-time frequency analysis. A cantilever beam model conducted vibration tests of hybrid bagasse/E-glass fibre plates.

Figure 2.23 - Vibration experimental setup (Trivedi *et al.* 2018)

Figure 2.23 depicts the entire vibration test setup (a). The TMR-211 analyzer receives signals from an accelerometer mounted to plates and sent them to a computer. Figure 2.23 shows an accelerometer attached to a plate (b). Following the completion of the setup, the plate is given free vibration with a small force, and data recording begins. The rate of recording acceleration is pre-programmed in the software. In this scenario, 200 readings per second are used because they are sufficient for obtaining a satisfactory result. The following figures demonstrate the graphical output of a hybrid bagasse/E-glass polyester plate containing 3% bagasse fibre.

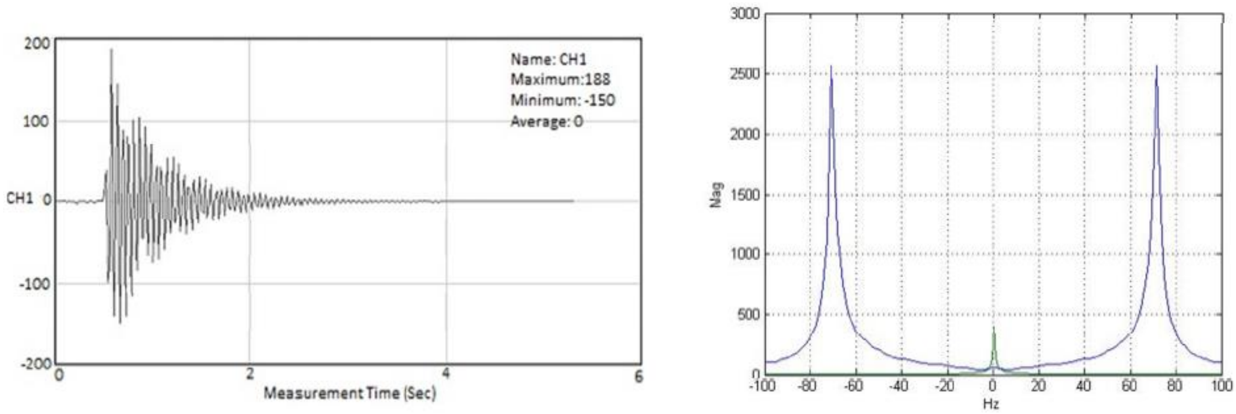

Figure 2.24 – Vibration signals from a hybrid composite (Trivedi *et al.* 2018)

Figure 2.24 shows the output of a multi-recorder in terms of magnitude vs time (a). Fast Fourier Transform is necessary to get the natural frequency from TMR-211-01 output. FFT is conducted in MATLAB, which produces the required \results as shown in Figure 2.24 (b) (b). This method was performed for all plates to determine each plate's natural frequency.

2.7 Existing knowledge gaps

Timber sleepers have a life span of fewer than 20 years and are easy to work with. Nevertheless, timber sleeper challenges that fail the sleeper are termite attack, end splitting and fungal decay. On the other hand, cutting down trees has negative effects on the ecosystems and environment. Suitable ways of replacing timber sleepers are essential. Steel sleepers have a life service of 50 years (Manalo et al. 2010) . However, steel sleeper has early failure due to several reasons. Salts from soil that come into contact with steel sleepers cause premature failure. The root cause of early failure and corrosion in steel sleepers are; ground water, metallic slag base-ballasts, moist environment or rain region and aggregates. Corrosive materials attached to the track system are also a threat. Measures that are used to minimize failure from sleeper are coat that is applied to steel

Although Concrete sleepers have a great compression strength of 51.2 MPa and 61.3 MPa at 7 and 28 days and are commonly used in railway sleepers, Concrete sleepers have low flexibility and elasticity. Major failures of concrete sleepers are longitudinal cracking and rail-seat deterioration. However, protective measures can be used to eliminate failures in concrete sleepers. The rail seat weakening can be eliminated by applying epoxy, using steel as reinforcement, adding fly ash on the surface of the rail seat or adding silica fume. Furthermore, using a combination of steel aggregates in the rail seat region, spread creates an abrasion-resilient pad that can strengthen the rails. Longitudinal cracking can be eliminated by presenting superior expansive concrete inside the bolt-hole region and placing traverse reinforcement bars to strengthen it transversely around the bolt hole.

Many different technologies have been developed as substitutes for timber sleepers but the durability and vibration damping capabilities of timber sleepers have not been satisfactorily met. Composite materials can be used to create a railway sleeper material with improved vibrational dampening properties while maintaining sound structural integrity.

CHAPTER 3: METHODOLOGY

3.0 Introduction

This chapter covers the methodology used to characterise raw materials used to fabricate the composite, including waste rubber tyre particles. After that, the fabrication method of the composite is outlined. The subsequent section presents the methodology used in the characterization of the mechanical and vibration properties of the composite. The last section presents the methods used to optimize the properties of the composite.

3.1 Conceptual framework

This research involved the characterization of raw materials, including rubber particles. Thereafter, the composite was fabricated using hand layup, as shown in the flow chart in Figure 3.1. Mechanical properties and vibration test was then carried out on the fabricated composites.

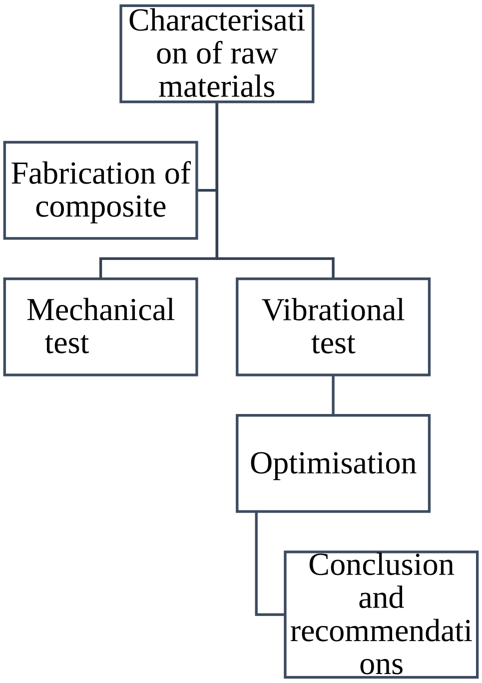

Figure 3.1 - Conceptual framework of the study

3.2 Characterization of rubber particles

The following sub-section shows the characterization tests carried out on the rubber particles, including sieve, moisture, and morphology analysis.

3.2.1 Particle size distribution test

Mathe Group, Kwazulu Natal branch supplied the waste tyre rubber particles tyres. Sieve analysis was carried out according to ASTM C 136-1 and ASTM E11 (Statements and Size 2007) to obtain a size of 150 and 300 µm to fabricate composites. Sieve of sizes of 600 µm, 425 µm, 300 µm, 150 µm and 75 µm were arranged from largest to smallest, with a pan placed at the bottom. The mass of rubber particles to be sieved was recorded using a digital scale to an accuracy of 0.01. The sieves were stacked on the shaker base, as shown in Figure 3.2. Rubber particle samples were then added to the top of the sieve using a scoop, and the sieve shaker was allowed to run for 15 minutes. After that, the rubber particles were quantified according to their particle size.

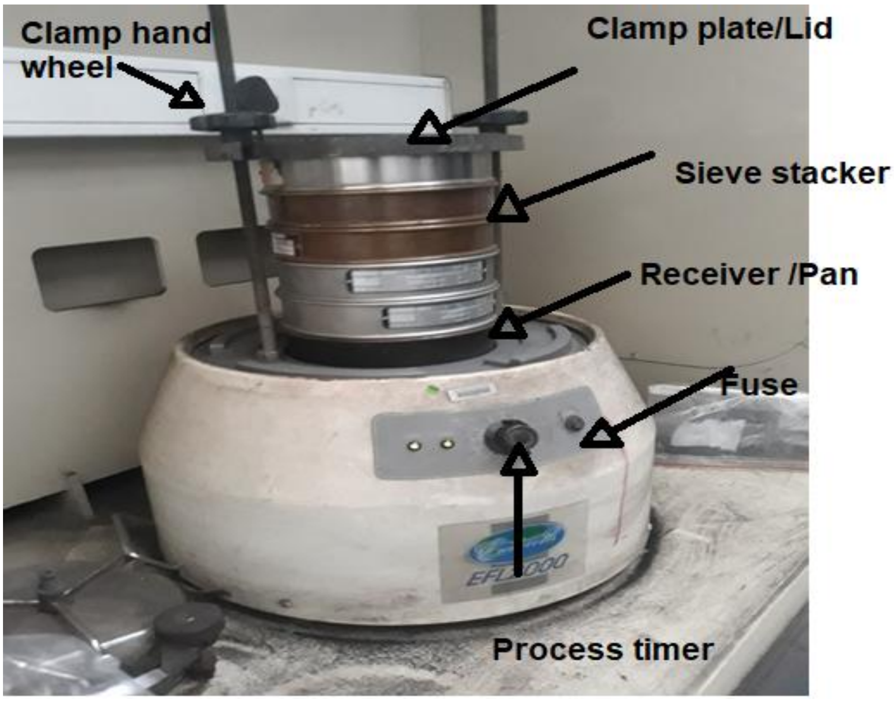

Figure 3.2 - Sieve shaker

Rubber particles of sizes 150 µm and 300 µm were selected to fabricate the composite of the current study sieves certificate shown in appendix A. Rubber particles of size 150 µm and 300 µm are rougher and have a larger specific area that could enhance the interfacial particle bond to the resin hence this were chosen in this study.

3.2.2 Moisture absorption test

Moisture absorption test of the rubber particles was done according to A0AC 930.15 (930.15 *et al.* 1999) to obtain moisture of rubber particles. An oven preheated to a temperature of 135°C was used to carry out the test. The temperature of the oven was monitored using a thermometer attached to the top of the oven, as shown in Figure 3.3. Borosilicate glass was placed inside the oven for 20 minutes at a temperature of 135°C to remove any residual moisture within the vessel.

- Oven (a) and desiccator (b)

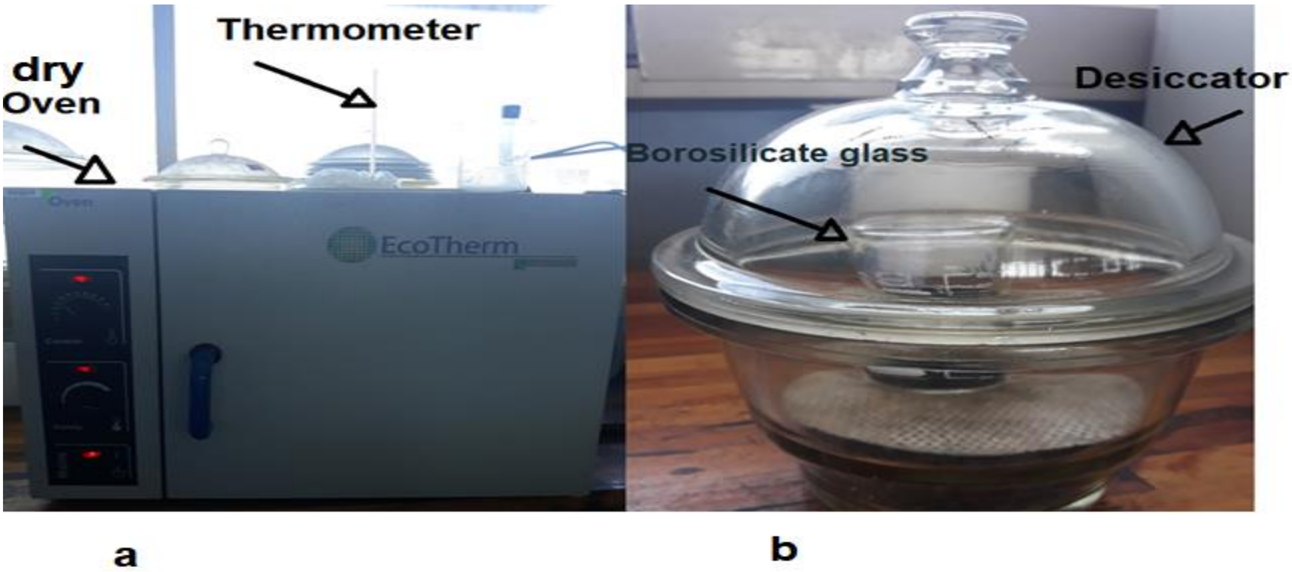

Figure 3.3 - Oven (a) and desiccator (b)

The borosilicate glass was then removed from the oven using metal tongs after 20 minutes and placed in a desiccator to cool off for 15 minutes. Thereafter, the borosilicate glass was placed on a scale as shown in Figure 3.4 this was done within a minute to avoid room moisture contamination. The weight of the dish was noted and recorded. A spatula was used to add 10g of rubber particles to the glass beaker. The rubber particles were then removed from the scale and sprinkled inside the borosilicate glass.

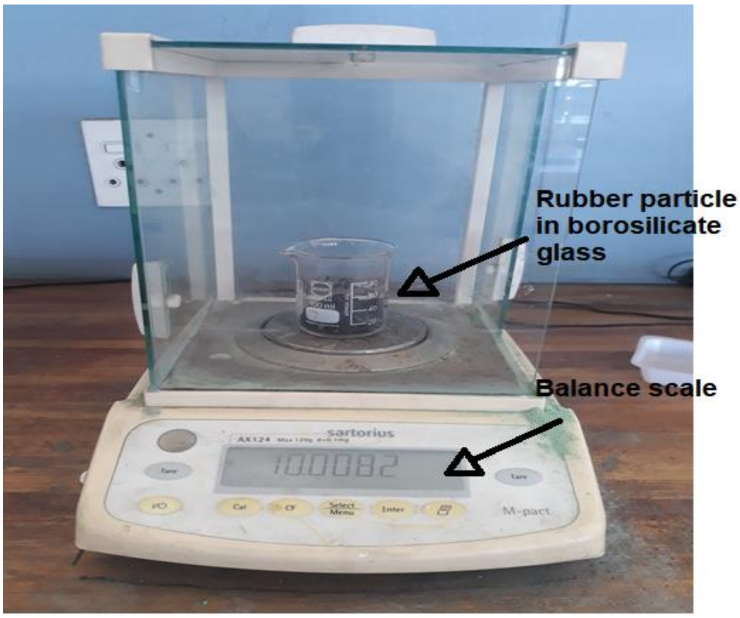

Figure 3.4 - Balance scale

The rubber particles were then placed in an oven for 2 hours and deposited in a desiccator to cool down. After the process of cooling, the rubber particles were measured again on a scale, and the mass was noted. This process was repeated three times until a constant mass was noted.

The moisture absorptions of the rubber particles were then calculated using equation 3.1.

$$Moisture = \frac{WS-(W2-W1)}{WS} X100 \qquad \{3.1\}$$

Where W_S mass of rubber particles (g), W_1 is the mass of rubber particles and borosilicate glass as combined in (g), and W_2 is the mass of the sample after being heated in an oven at a temperature of 135 ̊C until there was no change in (g) implying the sample was fully oven dry.

3.2.3 Scanning Electron Microscope analysis test.

Scanning Electron Microscope (SEM) morphology analysis of the rubber particles was carried out using SEM model number JSM IT500LA JEOL as shown in Figure 3.5. This test was conducted to determine the rubber particle morphology, lateral size features, roughness and topography. The morphology properties of rubber particles are attached in appendix D.

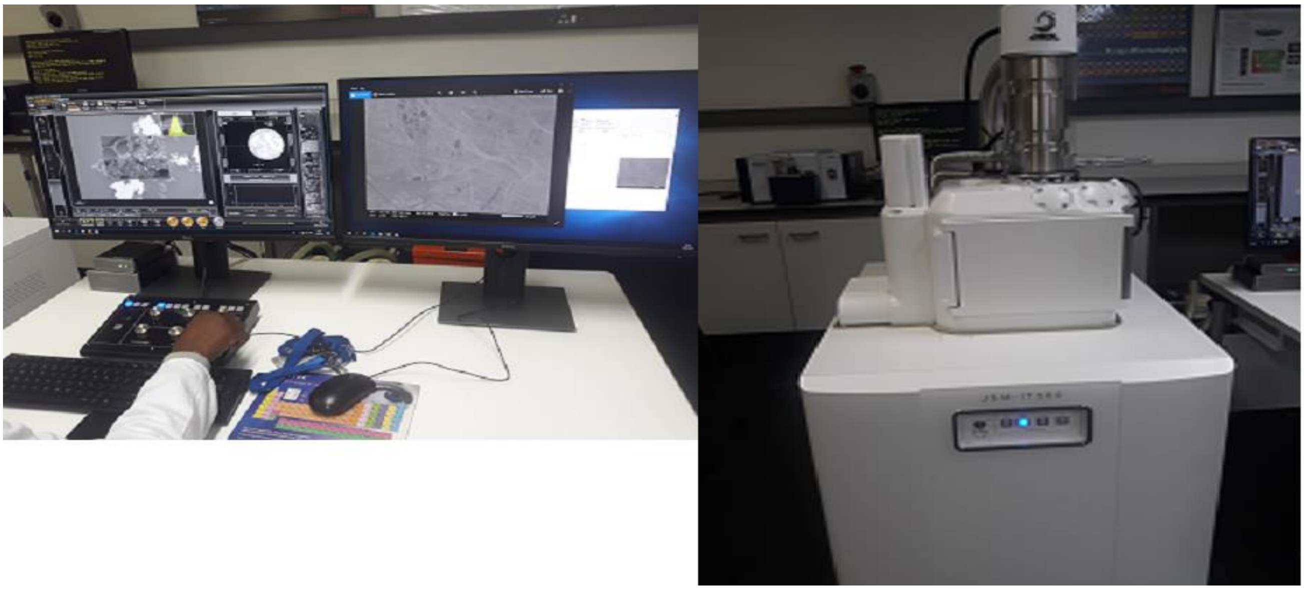

Figure 3.5 - JSM IT500LA JEOL SEM Scanning Microscope analysis

The rubber particles were placed on a sample holder and placed in the specimen chamber. The navigation flow to take a CCD image for zero mag software to enhance the image was used to view the image. The CCD image that was displayed in the image observation window was captured. The Zeromag software was used to locate the sample area, and the target was set. The software was used to zoom in. The optical image view changed to an SEM view automatically. The results were then saved on the external storage device.

3.3 Fabrication of the composites

The fabrication process of the composites was done using the hand layup method. The full factorial experimental design of the composites was done using Minitab V17 software. A full factorial experimental design was used with three factors and two levels. Fibreglass, rubber particles and polyester resin were used to fabricate the composite samples. A gel coat was applied to the surface of the mould in order to impact smoothness and aesthetically pleasant finishing. Figure 3.6 shows the materials and equipment that were used in fabricating the composite. The rubber particles used ranged from 5 - 20 %, the fibreglass ratio ranged from 5 - 8%, and the polyester resin ratio ranged between 72 - 90%.

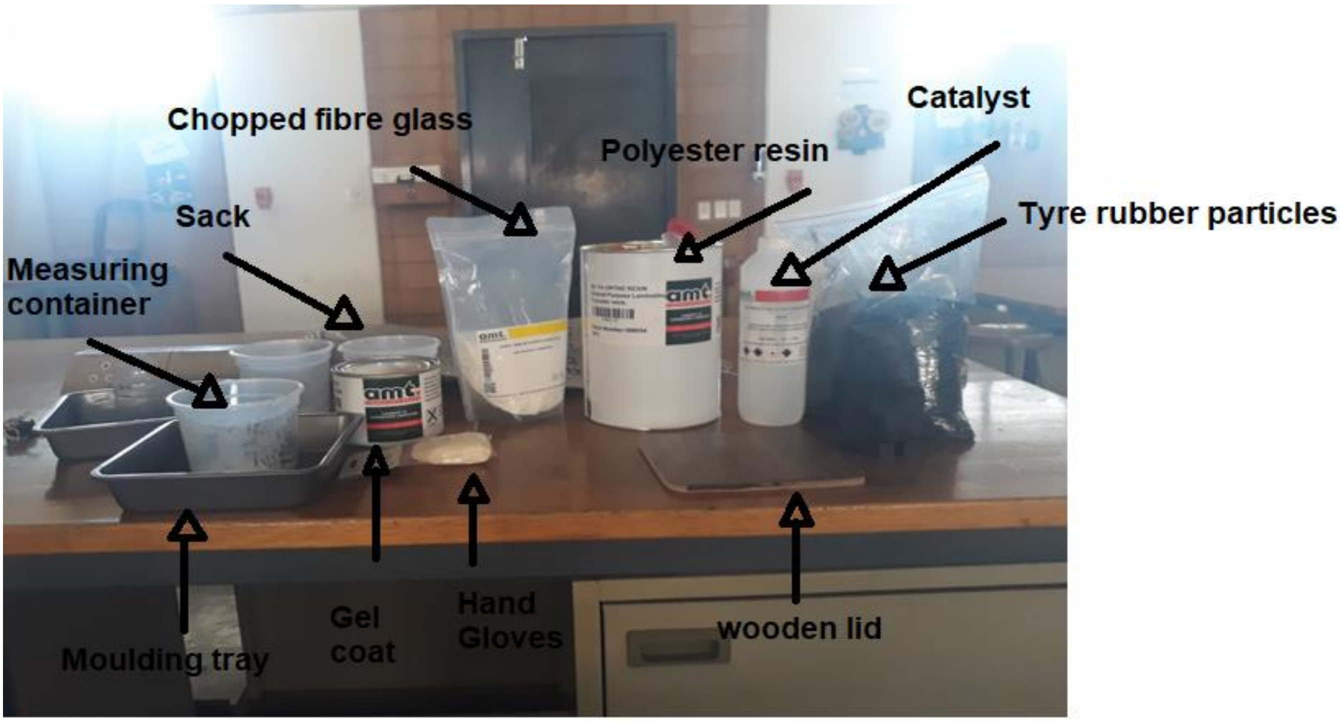

Figure 3.6 - Materials used in the fabrication of the composite

Moulding trays made of stainless steel of size 22,5 cm x 22,5 cm were used for the fabrication of the composites. The properties of polyester resin and fibreglass are attached in Appendix B and C.

3.3.1 Full Factorial Experimental design

Table 3.4 shows the experiment design that was used in the fabrication of the composite test specimens. In the fabrication of the composites, 150 μm and 300 μm rubber particle sizes were used. These rubber particles were added to the composites in accordance with the experimental design presented in table 3.1.

Table 3.1 - Showing the full factorial experimental design used in the composite fabrication

Run Order	Rubber particles (g)	Rubber particles Volume fraction (%)	Fibreglass (g)	Fibreglass Volume fraction (%)
1	0	0	0	0
2	0	0	20	5
3	0	0	24	6
4	0	0	28	7
5	0	0	32	8
6	20	5	0	0
7	20	5	20	5
8	20	5	24	6
9	20	5	28	7
10	20	5	32	8
11	40	10	0	0
12	40	10	20	5
13	40	10	24	6
14	40	10	28	7
15	40	10	32	8
16	60	15	0	0
17	60	15	20	5
18	60	15	24	6
19	60	15	28	7
20	60	15	32	8
21	80	20	0	0
22	80	20	20	5
23	80	20	24	6
24	80	20	28	7
25	80	20	32	8

3.3.2 Method of fabrication

The polyester resin was shaken before use to ensure that there was no liquefaction in the resin. Figure 3.7 shows the composite fabrication process. The polyester resin was then mixed with a 2% MERK catalyst thereafter, the fibreglass and rubber particles were measured using an analytical scale in accordance with the experimental design in table 3.1.

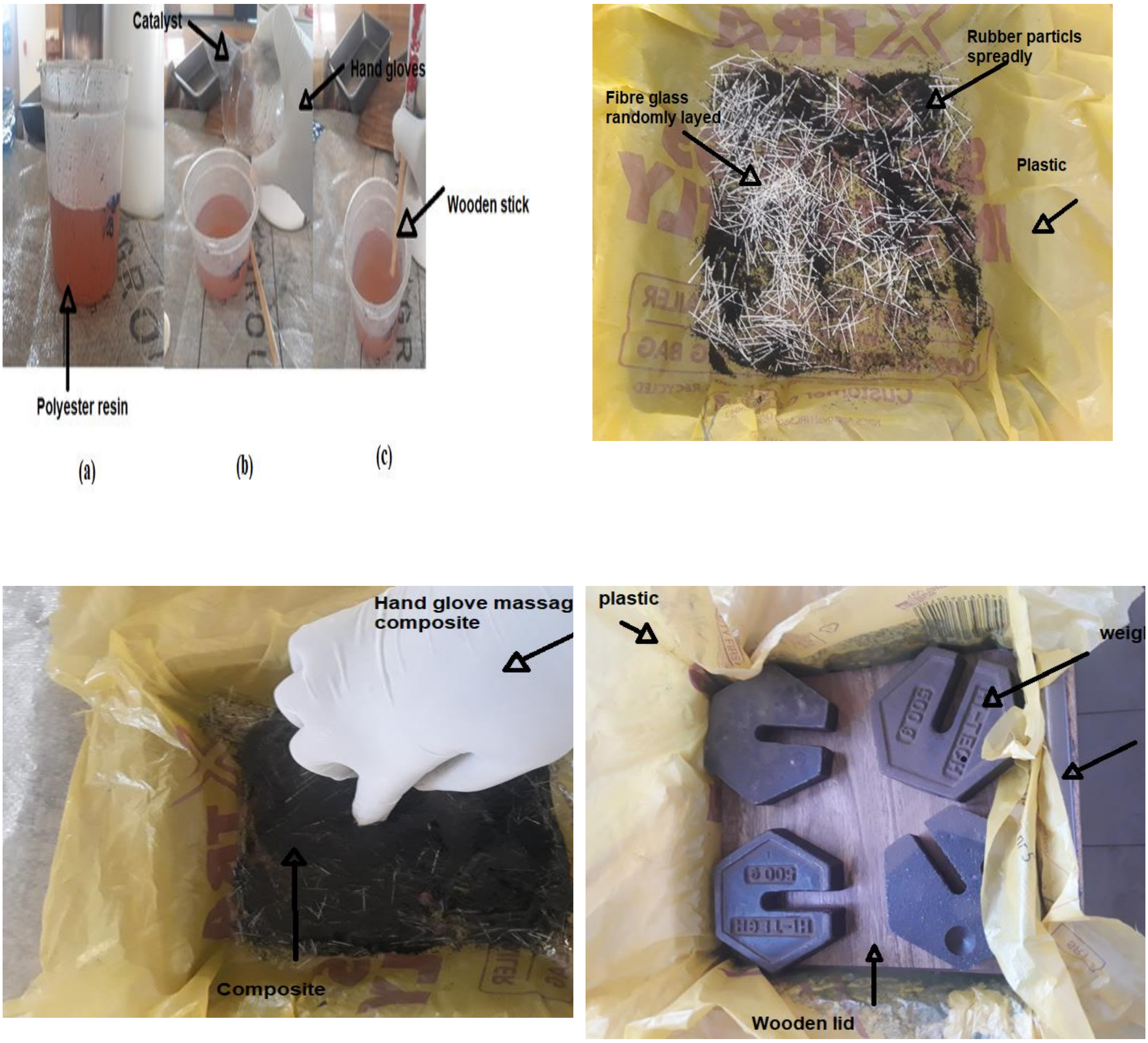

Figure 3.7 - (a) Process of fabrication of composites (b) (c) (d)

In order to make the de-moulding of the composite easier, a plastic release film was placed inside of the moulding tray, as shown in Figure 3.7. The hand layup process for composite formation included placing a fibreglass mat and then adding and evenly distributing the rubber particles in the moulding tray. The polyester resin was poured into the moulding tray, submerging the fibreglass and rubber particles and spread evenly using a rubber roller. The mixture was also kneaded to ensure uniform resin distribution, as shown in Figure 3.6. Fibreglass and rubber particles were progressively added to build laminate thickness, and this process was repeated until the desired thickness was attained. A wooden lid with a mould release film covering it was then placed over the composite mould, ensuring that there were no trapped air pockets Weights of 500 g each were placed on top of the lid to build pressure to consolidate the composite.

The composite was given 24 hours to cure in the lab at a temperature of 23^0C.Catalyst speed up chemical reaction of resin and add heat hence trmperature of 23^0C must be maintain to avoid boiling point that might form voids inside the composite. After the curing period, the composite was de-moulded, giving composite boards as shown in Figure 3.8.

Figure 3.8 - Fabricated composites

3.3.3 Cutting of composite

CREO software was used to plot the cutting pattern for the various samples necessary for testing. The samples were then precision cut using an electric saw with a blade of a diameter of 230 mm in preparation for mechanical and vibration tests.

3.4 Characterization of composite

Mechanical and vibration tests were carried out to characterize the fabricated composite.

3.4.1 Mechanical characterization

The mechanical tests included hardness, tensile, compression and flexural strength.

3.4.1.1 Tensile strength test

The tensile strength test was conducted in accordance with ASTM D3518/D3518M-18 (D 3518 2007), which uses a specimen size of 250 mm long and 25 mm wide, having an unsupported (gauge) length of 150 mm when installed in the fixture. The universal testing machine INSTRON model 3369, shown in Figure 3.9, was used to conduct the tensile test.

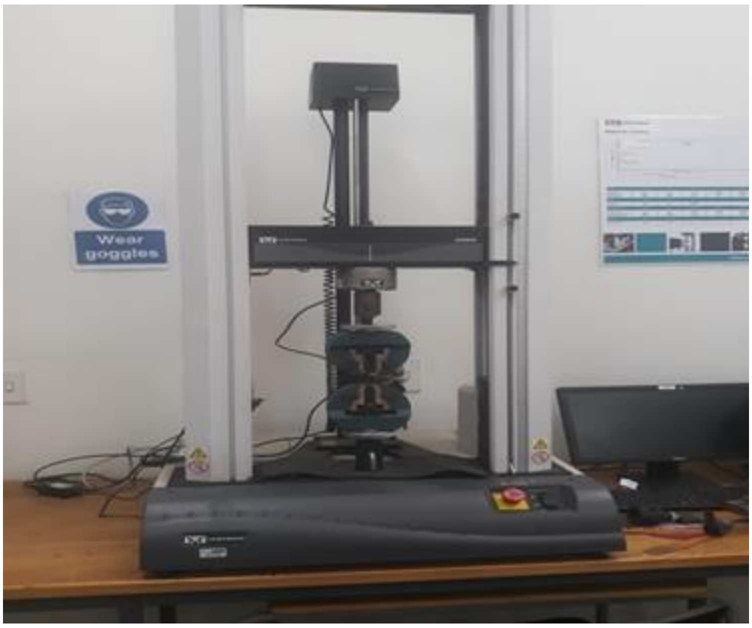

Figure 3.9 - UTM Equipment for tensile Test

The jaws suited for the tensile strength test were attached to the universal testing machine. The INSTRON Blue hill software version 3.65 was used to set up and adjust the machine's working parameters and to control the function of the universal testing machine. The machine gauge length was set with sliding electronic limit switches. A Static load cell of 5 kN was used to conduct the test. The machine was operated at a continuous speed of 5 mm/s, and a gauge length of 150 mm was used. The specimen was held in place by means of jaw grips, as shown in Figure 3.10, and the machine zeroed before running the test.

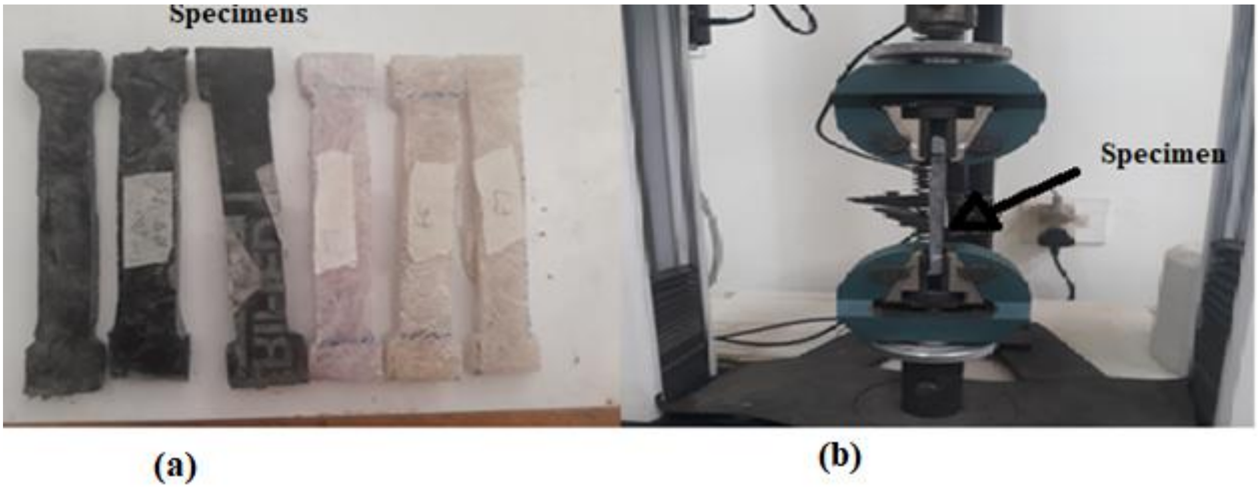

Figure 3.10 - (a) Specimens preparation for tensile strength test (b) specimens in the jaw of UTM

The tensile test was run until the specimen snapped, and the universal testing machine automatically stopped. After each test run, the UTM machine was returned to its home position in preparation for the next test.

3.4.1.2 Compressive strength test

Flexural strength test was done at the Vaal University of Technology, metallurgy Lab main campus Vanderbijlpark. The specimen test was conducted in accordance with ASTM D3410/D3410M (ASTM D3410 2014), which uses a specimen size of 140 mm long and 13 mm wide, having an unsupported gauge length of 13 mm when installed in the fixture. The universal testing machine INSTRON model 3369, shown in Figure 3.11, was used to conduct the compression strength test.

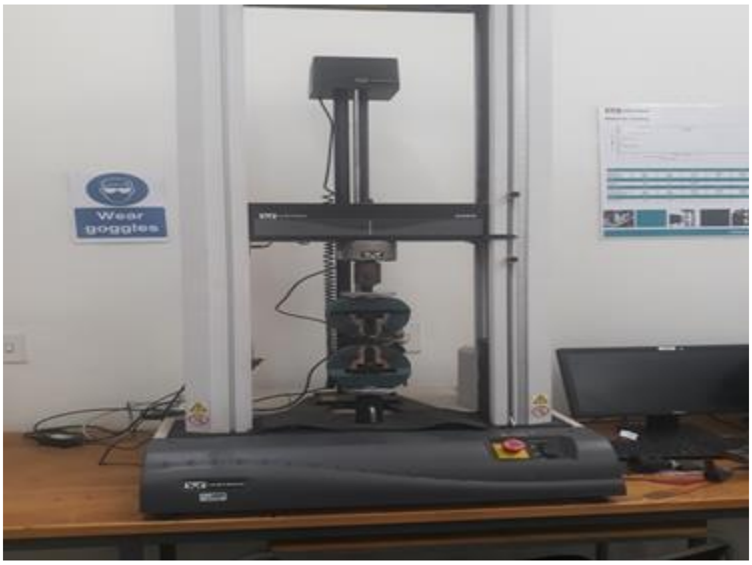

Figure 3.11 – UTM Equipment for compression Test

The grips for the compressive strength test were attached to the universal testing machine. The machine gauge length of 13 mm was set with sliding electronic limit switches. A Static load cell of 5 kN was used to conduct the test, and the machine was operated at a continuous speed of 5 mm/s. The specimen was then placed in the grips and tightened, as shown in Figure 3.12 (b), and the machine zeroed before running the test.

(a) (b)

Figure 3.12 - (a) Specimens preparation for compression strength test (b) specimen in the grips of UTM

The compressive test was run until the specimen was completely crushed, and the universal testing machine automatically stopped. After each test run, the UTM machine was returned to its home position in preparation for the next test. The compressive strength of the composites material was calculated according to equation 4

$$C = \frac{F}{A} \qquad \{3.2\}$$

Where C is compression strength (MPa), F is applied force (N), and A is the area (m^2)

3.4.1.3 Flexural strength test

Flexural strength test was done at the Vaal University of Technology, metallurgy Lab main campus Vanderbijlpark. The flexural strength test was conducted in accordance with ASTM D8058-19 (ASTM D8058-19 2019). A Universal Testing Machine, INSTRON model 3369, was used to conduct the flexural tests. Three-point bending tests were carried out in accordance with the ASTM standard, as shown in Figure 3.13.

Figure 3.13 - UTM Testing Flexural strength

The three-point flexural strength test attachment was mounted on the universal testing machine. The machine gauge length was set at 120 mm with sliding electronic limit switches. A Static load cell of 5kN was used to conduct the test at a continuous speed of 5 mm/s. The flexural strength specimens with dimensions of 160 mm x 40 mm were placed on the supports, as shown in Figure 3.14.

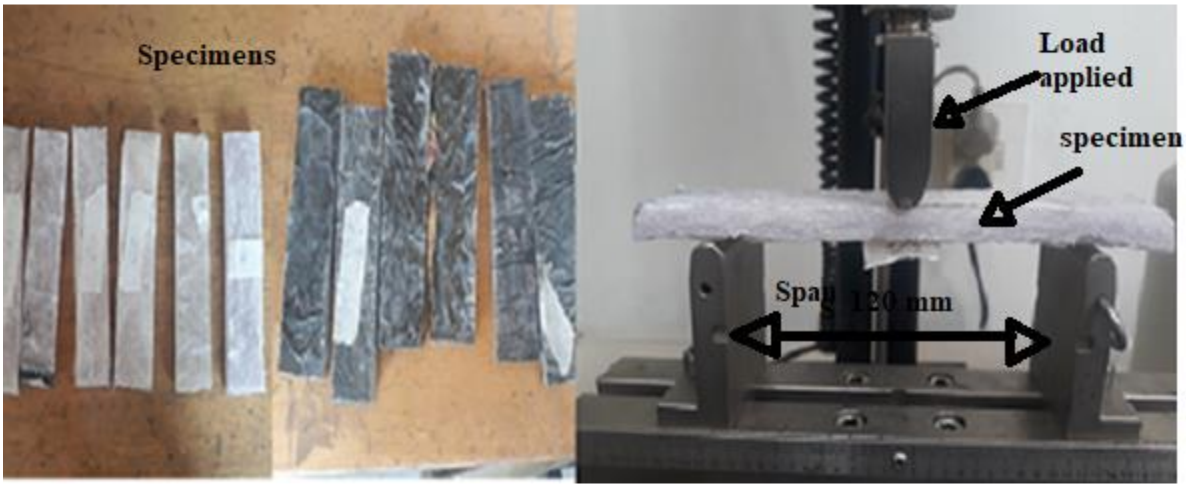

Figure 3.14 - (a) Specimens preparation for flexural strength test (b) flexural test arrangement

The flexural strength test was run until the specimen completely failed, and the machine stopped when the resistive force had fallen below 20 N. After the test run, the UTM machine was returned to its home position in preparation for the next test. The flexural strength was calculated for each specimen using equation 3.3

$$R = \frac{3PL}{2bd^2} \qquad \{3.3\}$$

Where R is the flexural strength of the specimen (MPa), P is the breaking load of the specimen (N), L is the length of span (mm),b is the width of the specimen (mm), and d is average thickness specimen (mm).

3.4.1.4 Hardness test

The composite hardness was measured using a model Time 5330 hardness tester shown in Figure 3.15. The test method used was based on the dynamic rebound principle, and the test was carried out in accordance with ASTM A-956 (ASTM A-956 1998).

Figure 3.15 - Portable hardness tester

A hacksaw was used to cut the specimens to appropriate dimensions, and subsequently, sanding papers of grit A80, A120 and A320 were used to polish the composites to obtain a flat surface. The hardness tester was switched on, and the impact device was placed on the testing block for calibration. The specimen was positioned on the stage of the hardness tester as shown in Figure 3.16, and the impact probe was placed vertical to the specimen, and then the plunger was released. The test was repeated 4 times in accordance with the standard at various points on the sample.

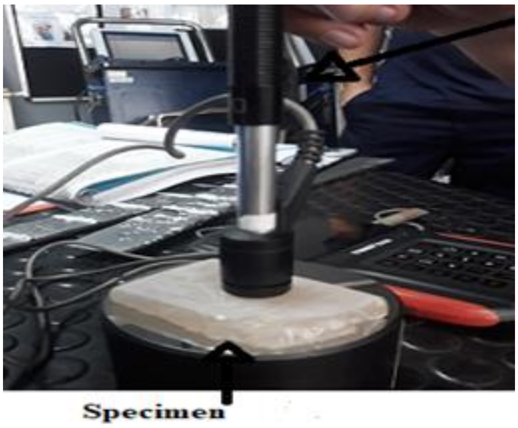

Figure 3.16 - Test preparation for hardness test

3.4.2 Vibration test analysis

The composite vibration test was carried out using a shaker table, as shown in Figure 3.18. This test was conducted according to the ASTM E756 standard (ASTM E756 2009). This test method measures the loss factor, young modulus or shear modulus, and vibration properties of materials and is accurate over a frequency range of 50 to 5000 Hz over the useful temperature range of materials. The vibration specimens with dimensions of 140 mm x 14 mm x 5 mm, as shown in Figure 3.17, were used for the vibration tests.

Figure 3.17 - Specimen preparation for vibration and damping test

The vibration specimens test setup is shown in Figure 3.18. The base of the cantilever beam was clamped over a length of 20 mm, with 120 mm free to vibrate in the air. There are a number of ways in which to measure the damping characteristics of a material. In this case the testing consisted of clamping a beam specimen on a steel base on a vibrating table, in such a way that the test sample acts as a simple cantilever, as shown in the sketch and photograph in the Figure 3.18. The principle of the test was then to apply a vertical vibration spectrum to the fixed end and measuring the responsive vibration at the free end of the beam. Accelerometers were used to determine the vibration spectra, one at the fixed end to measure the input vibration spectrum, and another at the free end of the beam.

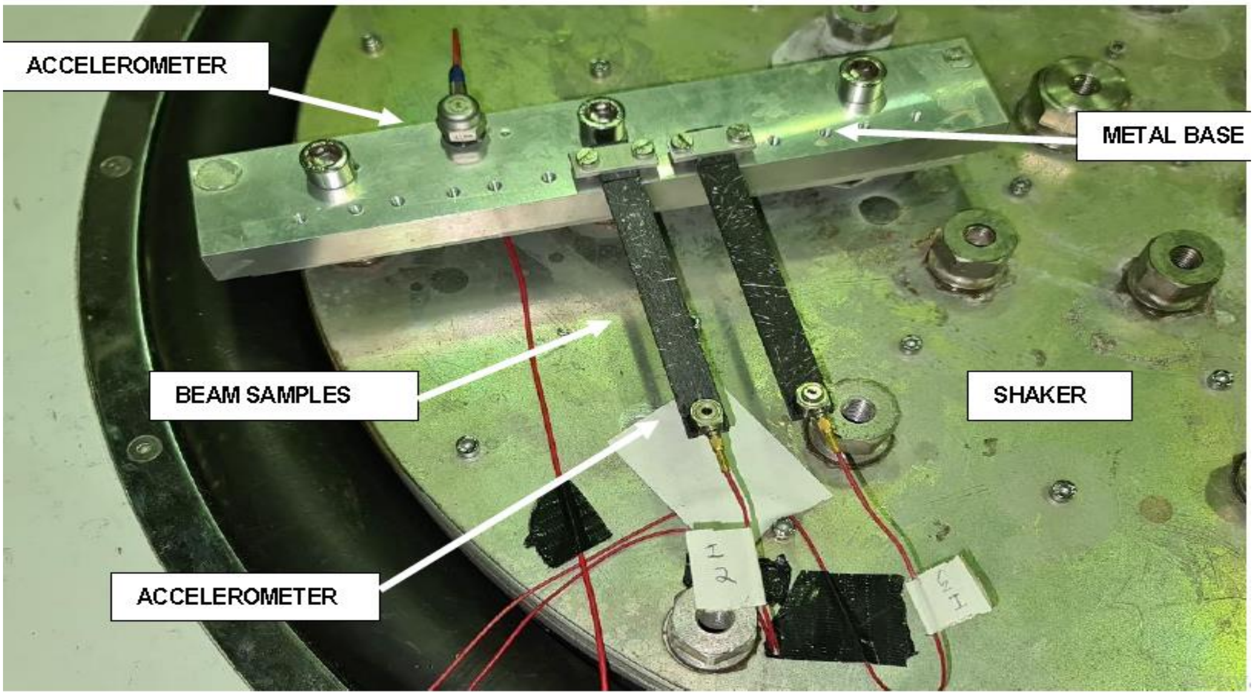

Figure 3.18 - Vibration and damping test set up

The metal bases were securely bolted to the shaker table, and the individual test specimens were clamped tightly to the metal base. The specimens were clamped onto the steel base on the vibrating table, so the test specimen acted as a simple cantilever, as shown in Figure 3.18. The principle of the test was to apply a vertical vibration spectrum to the fixed end and then measure the responsive vibration at the free end of the specimen. An accelerometer was used to determine the vibration spectra, with one at the fixed end to measure the input vibration spectrum and the other at the free end of the specimen.

3.4.2.1 Vibration specimen modelling

Finite element analysis using CAD software was used in the vibration analysis. This model was done to determine the optimum vibration spectrum to be used and the expected outcome. The following were made E (young's modulus) = 3.3 GPa , ν (Poison ratio) = 0.35 and ρ (Density) = 1150 kg/m^3 for this analysis to see which amplification peaks to expect. The parameters were based on typical resin materials properties, as the literature ascertained. The model was built with an infinite element method and hexahedrons , as shown in Figure 3.19.

The model was developed using finite element Software where a three-dimensional model was selected and the modal vibrational. After that, nodes were selected and inserted together with the dimensions of the specimen. Using the tools element button, all points that appeared on the screen were connected respectively. After that, the element face was selected. Under Tools, the element refine tool was selected to convert it to a quadratic element. Under default setting, new materials were inserted, young modulus, thickness, poison ratio and density of specimen were inserted. Then left edge of 20 mm was selected and fixed.

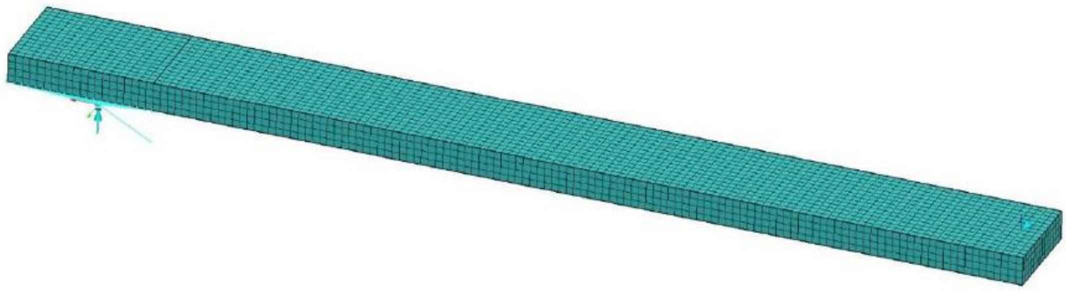

Figure 3.19 - Computing modelled beam, clamped over a length of 20mm (on the left)

The amplification (Q) was determined from the acceleration at the beam's free end versus the input acceleration. In this case, the input acceleration Z (input) was kept at a constant 1 Z. In this case, the amplification was determined because Z (output) is equal to Z (input), and equation 3.4 was used to calculate the critical damping (ζ):

$$\varsigma = \frac{1}{2 \times Q} \quad (Dimensionless) \qquad \{3.4\}$$

Structural damping (G) was then calculated using equation 3.5

$$G = 2 \times \varsigma \ (Dimensionless) \qquad \{3.5\}$$

Critical damping, as well as structural damping, were used to compare the vibration properties of the different composite mix designs.

3.5 Modeling process

The optimization process was carried out using Minitab software version 17.1.0. The full experimental design factors shown in section 3.2.1 were used in the software and obtained results to optimize, as shown in Figure 3.20.

Minitab - Minitab optimazation.MPJ - [Worksheet 1 ***]

File Edit Data Calc Stat Graph Editor Tools Window Help Assistant

↓	C1	C2	C3	C4	C5	C6	C7	C8	C9
	Rubber particles Volume fractio	Fibre glass Volume fraction (%)	Particle size	Tensile strength	Compression strength	Flexural strength	Hardness	Damping	
1	0	0	0	7.50	*	*	*	0.050	
2	0	5	150	7.98	40.004	27.513	592	0.061	
3	0	6	150	8.01	42.051	34.341	622	0.071	
4	0	7	150	9.17	49.414	39.159	745	0.077	
5	0	8	150	12.13	55.164	42.658	622	0.089	
6	5	0	150	8.27	20.300	20.369	648	0.077	
7	5	5	150	8.98	41.258	32.856	568	0.103	
8	5	6	150	9.18	44.346	34.785	593	0.103	
9	5	7	150	10.83	33.485	38.275	640	0.105	
10	5	8	150	13.63	31.305	42.219	759	0.118	
11	10	0	150	8.86	24.547	19.835	566	0.105	
12	10	5	150	8.02	33.857	26.608	623	0.146	
13	10	6	150	13.58	39.183	34.329	645	0.155	
14	10	7	150	13.34	33.287	36.771	608	0.158	
15	10	8	150	12.08	30.749	23.382	561	0.192	
16	15	0	150	7.90	16.363	15.300	538	0.111	
17	15	5	150	7.21	26.497	23.515	622	0.121	
18	15	6	150	9.18	29.792	24.407	576	0.141	
19	15	7	150	9.95	22.611	27.242	504	0.162	
20	15	8	150	14.23	21.152	21.715	661	0.162	
21	20	0	150	5.67	23.346	12.600	659	0.162	
22	20	5	150	4.87	7.987	9.414	695	0.172	
23	20	6	150	10.67	13.835	21.975	656	0.213	
24	20	7	150	10.18	12.528	23.722	639	0.220	

Figure 3.20 – Optimization process

The following steps were used on Minitab software to optimize Statistics then the design of the experiment (DOE) was selected. Response surface and Response optimiser were then selected, respectively. The maximise target values were then selected, as shown in Table 3.2, for the optimisation process.

Table 3.2 - The target response outputs

Property	Optimum
Tensile strength	Maximise
Flexural strength	Maximise
Compressive strength	Maximise
Vibrational damping	Maximise

All the parameters were set at maximum in order to obtain the best possible mechanical strength as well as vibrational damping.

3.5.1 Optimization process

The optimization analysis process was carried out using an overlaid counter plot to show optimum regions for all responses. Numerical optimization was carried out to determine the specific composite composition. The numerical optimization was carried out after inputting the target response outputs. The following steps were used to get optimum results Statistics. Then Response surface was selected.Thereafter Overlaid contour plot graph was selected to identify the optimum region on the plot. The responses were then selected and the contours defined.

3.5.2 Model validation

The Model validation process was carried out by running experimental tests on the optimum composite composition computed from the ANOVA software developed numeric model. The composite was fabricated using an optimum ratio of rubber particles volume fraction, particle size and fibreglass volume fraction. The experiment characterization results, which included the mechanical and vibrational results, were then statically compared with those obtained from the model to validate the model's fit to experimental data.

Chapter 4: Results and Discussion

4.0 Introduction

This chapter consists of three main sections. The first section, 4.1, covers the analysis of the raw material characterization results. The second section, 4.2, discusses the mechanical and vibration results of the fabricated composites. The last section, 4.3, focuses on developing a model to optimize the mechanical and vibrational properties of the fabricated composite railway sleeper.

4.1 Characterization of rubber particles

The rubber particle characterization results, including SEM morphology results, particle size and moisture analysis, are discussed in the subsequent subsections.

4.1.1 Particle size analysis

Sieve analysis was carried out on the rubber particle sample to obtain 150 and 300 µm rubber particle sizes Figure 4.1 presents the particle size distribution results obtained from sieve analysis.

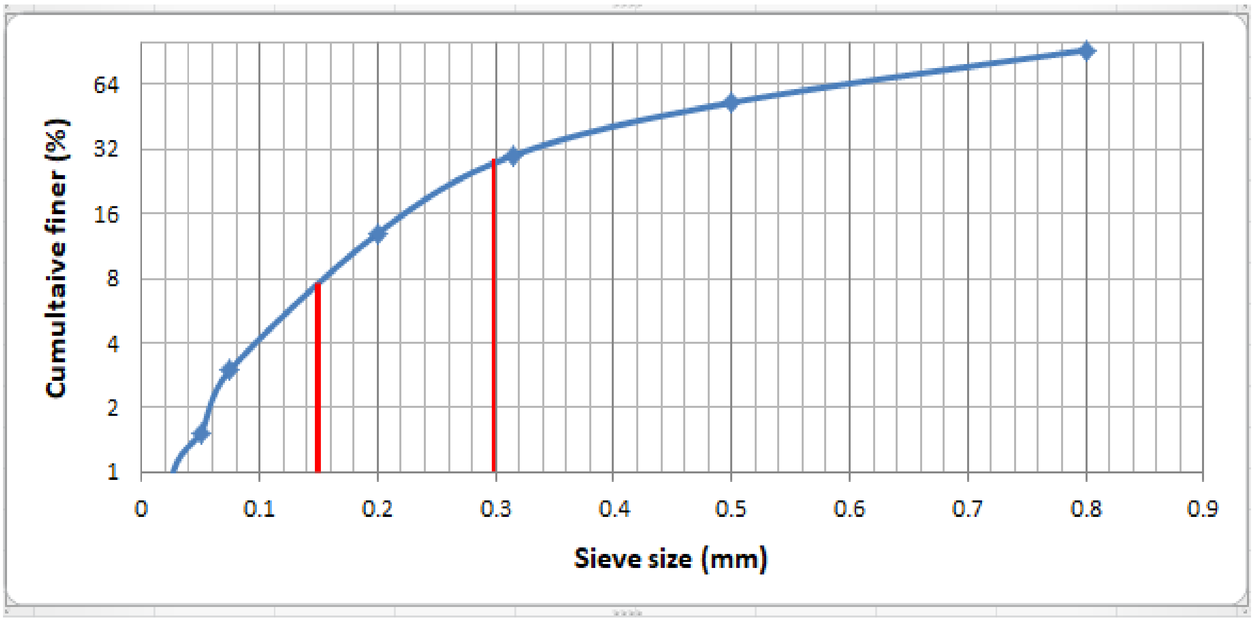

Figure 4.1 - Rubber particle size distribution

Figure 4.1 presents a general trend in the volume fraction of rubber particles with an increase in the sieve size. The cumulative finer increased by 93% from particle size 0 to 0.8 mm. Rubber particles are hard to mill due to their inherent toughness and elasticity. Rubber particles tend to expand and shrink when in contact with the grinding meshing gears making it extremely difficult to grind very fine rubber particles of less than 75 µm. Hence, the results in Figure 4.1 indicate that the milling machine produced higher volume fraction of rubber particles greater than 75 µm. It was also observed during the sieving process that rubber particles tend to stick in the sieve mesh pores due to the expansion and shrinkage of the rubber. Rubber particles of 150 and 300 were selected to fabricate composite.

Fabricating composites using rubber particles that are less than 300 µm has numerous advantages as was reported by Wang *et al.* (2014). A study by Wang *et al.* (2014) concluded that rubber particles exceeding 300 µm are normally inefficiently dispersed within the composite, resulting in low mechanical strength properties. Fabricating composites using smaller rubber particles of sizes less than 300 µm is advantageous because smaller particles are rougher and have a larger specific area that could enhance the interfacial particle bond to the resin. This current study selected rubber particle sizes of 150 µm and 300 µm to fabricate the composites. It was essential to use different sizes of rubber particles for optimization of composite and to identify particle size influence.

4.1.2 Moisture absorption properties of rubber particles

Figure 4.2 presents the moisture absorption over time of the rubber particle samples.

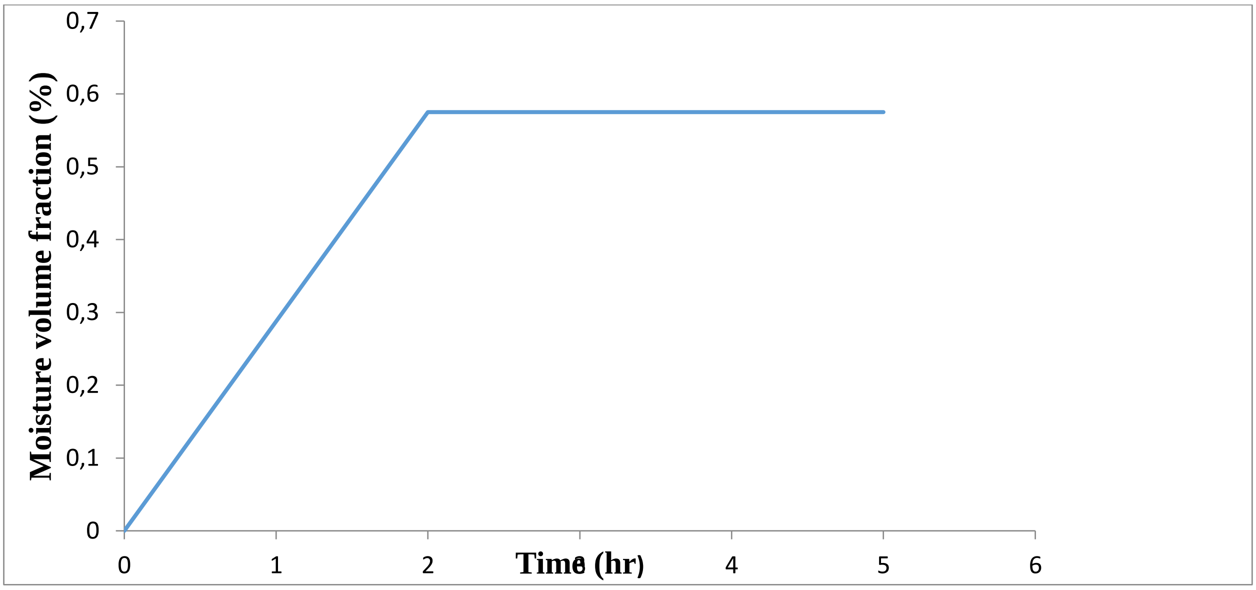

Figure 4.2 - Moisture absorption analysis of rubber particles

Figure 4.2 shows a general increasing trend in the water absorption of rubber particles over time up to 2 hours. Maximum moisture absorption of 0.575% was recorded after 2 hours at a temperature of 135^{0}C. The low moisture absorption of the rubber particles effectively classifies them as low hydrophilic (Abdul *et al.* 2016). The moisture absorption affinity of rubber particles directly correlates to the quantity of resin absorbed by the particles. The moisture absorption was necessary for developing a working polyester resin-to-rubber particle mix ratio.

Railway sleeper composites are subjected to harsh operating conditions, which include frequently being in contact with or submerged in water. The low moisture absorption recorded of the rubber particles will help prevent swelling of the railway sleeper, which could alter its dimensional stability. Furthermore, polymer composites are generally susceptible to environmental attack from the water. Water that ingresses into the composite can encourage the development of cracks and ultimately lead to catastrophic failure of the composite material (Shohag et al. 2017). Moreover, composites that absorb water can suffer compounded effects of environmental damage from both the water volume fraction and Ultraviolet (UV) effects expatiating the damage (Awuchi *et al.* 2021).

Railway sleepers are subjected to numerous spills, which can include oils and chemicals from the cargo or from the trains' internal mechanical components if there is a leak. Low moisture absorption, as recorded in this study, can aid in avoiding chemical absorption into the composites, which can cause them to fail prematurely. A survey carried out by Zong *et al.* (2014) reported that low moisture absorption of the rubber particle filler in composites could aid in resistance to chemical ingress into the composite. Chemicals such as chloride ions, alkali ions and sulfate ions can react with polyester resin, effectively lowering its mechanical strength through a chemical process of bond scission (Tikish *et al.,* 2021).

4.1.3 SEM analysis results

SEM analysis was carried out on the rubber particles to determine their morphology, lateral size and roughness, as shown in Figure 4.3.

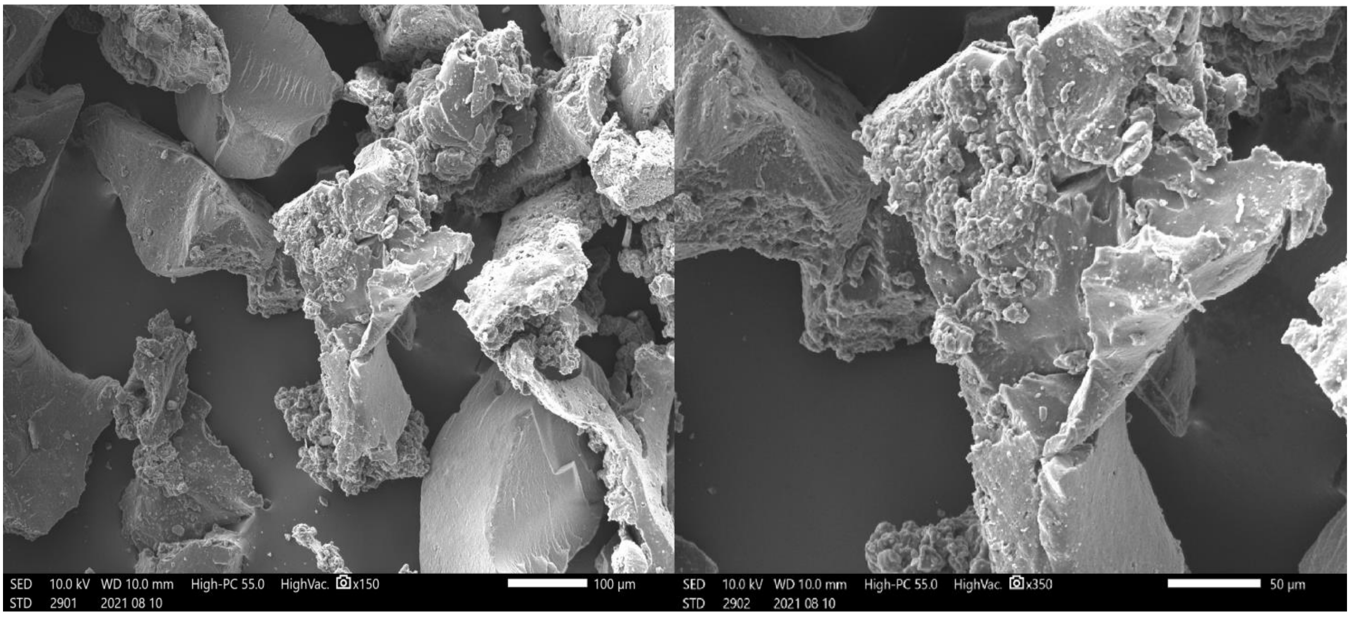

Figure 4.3 - SEM images of rubber particles

When observed under SEM, the rubber particles showed a heterogeneous appearance, with the surface of the particles being rough, elongated, and porous. The rubber particles were observed to consist of particles having varying sizes making it difficult to approximate the specific size of the particles. The rubber particles milling machine is responsible for the heterogeneous shape of the rubber particles.

A smooth surface on the rubber particles helps with workability during fabrication. However, a rougher rubber particle surface, as observed in Figure 4.3, helps to build a strong bond between the resin and filler, increasing the mechanical strength of the composite. Hence, the roughness observed on the surface of the rubber particles is expected to increase the mechanical strength of the composite material made from these particles. This rough morphology will assist in improving the interfacial bond strength with the matrix of the composite (Rodrigue *et al.*, (2021).

4.1.3.1 Chemical composition analysis

The chemical composition of the rubber particles was carried out using EDS as an attachment on the SEM machine, and the results obtained are as shown in Figure 4.4.

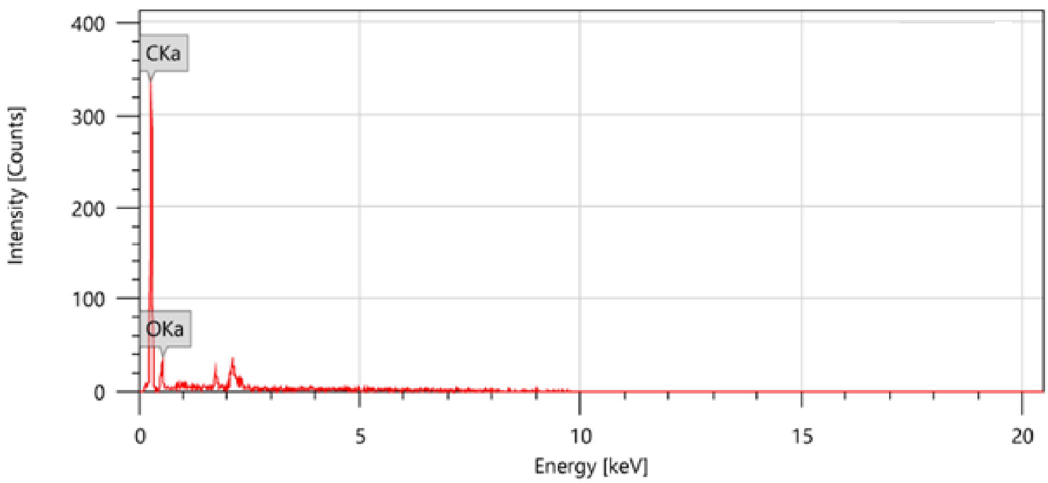

Figure 4.4 - EDS spectra of rubber particles

The EDS analysis shows the predominant elements in the rubber particles sample to contain C (Carbon) and O (Oxygen). The Ka indicated in Figure 4.4 is the wavelength used to obtain elements within the particles. The intensity of CKa (Carbon K alpha) is 350, and for Oka (Oxygen K alpha) is 40 at the energy level for both carbon and oxygen below 1 KeV (Kilo electron volt). CKa (Carbon K alpha) and Oka (Oxygen K alpha) There are some trace elements of impurities in the rubber particles indicated by the minor peaks at 2.4KeV and 2.6KeV, which would warrant further investigation with XRD (X-ray diffraction). The vulcanization process of the rubber could have caused these impurities during tyre manufacture.

Table 4.1 - Showing EDS report on elements of the rubber particles

Element	**Line**	**Mass%**	**Atom%**
C	K	82.49±0.83	86.26 ± 0.87
O	K	17.51±1.16	17.00 ±0.91
Total		100	100

The rubber particles contain 82.49 ± 0.83 % of carbon and 17.51 ± 1.16% oxygen elements, as shown by the EDS report in Table 4.1. The observed results are consistent with those obtained by Formela *et al.* (2014), who studied and characterized waste tyre rubber particles. The carbon helps trap heat and energy received from the sun, which could help with the chemical reaction of rubber particles and resin. The high carbon volume fraction in the rubber particles is expected to give it high mechanical strength (Formela *et al.* 2014).

The presence of oxygen in the rubber particles could assist in marginally protecting the composites from harmful ultraviolet rays (Inagaki *et al.,* 2009).

4.2 Mechanical Properties of Composite

This section discusses the composite mechanical characterization results for tensile strength, compression strength, flexural strength and hardness properties. The fibre ratio of 0 – 8% and rubber particles of 0- 20% are adopted in this study. Control samples of fibreglass and rubber particles are adopted in this study to isolate the experimental effect. Furthermore, without control samples, the experiments are less clear and misleading.

4.2.1 Tensile strength properties

This section analyses the composite tensile strength results in accordance with the experimental design of the study.

4.2.1.1 Effects of fibreglass on the tensile strength of the composite.

Figure 4.5 presents the effects of fibreglass volume fraction on the composite tensile strength.

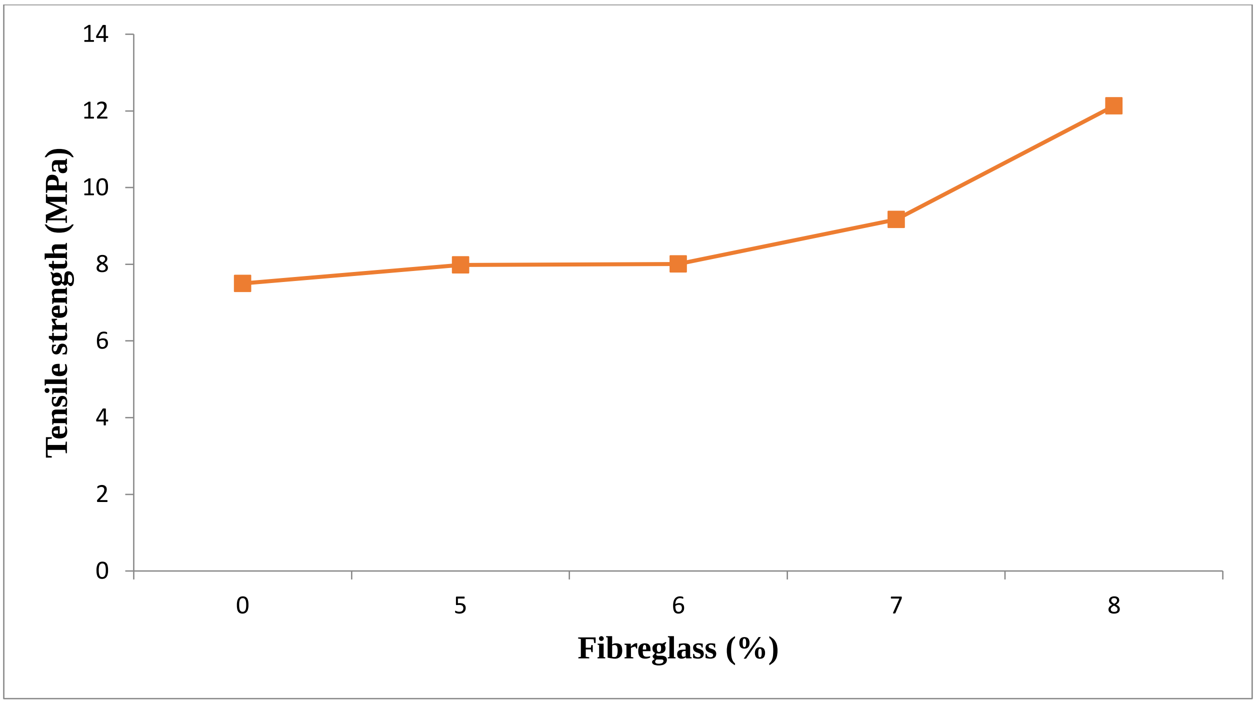

Figure 4.5 - Effect of fibreglass volume fraction on the tensile strength of the composite

Figure 4.5 presents a general increasing trend in the tensile strength of the composite with an increase in the fibreglass volume faction. The graph shows an increase in tensile strength from 6.71 MPa to 12.13 MPa with an increase in fibreglass volume fraction of 5 to 8%, respectively. An overall tensile strength gain of 38% was realized with an 8% fibreglass volume fraction compared to the control sample.

The results in Figure 4.5 suggest that a higher fibreglass volume fraction must be used in the composites as the tensile strength increases with the increase in reinforcing fibreglass volume fraction. Low fibreglass volume fractions of less than 5% do not give adequate reinforcement. The dominant tensile strength failure mode at low fibreglass volume fraction less than 5% is largely fibre breakage and matrix cracking. However, when fibreglass volume fraction was increased to greater than 8%, the dominant failure mode was fibre pull out and fibre breakage. This failure mode could be attributed to fibres tending to take up the bulk of the tensile forces before failure resulted in matrix cracking and propagation of cracks.

4.2.1.2 Effects of rubber particles on the tensile strength of the composite

Figure 4.6 presents the effects on composite tensile strength of rubber particles of sizes 150 and 300 µm.

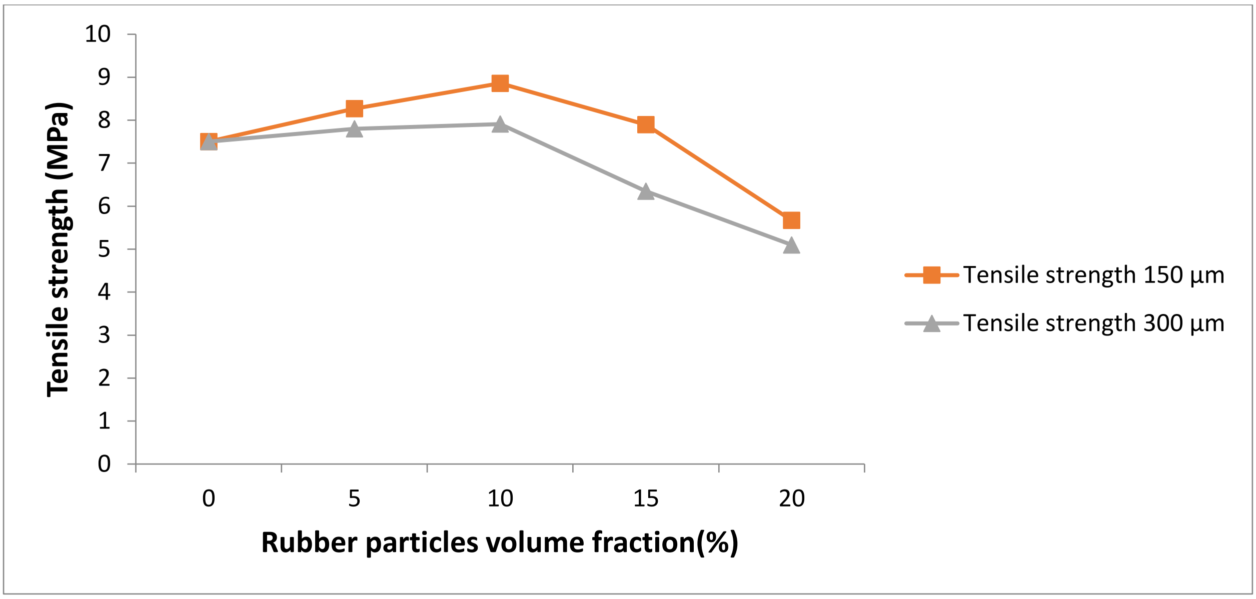

Figure 4.6 - Effect of rubber particles on tensile strength

Figure 4.6 presents that the addition of rubber particles had an adverse effect on the tensile strength of the composite for 150 µm rubber particles. The initial strength at 5% rubber particle loading is 8.27 MPa. As the volume fraction increases to 10%, there is a marginal increase in tensile strength to 8.86 MPa. However, any further addition of rubber particles resulted in a decrease in tensile strength. This is seen with a 15% rubber particle volume fraction giving tensile strength of 7.90 MPa. Further increase in rubber particle volume fraction to 20% gave tensile strength of 5.67 MPa.

Rubber particle sizes of 300 µm gave an initial strength at a 5% volume fraction of 7.80 MPa, as shown in Figure 4.6. As the rubber particle volume fraction increased to 10%, there was a marginal increase in tensile strength to 7.91 MPa. However, any further addition of rubber particles resulted in a decrease in tensile strength. This is seen with a 15% rubber particles volume fraction giving a strength of 6.35 MPa. Further increase in volume fraction to 20% gave tensile strength of 5.10 MPa.

The 150 µm rubber particle results show that increased rubber particle volume fraction decreases the composites' tensile strength. The results obtained for composite tensile strength are consistent with a study by Abu-jdayil *et al.* (2016). They concluded that increasing rubber particle volume fraction in composites reduces its tensile strength. The highest tensile strength of the composite is realized at a low volume fraction of rubber particles, less than 5%. This phenomenon can be attributed to the even distribution of the rubber particles at lower volume fractions, minimising voids' formation. The results for 300 µm rubber particles show that an increase in rubber particles' volume fraction lowers the tensile strength of the composites in a similar trend to the 150 µm rubber particles. The composites containing 20% rubber particles were observed to contain voids, as shown in Figure 4.7. The presence of the voids could be attributed to the poor dispersal of rubber particles within the composite. Therefore, the use of rubber particles alone as the filler material is not feasibly at percentages exceeding 15%. Figure 4.7 presents the primary mode of composite failure observed in composites containing only rubber particles.

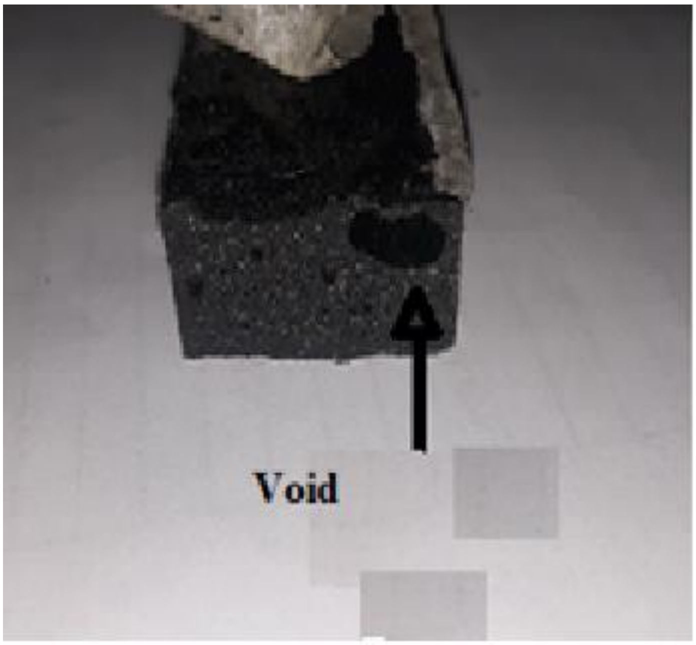

Figure 4.7 - Failure mode of a composite containing rubber particles only

This research work aligns with the study by Hisham *et al.* (2011), who reported that an increase in rubber particle volume fraction reduces tensile strength. The workability during fabrication of the composite was easier at a low volume fraction of rubber particles. Furthermore, composite cutting was easier for these specimens. The composites containing higher rubber particle volume fraction greater than 15% did not cure quickly and took an excess of 48 hours to reach acceptable hardness.

The results obtained in this study align with the research by Wang *et al*. (2019), who reported that the smaller the size of rubber particles used, the higher the composite tensile strength. This analogy is attributed to the even dispersion possible with finer rubber particles compared to coarser rubber particles. Furthermore, finer rubber particles have a larger surface area resulting in enhanced interfacial bonds with the polyester resin.

Even though rubber particles of size greater than300 µm can significantly improve the damping properties of the composite in comparison to rubber particles less than150 µm, the tensile strength of coarser rubber particles would be adversely affected.

4.2.1.3 Effect of combination of rubber particles and glass fibre on composite tensile strength

The graph in Figure 4.8 presents the effect on the tensile strength of a hybrid composite consisting of rubber particles and glass fibres.

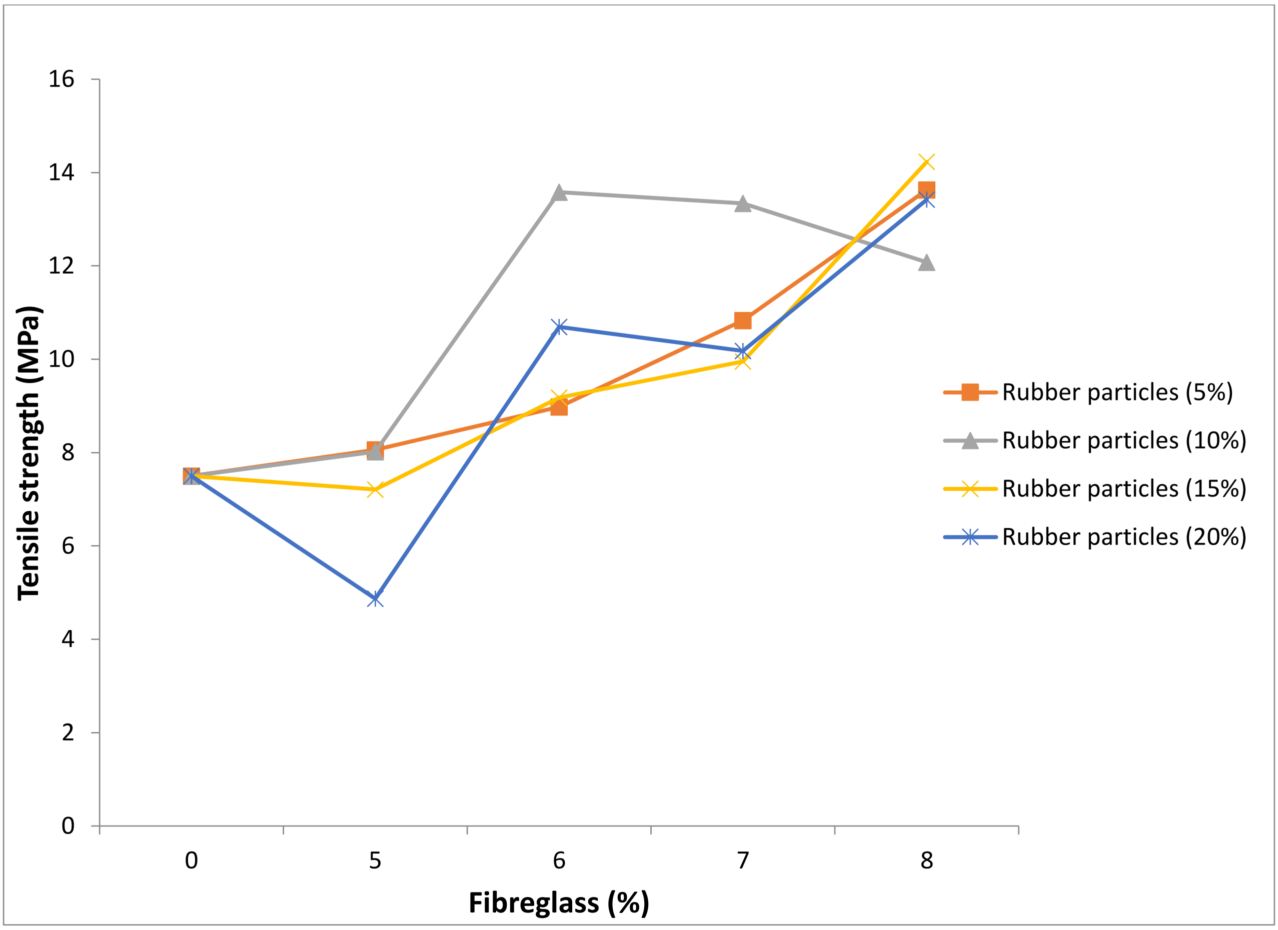

Figure 4.8 - Effect of 150 µm rubber particles and glass fibre on tensile strength of composite

Figure 4.8 shows that an increase in fibreglass volume fraction positively affects the tensile strength regardless of the rubber particle volume fraction. The tensile strength of 5% rubber particle volume fraction increased from 8 MPa to 14 MPa with an increase in fibreglass volume fraction from 5 to 8 %. The tensile strength of rubber particles with a 10 % volume fraction increased from 8 MPa to 14.5 MPa when fibreglass volume fraction was increased from 5 to 8 %. The tensile strength of composite containing 15 % rubber particle volume fraction increased from 7 MPa to 13.5 MPa when fibreglass volume fraction was increased from 5 to 8 %.

The graph in Figure 4.9 presents the effects that a hybrid composite consisting of 300 µm rubber particles and glass fibres has on tensile strength

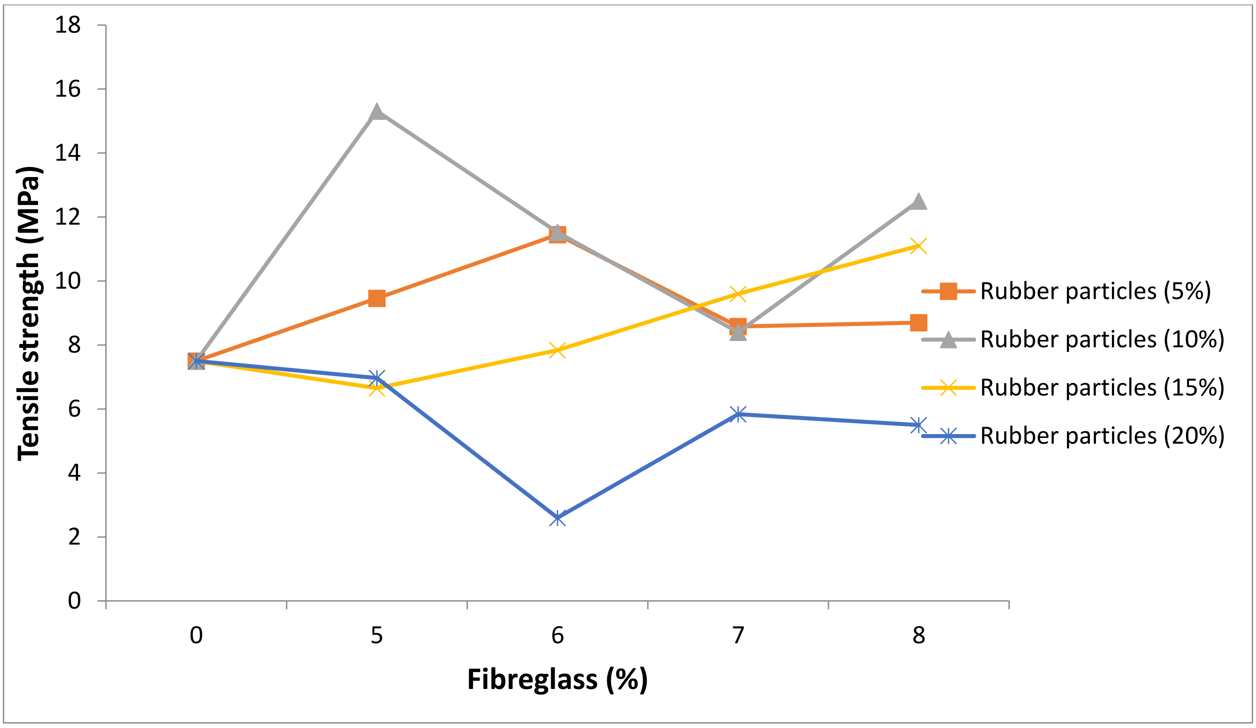

Figure 4.9 - Tensile strength of 300 µm particles at various fibre volume fractions

Figure 4.9 presents that the tensile strength of composite containing 5% rubber particles increases when fibreglass volume fraction of 5 to 6% is used, then drops from 6 to 8% of fibreglass volume fraction. The results indicate that the tensile strength of composites with a rubber volume fraction of 10 % reduces when adding fibreglass volume fraction of 5 to 7% and rises from 7 to 8%. The results indicate that the tensile strength of composites with a rubber volume fraction of 15% increases after adding fibreglass volume fraction of 5 to 8%.

The tensile strength decreases from 10 MPa to 6 MPa because of an increase in the volume fraction of fibreglass. The tensile strength of fibreglass decreases by 40 % with an increase in fibreglass from 5% to 8%. The tensile strength of 150 µm rubber particle composite with 5% loading improved from 8.2 MPa to 14 MPa when 6% fibreglass loading was incorporated, ranging from 5 - 8%. The tensile strength of 150 µm rubber particle with a 10% loading improved from 9 MPa to 13.9 MPa when fibreglass was incorporated, ranging from 5 - 8%. Tensile strength of 150 µm rubber particles at 15% composite loading improved from 8 MPa to 14.2 MPa when fibreglass was incorporated, ranging from 5 - 8%. Tensile strength of 150 µm rubber particle size with a volume fraction of 20% improved from 5.8 MPa to 13.5 MPa when fibreglass was incorporated, ranging from 5 - 8%.

The tensile strength of composite consisting of 300 µm rubber particles at 5% loading improved from 7.5 MPa to 11.5 MPa when fibreglass was incorporated, ranging from 5 - 8%. Tensile strength of 300 µm rubber particle size with volume fraction of 10 % improved from 8 MPa to13.9 MPa when fibreglass was incorporated. Tensile strength of 300 µm rubber particle size at 15% loading improved from 6.2 MPa to 14.2 MPa when fibreglass was incorporated, ranging from 5 - 8%. Tensile strength of 300 µm rubber particle size with a volume fraction of 20% improved from 5 MPa to 6.9 MPa when fibreglass was incorporated, ranging from 5 - 8%.

Figure 4.8 and Figure 4.9 show that increase in rubber particle volume fraction regardless of particle size has an adverse effect on the composite tensile strength. This phenomenon can be attributed to the low inherent tensile strength of the rubber particles.

Figure 4.10 shows the failure mode of the hybrid composite containing rubber particles and fibreglass reinforcement. The dominant failure modes for composites contain 5 - 15% rubber particles and 5 – 8% fibreglass volume fraction of fibre breakage. However, matrix cracking is observed in the dominant composite failure mode when the rubber particles' volume fraction is increased to 20%. When the fibreglass volume fraction is increased to 8%, the interfacial bond of the fibre to the polyester resin is weak due to the poor dispersal of fibreglass. This results in fibre pull out, fibre breakage and matric breakage.

Figure 4.10 - Failure mode of composites

A study by Lim *et al.* (2021) stated that the tensile strength of a plastic sleeper is 4.94 MPa and the highest recorded tensile strength in this study is 15.3 MPa. The tensile strength of the current study is three times that of plastic recorded by Lim et al. (2021). Furthermore, heating can re-hardened composite sleepers made of thermoplastic materials when cooled and softened by heating, and a reversible process can influence the change of mechanical properties.

The fabricated composites showed better tensile strengths when compared with concrete sleepers, which have a tensile strength of 6.5 MPa. However, the tensile strength of the concrete is negatively impacted, as noted with this fabricated composite.

4.2.2 Compression strength properties

This section analyses the composite compression strength results in accordance with the experimental design of the study.

4.2.2.1 Effects of fibreglass on the compression strength of the composite.

Figure 4.11 presents the effects of fibreglass volume fraction on the composite compressive strength.

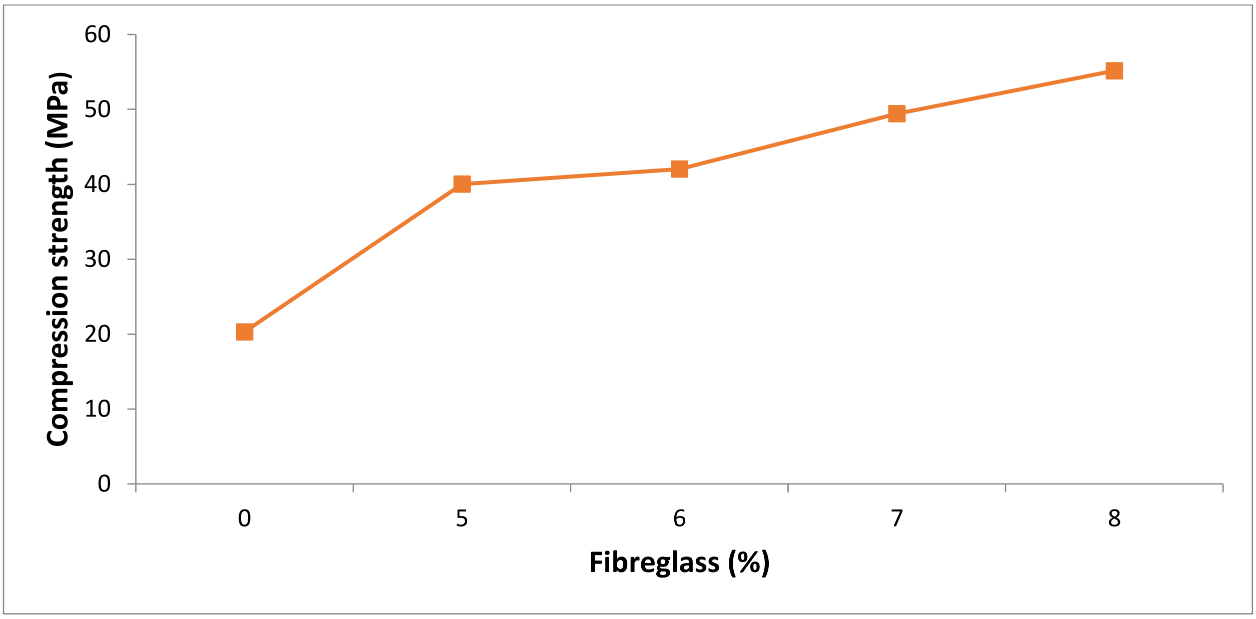

Figure 4.11 - Effects of fibreglass volume fraction on the compression strength of the composite

Figure 4.11 presents a general trend in the compression strength with an increase in the fibreglass volume faction. The graph shows an increase in compression strength from 20.30 MPa to 55.16 MPa with fibreglass volume fractions of 0 to 8%, respectively. There is an increase in compressive strength between 0 and 8% fibreglass volume fraction. An overall compression strength gain of 63% was realized with an 8% fibreglass volume fraction compared to the control sample.

The increase in compressive strength with progressive increment in fibreglass volume fraction can be attributed to hybrid composite increasing strength due to the interfacial bond between fibres and polyester.

The results observed in this study are consistent with research by Prema *et al.* (2020) and Srivastava *et al.* (1991). They both reported that an increase in fibreglass volume fraction also increases the composite compression strength. It was observed that fibreglass volume fraction greater than 5% gave even fibre distribution resulting in a composite with acceptable compressive strength.

4.2.2.2 Effects of rubber particles on the compression strength of the composite

Figure 4.12 presents the effects on compression strength of rubber particles of sizes 150 and 300 μm.

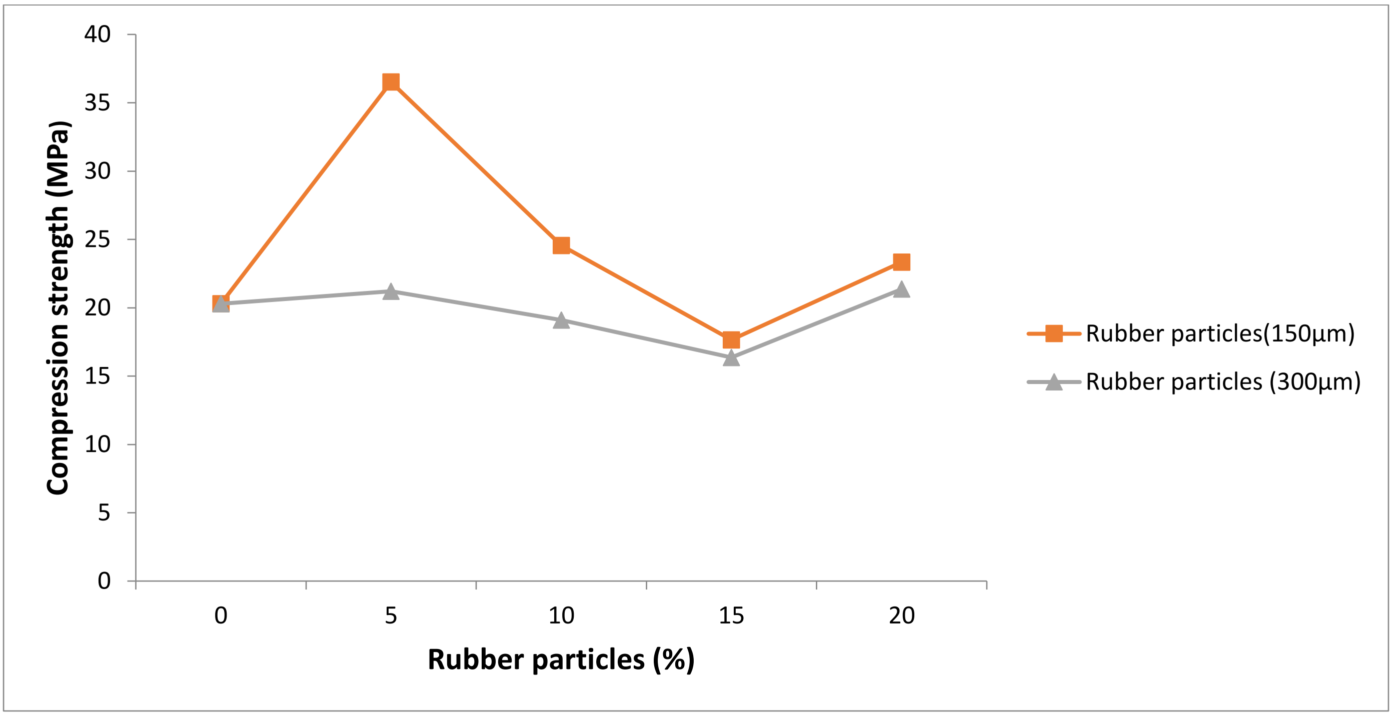

Figure 4.12 - Effects of rubber particles on composite compression strength

Figure 4.12 presents that for 150 μm rubber particles, the initial composite compressive strength at 5% rubber particle loading is 36.52 MPa. As the rubber particle volume fraction increased to 10%, there was a marginal decrease in compression strength to 24.55 MPa. Furthermore, any further addition of rubber particles resulted in a reduction of composite compression strength. As observed with 15% rubber particles, the volume fraction gives the strength of 16.36 MPa. Further increase in rubber particle volume fraction to 20% showed an increase in compression strength to 23.35 MPa.

Rubber particle sizes of 300 μm gave initial compression strength at 5% of 21.208 MPa. As the particle volume fraction increased to 10%, there was a marginal decrease in compression strength to 19.09 MPa. Furthermore, any further addition of rubber particles resulted in a reduction of compression strength. This is seen with 15% rubber particles giving a strength of 16.36 MPa. Further increase in volume fraction to 20% increases compression strength of 21.36 MPa. This could be the result of adding more catalyst to the composite since it was not curing after 24 hours

Rubber particle sizes of 150 µm decreased composite compressive strength with increased rubber particle volume fraction. This decrease in strength could be attributed to the rubber particles' low hydrophilicity, which gave a weak interfacial bond between the rubber particles and the polyester resin. Abu-jdayil et al. (2016) found a similar decrease in composite compressive strength with incremental rubber particle volume fraction. The low volume fraction of rubber particles, less than 5%, enhances the composite compression. This trend could be attributed to the even distribution of the rubber particles in the matrix, creating a robust interfacial bond with the absence of voids.

The results for 300 µm rubber particles show that an increase in rubber particles volume fraction negatively affects the composite compression strength. However, there is a moderate increase in composite compression strength between 15 and 20% rubber particle volume fraction. The results align with a study by Abu-jdayil et al. (2016), who stated that when you increase rubber volume fraction in composites, the compression strength progressively reduces. The low volume fraction of rubber particles enhances the mechanical strength of the composites due to the even distribution of the rubber particles in the matrix, creating a solid interfacial bond with the absence of voids. From Figure 4.12, it was observed that composite compression strength decreases with an increase in the size of rubber particles. The 300 µm rubber particles had a generally lower compressive strength than the 150 µm rubber particles. Smaller rubber particles have a larger surface area than bigger rubber particles, which increases the matrix bond.

An increase in composite rubber particle volume fraction positively affects the composite flexibility, elasticity and damping properties (Meesit et al., 2017). However, stress transfer between rubber particles and polyester resin is low due to the weak bond strength between the rubber particles and the polyester resin. A study by Wang *et al*. (2019) aligns with a current study that finer rubber particles as composite fillers give higher composite compression strength than coarser rubber particles. This analogy is attributed to the even dispersion possible for finer rubber particles within the composite. Furthermore, the larger surface area presented by finer rubber particles increases their bond strength compared to the coarser rubber particles (X.Lu, W.Wang, L.yu, 2014).

The composites with greater than20% rubber particles volume fraction were observed to contain voids. The presence of the voids could be attributed to the poor dispersal of rubber particles within the composite. Therefore, using rubber particles alone as the filler material is not feasibly at percentages exceeding 15%.

The workability in the fabrication of the composite was easier at a low volume fraction of rubber particles of less than 15%. Furthermore, composite cutting was more straightforward for these specimens. The composites containing higher rubber particle volume fraction greater than 15% did not cure quickly and took an excess of 48 hours to reach acceptable hardness.

4.2.2.3 Effects of a combination of rubber particles and glass fibre on composite compression strength

The graph in Figure 4.13 presents the effects that a hybrid composite consisting of rubber particles size 150 µm and glass fibres has on composite compression strength.

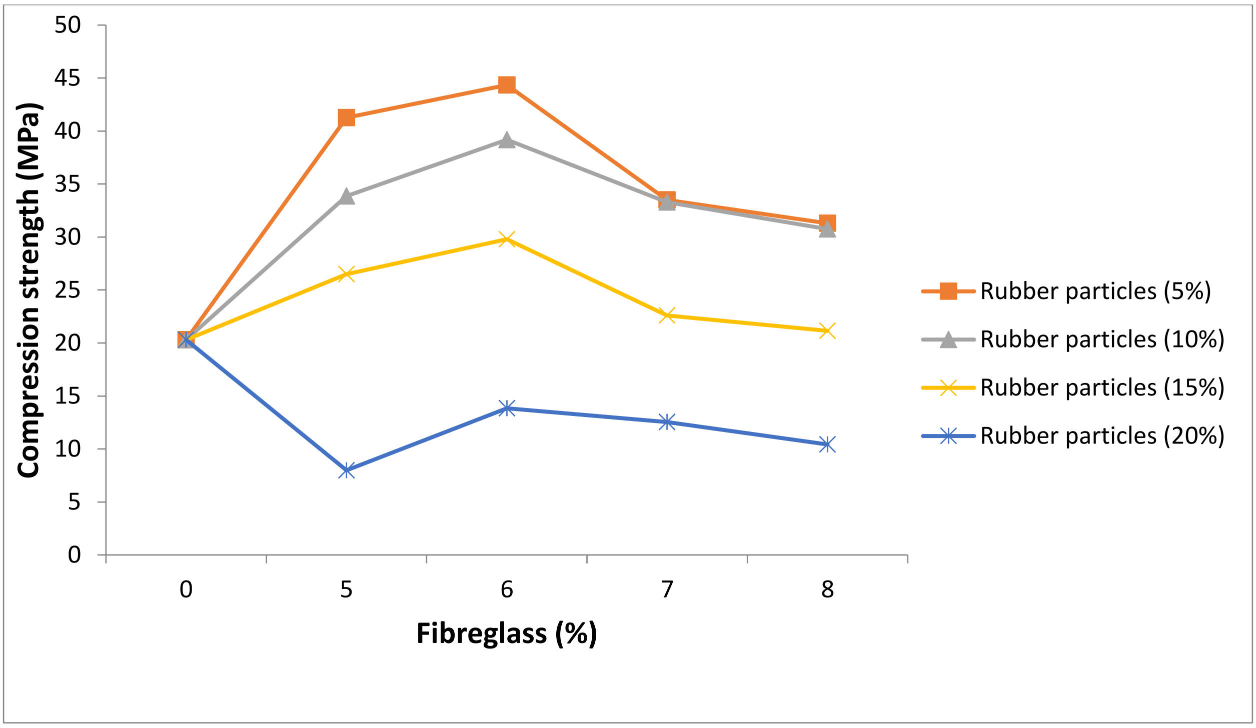

Figure 4.13 - Effects of 150 µm rubber particles and glass fibre on compression strength of composite

Figure 4.13 shows that hybrid composites containing 5 % rubber particles and 5% fibreglass have a compressive strength of 41.26MPa. As the fibreglass volume fraction increases to 6%, there is a marginal increase in compression strength to 44.35 MPa. Furthermore, any addition of fibreglass above 6% resulted in a decrease in hybrid composite compression strength, as observed with a composite containing 7 % fibreglass, giving 33.29 MPa of energy. Further increase in fibreglass volume fraction to 8 % decreases compression strength to 31.31 MPa.

The compression strength of rubber particles with 10 % and 5% fibreglass has a compressive strength of 33.86 MPa. As the fibreglass volume fraction increases to 6%, compression strength increases to 39.18 MPa. Furthermore, any addition of fibreglass decreased compression strength, which is seen with 7% fibreglass, giving a strength of 33.29 MPa. Further increase in fibreglass volume fraction to 8% resulted in a reduction in compression strength to 30.75 MPa.

The compression strength of 15% volume fraction rubber particles and 5% volume fraction fibreglass has an initial compressive strength of 26.50 MPa. As the fibreglass volume fraction increased to 6%, compression strength increased to 29.80 MPa. Further addition of fibreglass decreased composite compression strength, as observed with 7% fibreglass giving a strength of 22.61 MPa. Further increase in fibreglass volume fraction to 8% resulted in a reduction in compression strength to 21.15 MPa.

The compression strength of rubber particles with 20% and 5% fibreglass has an initial strength of 7.99 MPa. As the fibreglass volume fraction increased to 6%, composite compression strength increased to 13.84 MPa. Further addition of fibreglass decreased compression strength, as observed with composite containing 7% fibreglass, giving compressive strength of 12.53 MPa. Further increase in fibreglass volume fraction to 8% resulted in a reduction of compression strength to 10.42 MPa.

The graph in Figure 4.14 presents the effects that a hybrid composite consisting of 300 µm rubber particles and glass fibres has on compression strength

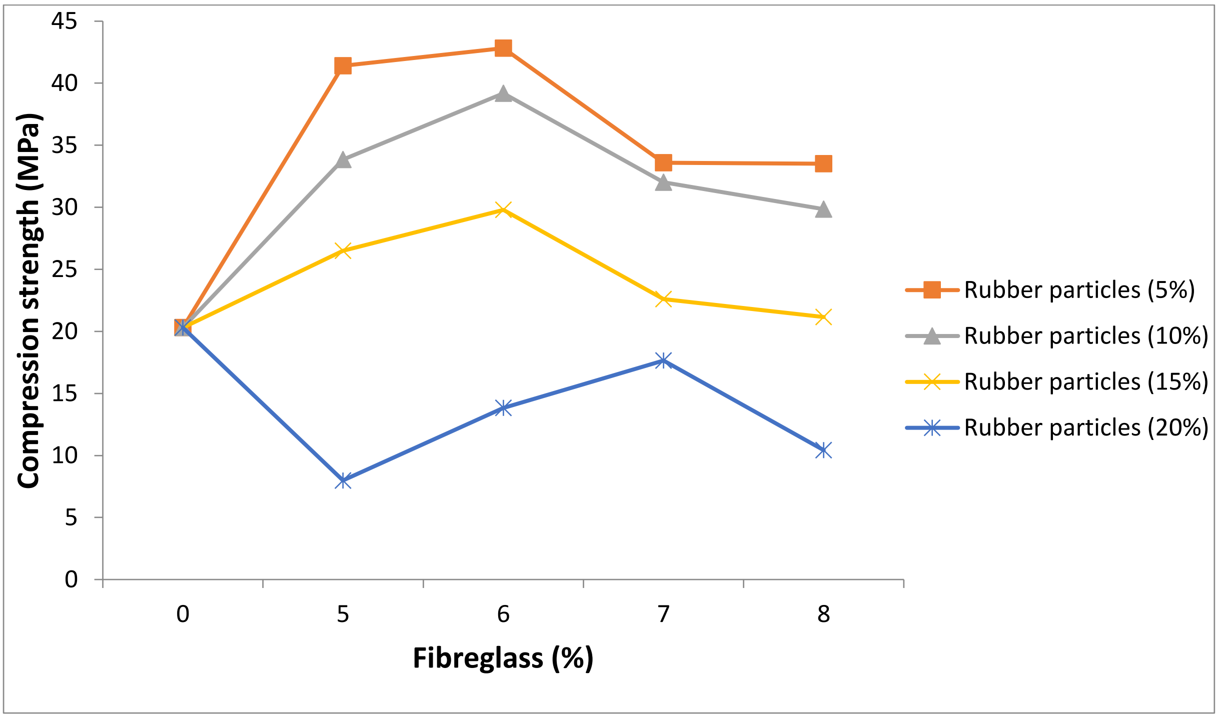

Figure 4.14 - Compression strength of 300 µm particles at various fibre volume fraction

Figure 4.14 present that a hybrid composite with 5% rubber particle volume fraction and 5% fibreglass volume fraction had initial strength of 41.42 MPa. As the fibreglass volume fraction increased to 6%, there was a marginal increase in compression strength to 42.83 MPa. Any further addition of fibreglass decreased compression strength, as shown in Figure 4.16, with a 7 % fibreglass volume fraction giving a strength of 33.59 MPa. Further increase in fibreglass volume fraction to 8 % resulted in a decrease in compression strength to 33.31 MPa.

The compression strength of 10% volume fraction of rubber particles with 5% volume fraction fibreglass gave an initial strength of 33.86 MPa. As the fibreglass volume fraction increased to 6%, compression strength increased to 39.18 MPa. Further addition of fibreglass decreased composite compression strength as observed in Figure 4.14 with 7 % fibreglass giving compressive strength of 32.03 MPa. Further increase in fibreglass volume fraction to 8% resulted in a reduction in composite compression strength to 29.84 MPa.

The composite compression strength of 15% volume fraction of rubber particles and 5% fibreglass volume fraction had an initial strength of 26.50 MPa. As the fibreglass volume fraction increased to 6%, composite compression strength increased to 29.80 MPa. Further addition of fibreglass volume fraction resulted in a decrease in composite compression strength as observed with 7% volume fraction fibreglass giving a strength of 22.61 MPa. Further increase in fibreglass volume fraction to 8 % resulted in the reduction in composite compression strength to 21.15 MPa.

The composite compression strength of 20% volume fraction rubber particles and 5% fibreglass volume fraction had an initial strength of 7.99 MPa. As the fibreglass volume fraction increased to 6%, composite compression strength increased to 13.84 MPa. Further addition of fibreglass increased compression strength. However, further fibreglass volume fraction increases beyond 8%, reducing composite compression strength to 10.42 MPa.

The compression strength of composite containing 150 µm rubber particles with 5% fibre volume fraction improved from the control 36.52 MPa to 44.346 MPa when fibreglass was varied from 5 to 8%. The compression strength of composite containing 150 µm rubber particles with fibreglass volume fraction of 10% improved from the control 24.547 MPa to 39.183 MPa when fibreglass was varied from 5 to 8%. The compression strength of composite containing 150 µm rubber particles with fibreglass volume fraction of 15% improved from the control compressive strength of 17.657 MPa to 29.792 MPa when fibreglass was varied from 5 to 8%. However, the compression strength of 150 µm rubber particle size with a volume fraction of 20% reduced from 23.346 MPa to 13.835 MPa when fibreglass was incorporated when fibreglass was varied from 5 to 8%. This results from poor dispersal of rubber particles and fibreglass, giving a weak interfacial bond of resin, glass fibres and rubber particles.

Compression strength of 300 µm rubber particle size with volume fraction of 5% improved from 21.208 MPa to 42.827 MPa when fibreglass was incorporated when fibreglass was varied from 5 to 8%. The compression strength of 300 µm rubber particles with a volume fraction of 10% improved from 19.09 MPa to 39.183 MPa when fibreglass was incorporated when fibreglass was varied from 5 to 8%. The compression strength of 300 µm rubber particle size with a volume fraction of 15% improved from 16.363 MPa to 29.792 MPa when fibreglass was incorporated when fibreglass varied from 5 to 8%. Compression strength of 300 µm rubber particle size with volume fraction of 20% reduced from 5 MPa to 6.9 MPa when fibreglass was incorporated when fibreglass was varied from 5 to 8%. Hybrid composites' workability becomes difficult and results in a poor dispersal of rubber particles and fibreglass since when the interfacial volume bond of resin increases, glass and rubber particles become weak.

Figure 4.13 and Figure 4.14 show that increasing rubber particle volume fraction regardless of particle size has an adverse effect on the composite compression strength. This phenomenon can be attributed to the low hydrophilicity of rubber particles to the resin resulting in weak interfacial bond strength. Both results of rubber particles size 150 and 300 µm suggest that hybrid composites with rubber particles volume fraction of less than10% and fibreglass volume fraction of less than 7% give optimal compressive strength.

The dominant failure modes of the composites containing rubber particles volume fraction of 5%, 10% and 15 % and fibreglass volume of 5 to 8% were fibre breakage, split failure and matrix failure, as shown in Figure 4.15. However, when the rubber particles' volume fraction was increased to 20%, fibre breakage was observed in the dominant composite failure mode. When fibreglass volume fraction is increased to 8%, the interfacial bond of polyester resin becomes weak, and the dispersal of fibreglass within the composite is poor. This resulted in the dominant failure mode being fibre pull out and matrix breakage.

Figure 4.15 - Failure mode of fibreglass/rubber particle composite under compressive force

The fabricated composite showed an optimum compressive strength of 42.83 MPa, which was acceptable; however, concrete sleepers have a much higher compression strength of 61.2 MPa. However, despite the high compression strength of concrete sleepers, they have poor vibrational damping properties, elasticity and flexibility compared to the fabricated hybrid composite. A study by Meesit *et al.* (2017) reported that adding rubber particles to concrete improves the vibrational damping properties. However, the concrete's compression strength reduces due to a weak interfacial bond between concrete and rubber particles.

The current study suggests composite sleepers possess great compression strength, elasticity, and durability. In addition, the fabricated composite has improved damping properties compared to traditional wooden and concrete sleepers.

4.2.3 Flexural strength properties

This section analyses the composite flexural strength results in accordance with the experimental design of the study.

4.2.3.1 Effects of fibreglass on the flexural strength of the composite.

Figure 4.16 presents the effects of varying fibreglass volume fractions on the composite flexural strength.

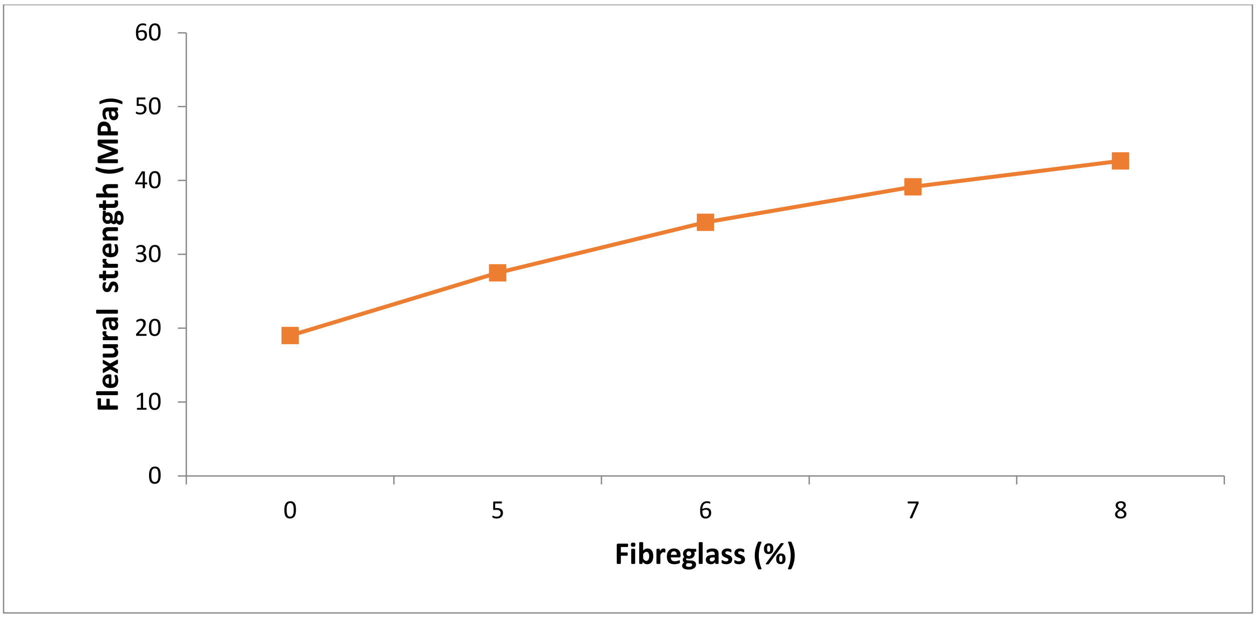

Figure 4.16 - Effects of fibreglass volume fraction on the flexural strength of the composite

Figure 4.16 presents a general increasing trend in the flexural strength with an increase in the fibreglass volume faction. The graph shows an increase in flexural strength from 27.51 MPa to 42.60 MPa with an increase in fibreglass volume fraction of 5 to 8%, respectively. The overall flexural strength gained from 5 to 8% fibreglass volume fraction is 35.50%.

The flexural strength of the composite increases as the glass fibre volume fraction is increased.

The results observed in this study align with the research by Rachchh et al. (2018) that showed an increase in flexural strength with an increase in fibreglass volume fraction. However, the study by Rach et al. (2018) noted that the composite flexural strength decreases when glass fibre volume fraction is greater than 9% due to insufficient polyester resin for the transmission of load from one fibre to another.

Figure 4.17 shows the dominant failure mode of the fabricated fibreglass composite. It was observed that at a high fibre volume fraction greater than 5%, the dominant composite failure modes mainly include fibre breakage, ultimately leading to matrix breakage.

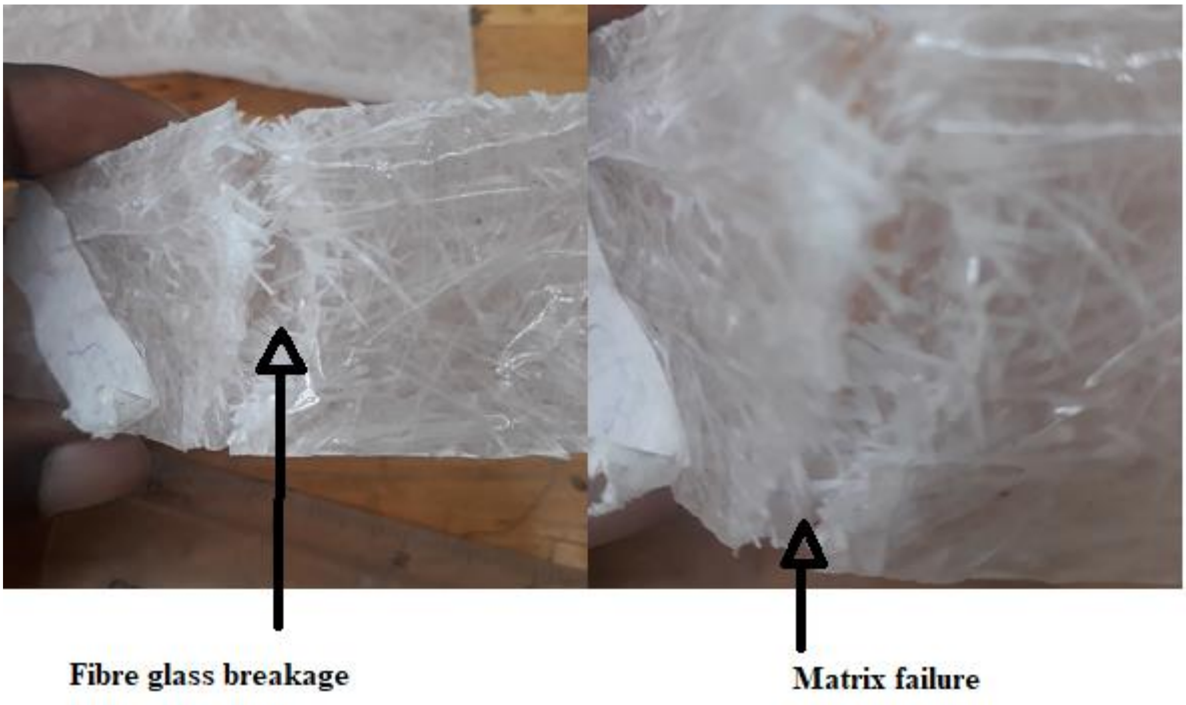

Figure 4.17 - Experimental failure mode of a composite containing fibreglass

4.2.3.2 Effects of rubber particles on the flexural strength of the composite

Figure 4.18 presents the effects on composite flexural strength of rubber particle fillers sizes 150 and 300 µm.

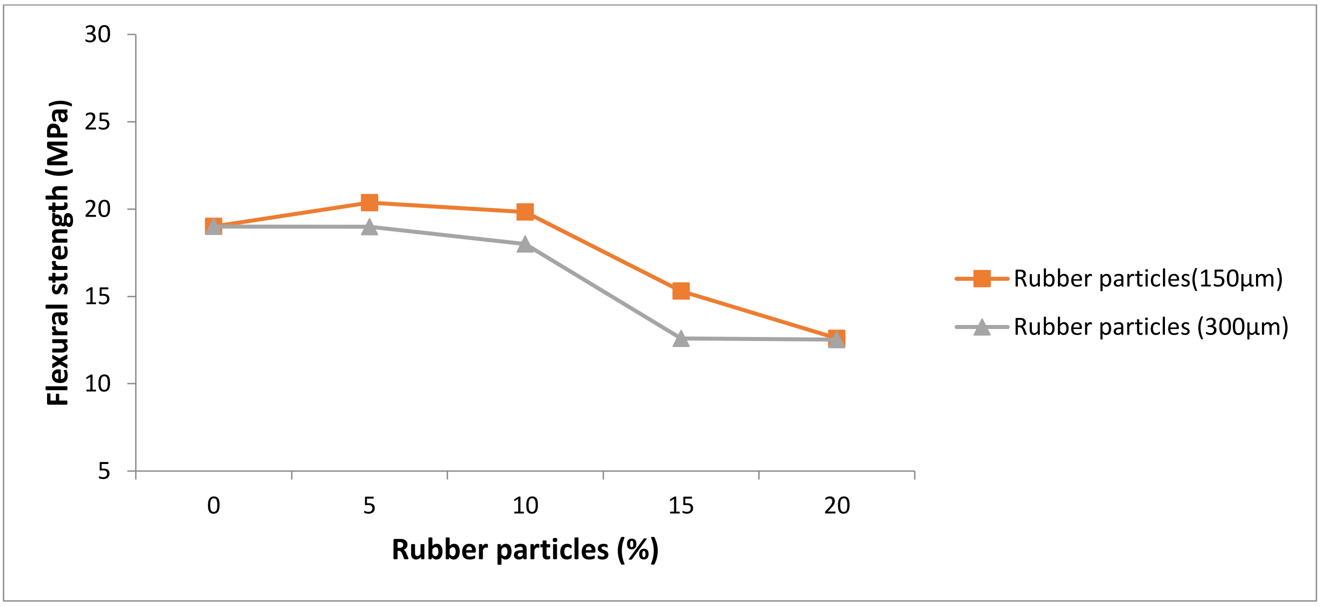

Figure 4.18 – Effect of rubber particles on composite compression strength

Figure 4.18 presents that for 150 µm rubber particles, the composite flexural strength at a 5% fibre volume fraction is 20.37 MPa above the control specimen, which had a flexural strength of 19.00 MPa. As the fibre volume fraction was increased to 10%, there was a marginal decrease in flexural strength to 19.84 MPa. However, any further addition of rubber particles beyond 10% resulted in a decrease in flexural strength as observed with a 15% rubber particles volume fraction giving a flexural strength of 15.30 MPa. Further increase in volume fraction to 20% gave a flexural strength of 12.60 MPa.

Rubber particle sizes of 300 µm had initial strength of 18.98 MPa at 5% rubber particle loading. As the rubber particle volume fraction increased to 10%, flexural strength decreased to 18.00 MPa. However, further addition of rubber particles beyond 10% decreased flexural strength, as observed with a 15% rubber particle volume fraction giving flexural strength of 12.60 MPa. Further increase in rubber particle volume fraction to 20% gave flexural strength of 5.80 MPa.

The results of 150 µm rubber particles suggest that a low volume fraction of less than 5% must be used in a composite to maximize flexural strength. The trend observed in Figure 4.18 for 150 µm rubber particle shows that an increase in rubber particle volume fraction decreases the flexural strength of the composite. The reduction in flexural strength can be attributed to the low rubber particle hydrophilicity giving a weak interfacial bond with the resin.

Rachchh et al. (2018) showed a similar trend to the current study that an increase in rubber particle volume fraction decreases the composite flexural strength due to insufficient bond strength to polyester resin.

The results shown in Figure 4.18 for 300 µm show that rubber particles of less than 5% must be used to maximize the flexural strength as the composite strength decreases when the rubber particle volume fraction is increased. This was attributed to low rubber particle hydrophilicity and weak interfacial bond between rubber particles and resin. The results obtained in Figure 4.18 align with a study by Abu-jdayil *et al.* (2016) and (Meesit et al. 2017). They reported that an increase in composite rubber particle loading increases the composite flexibility and elasticity.

The composites with greater than 20% rubber particle loading were observed to contain voids. The presence of the voids could be attributed to the poor dispersal of rubber particles within the composite. Therefore, using rubber particles alone as the filler material is not feasibly at percentages exceeding 15%.

The fabrication of the composite was easier when the rubber particle volume fraction was low. Furthermore, cutting composites for these specimens was easy. The composites with a more significant rubber particle volume percentage greater than 15% took longer to cure and required more than 48 hours to obtain an acceptable hardness.

4.2.3.3 Effects of a combination of rubber particles and glass fibre on composite flexural strength

The graph in Figure 4.19 presents the effects that a hybrid composite consisting of rubber particles and glass fibres has on flexural strength.

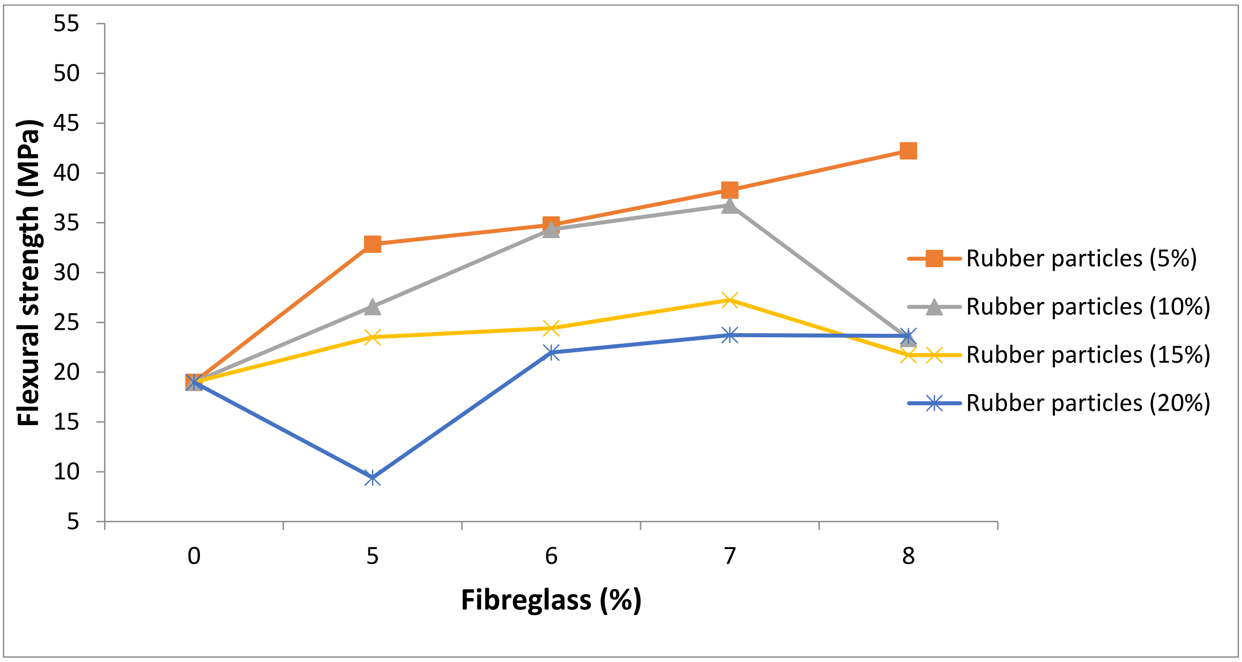

Figure 4.19 - Effects of 150 µm rubber particles and glass fibre on flexural strength of composite

The hybrid composite containing 5% rubber particles and 5% fibreglass had a flexural strength of 32.86MPa. As the fibreglass volume fraction increased to 6%, there was a marginal increase in flexural strength to 34.33 MPa. Any addition of fibreglass above 6% increased composite flexural strength as observed with 7 % fibreglass giving flexural strength of 38.28 MPa. Further increase in fibreglass volume fraction to 8% increased flexural strength to 42.22 MPa.

The flexural strength of 10% rubber particles volume fraction and 5% fibreglass had a flexural strength of 26.61 MPa. As the fibreglass volume fraction increased to 6%, flexural strength increased to 34.33 MPa. Further addition of fibreglass to 7% increased flexural strength to 36.77 MPa. Further increase in fibreglass volume fraction to 8% resulted in a reduction in flexural strength to 23.38 MPa.

The flexural strength of the composite with 15% rubber particles and 5% fibreglass volume fraction was 23.52 MPa. As the fibreglass volume fraction increased to 6%, there was an increase in flexural strength to 24.41 MPa. Further fibreglass addition to 7% resulted in flexural strength of 27.24 MPa. Further increase in fibreglass volume fraction to 8% resulted in a reduction in composite flexural strength to 21.72 MPa.

The flexural strength of the hybrid composite with 20% rubber particles and 5% fibreglass was 9.41 MPa. As the fibreglass volume fraction increased to 6%, flexural strength increased to 21.98 MPa. The addition of 7% fibreglass increased flexural strength to 23.72 MPa. Further increase in fibreglass volume fraction to 8% resulted in a reduction of flexural strength to 21.72 MPa.

The results for the flexural strength of 300 µm are presented in Figure 4.20.

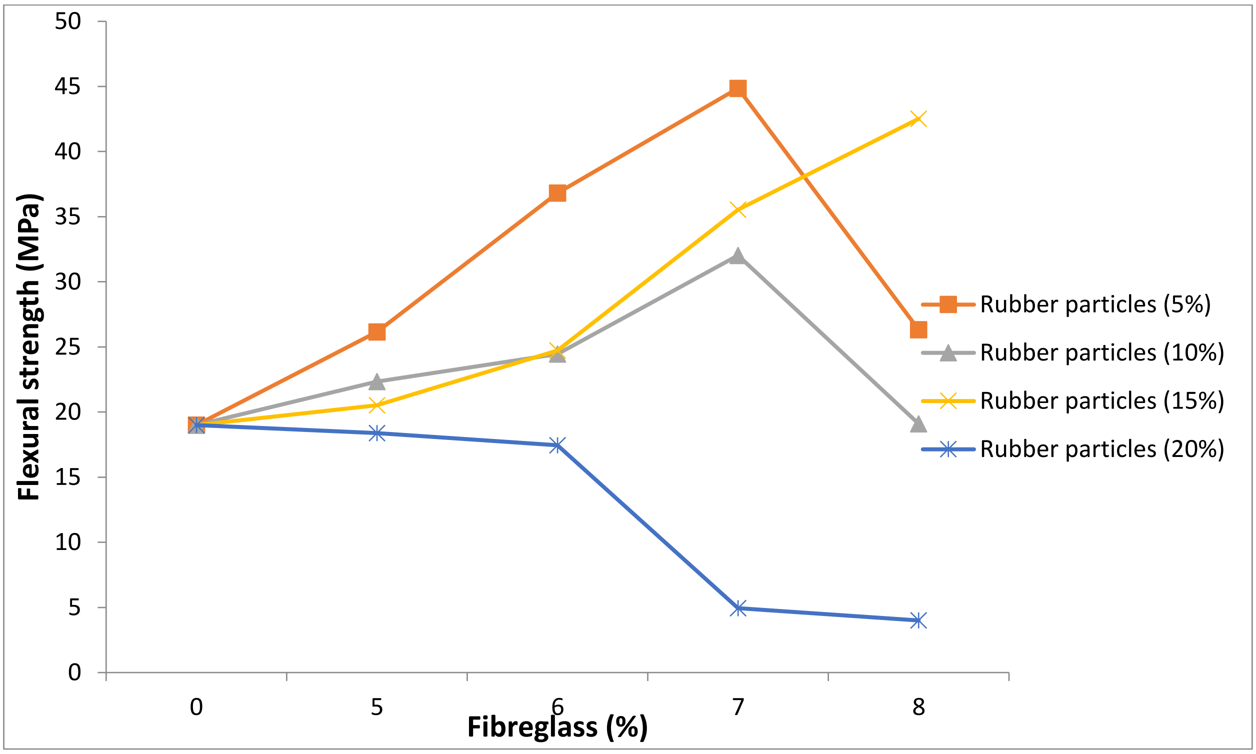

Figure 4.20 - Flexural strength of 300 µm particles at various mass

The composite containing 5 % rubber particles and 5% fibreglass had a flexural strength of 26.15 MPa. As the fibreglass volume fraction increased to 6%, there was a marginal increase in flexural strength to 36.82 MPa. The addition of fibreglass above 6% increased flexural strength. However, the addition of 8% fibreglass decreased flexural strength to 26.33 MPa.

The flexural strength of the composite with 10% rubber particles and 5% fibreglass was 20.53 MPa. As the fibreglass volume fraction increases to 6%, there is an increase in flexural strength to 24.724 MPa. The addition of fibreglass to 7% and 8% fibreglass resulted in flexural strength of 32.03 MPa and 19.09 MPa respectively.

The flexural strength of composite with 15% rubber particles and 5% fibreglass gave flexural strength of 20.53 MPa. As the fibreglass volume fraction increased to 6% there was an increase in flexural strength to 24.72 MPa. Further addition of fibreglass up to 7% gave a steady increase in flexural strength. However, the addition of 8% fibreglass resulted in a decrease

The flexural strength of composite with 20% rubber particles and 5% fibreglass gave a flexural strength of 18.39 MPa. As the fibreglass volume fraction increased to 6%, flexural strength decreased to 17.46 MPa. Further addition of fibreglass to 7% resulted in a decrease in flexural strength to 4.96 MPa. Further increase in fibreglass volume fraction to 8% gave flexural strength of 4.00 MPa.

The results indicate that rubber particle volume fraction less than15% must be used in composites for optimal flexural strength.

Figure 4.19 and Figure 4.20 indicates an increasing rubber particle volume fraction, regardless of particle size, has an adverse effect on the composite flexural strength. This phenomenon can be attributed to the low hydrophilicity of rubber particles to the resin resulting in weak interfacial bond strength.

The failure mode of hybrid composites containing fibreglass and rubber particles. Fibreglass was used to enhance the flexural strength of the hybrid composite and contour the effect of rubber particles that reduce the composite flexural strength. The dominant failure mode of composites with rubber particles volume fraction of 5% less than 15 % was fibre breakage. However, when the rubber particles' volume fraction was increased to 20%, the dominant composite failure mode was matrix breaking and fibre pulling out.

4.2.4 Hardness properties

This section discusses the composite hardness results according to the full factorial experimental design followed in this study.

4.2.4.1 Effects of fibreglass on the hardness of the composite.

Figure 4.21 presents the effects of fibreglass volume fraction on the composite hardness.

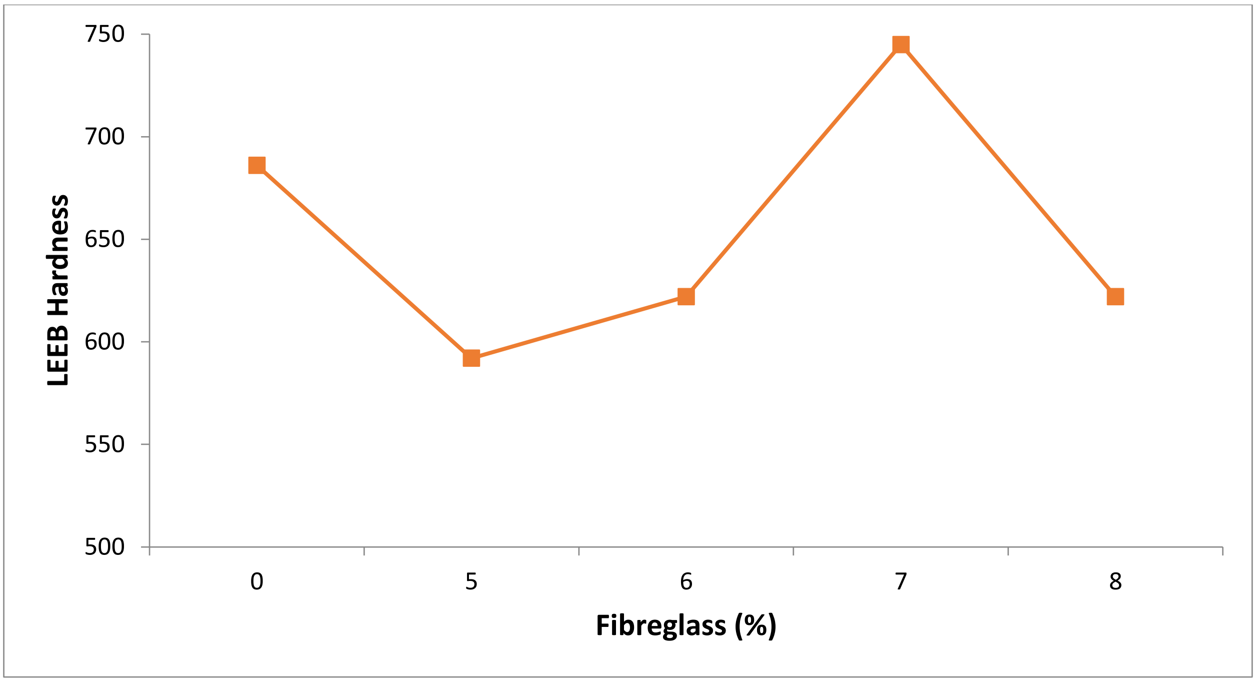

Figure 4.21 - Effects of fibreglass volume fraction on the hardness of the composite

As observed in Figure 4.21, a sharp drop in from the control specimen with the addition of 5% fibreglass, giving a hardness of 592 from 690. As the fibre volume fraction increased to 6%, there was a marginal increase in hardness to 622. Further addition of fibreglass to 7% resulted in an increase in hardness to 745. However, an increase in fibreglass volume to 8% decreased the hardness to 622.

The results indicate that fibreglass of volume fraction 5 to 7% increases the hardness of the composite. However, a fibre volume fraction greater than 8% decreases the hardness of the composite. This phenomenon can be attributed to the fibreglass having low efficiency of polyester resin absorption when fibreglass is greater than 8%. Furthermore, the fibreglass volume fraction of greater than 8% results in a stress transfer that becomes poor in a matrix.

The results observed in this study align with the research by Rachchh *et al.* (2018), Zoalfakar *et al.* (2017) and Araújo *et al.* (2006), who stated the hardness increases with fibre volume fraction as observed up to 7% in Figure 4.21. However, the decrease in hardness observed in the current study beyond 8% can be attributed to insufficient polyester resin cover to transmit the load from one fibre to another. Furthermore, the matrix's poor fibre dispersion and distribution could result in low composite hardness at high fibre loading.

4.2.4.2 Effects of rubber particles on the hardness of the composite

Figure 4.22 presents the effects on the composite hardness of rubber particles of sizes 150 and 300 µm.

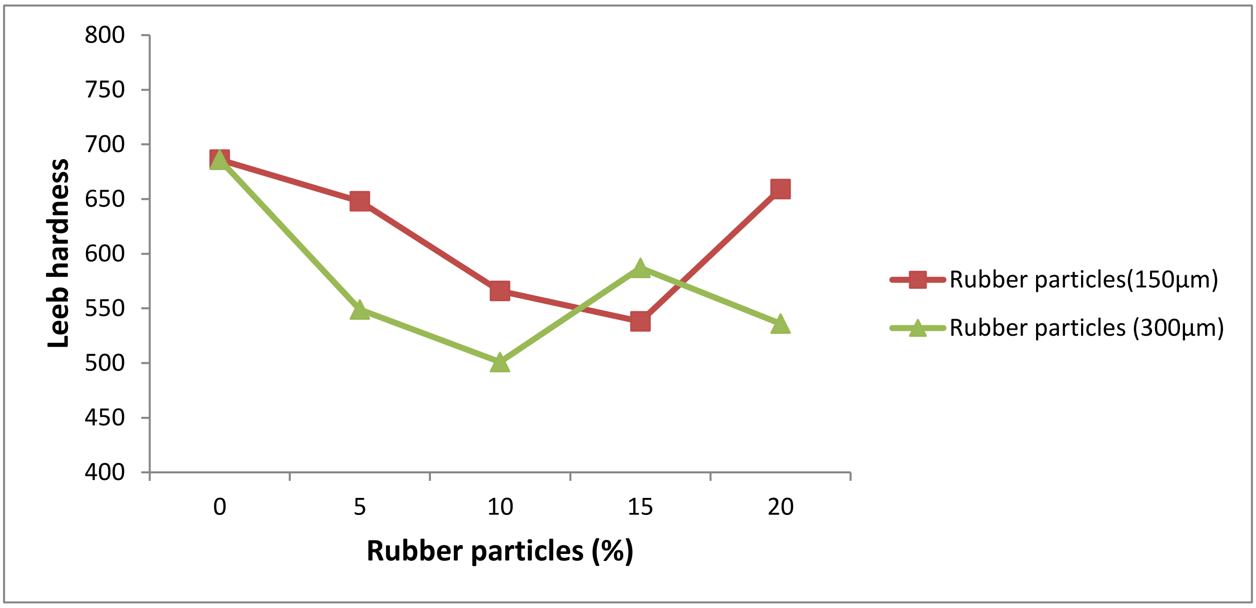

Figure 4.22 – Effect of 150 and 300 µm rubber particles on the composite hardness

Figure 4.22 presents that for 150 µm rubber particles, the initial Leeb hardness at 5% is 648. As the rubber particle volume fraction increased to 10%, there was a marginal decrease in hardness to 566. Further addition of rubber particles beyond 5% resulted in a decrease in composite hardness as observed with composite containing 15% rubber particles giving a hardness of 538. However, a further increase in volume fraction to 20% resulted in an increase in hardness to 659 MPa.

Composite containing 300 µm rubber particles gave Leeb hardness at 5% rubber particle loading of 549. As the rubber particle volume fraction increased to 10%, there was a marginal decrease in hardness to 501. However, further addition of rubber particles to 15% resulted in an increase in composite hardness to 587. Further increase in rubber particle volume fraction to 20% gives a composite hardness of 536.

The results for 150 µm present that an increase in rubber particles volume fraction from 5% to 15% decreases the composite hardness. However, the hardness increases at 20% particle volume fraction to 660. This could be a result of adding excess catalyst at higher particle volume fractions to ensure composite cures.

The results for 300 µm present that an increase in rubber particles volume fraction from 5% to 10% decreases the composite hardness. On the other hand, there is an increase in composite hardness at a rubber particle volume fraction of 15%. However, further addition of rubber particles to 20% loading decreases the composite hardness due to the presence of voids.

The current study shows that composites fabricated from 300 µm rubber particles have a lower hardness than composites made with 150 µm rubber particles. The larger rubber particles of sizes 300 µm are inefficiently dispersed and result in low hardness. Smaller rubber particles of 150 µm are rougher and have larger specific areas that enhance the matrix bond with the polyester resin and hence have higher hardness (X.Lu, W.Wang, L.yu, 2014).

4.2.4.3 Effects of a combination of rubber particles and glass fibre on the composite hardness

The graph in Figure 4.23 presents the effect that a hybrid composite consisting of rubber particles size 150 µm and glass fibres at varying proportions has on composite Leeb hardness.

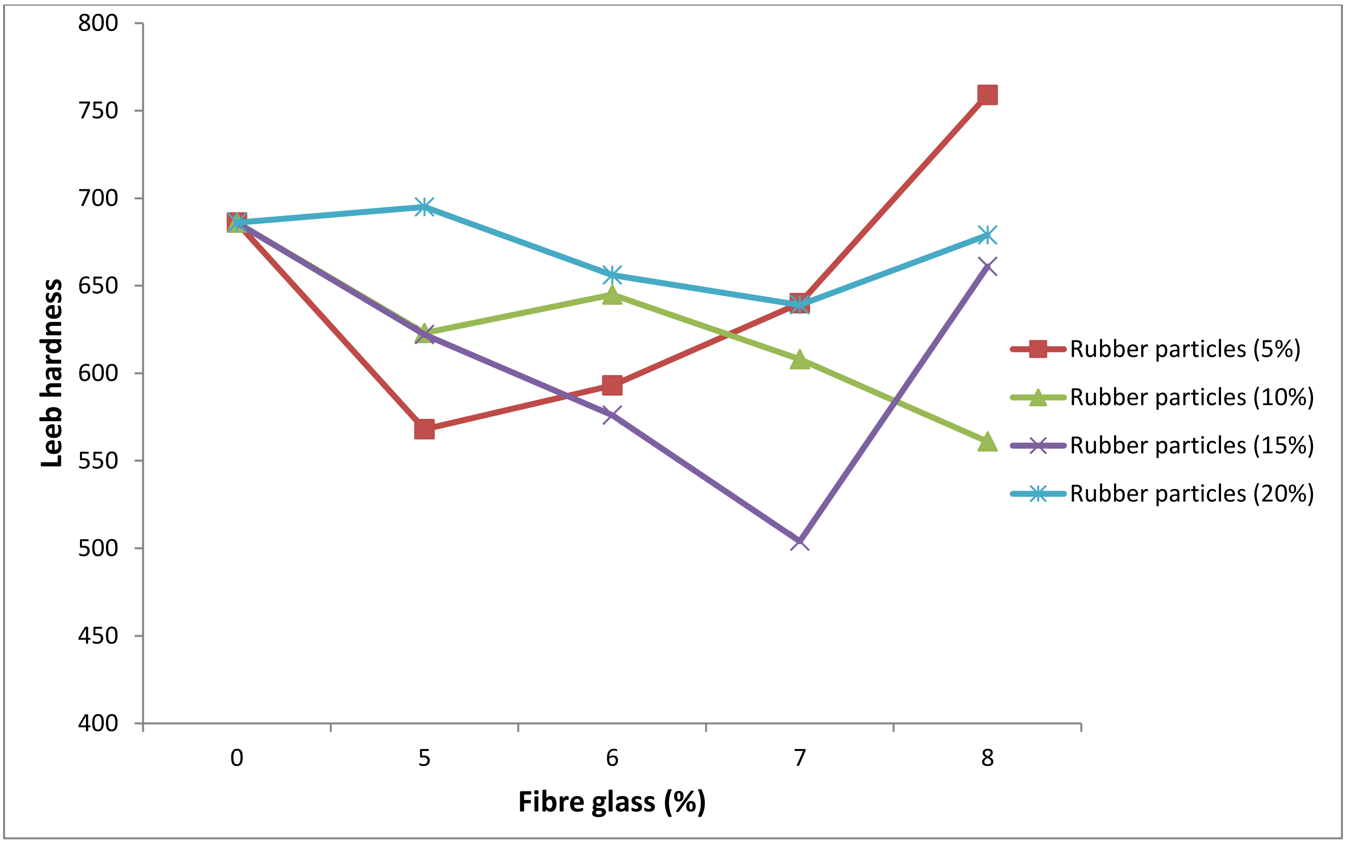

Figure 4.23 - Effects of 150 µm rubber particles and glass fibre on the hardness of composite

Figure 4.23 shows that the hybrid composite containing 5% rubber particles and 5% fibreglass had a hardness of 568. As the fibreglass volume fraction increased to 6%, there was a marginal increase in hardness to 593. Further addition of fibreglass above 6% increased composite hardness as shown with composite containing 7 % fibreglass giving a hardness of 640. Further increase in fibreglass volume fraction to 8% increased hardness to759.

The composite containing 10% rubber particles and 5% fibreglass had hardness of 623. As the fibreglass volume fraction increased to 6%, there was an increase in the hardness to 645. However, any further addition of fibreglass decreased the composite hardness, as observed with 7% fibreglass giving a hardness of 608. Further increase in fibreglass volume fraction to 8% reduced hardness to 561.

The composite made up of 15% rubber particles, and 5% fibreglass had a hardness of 622. There was a decrease in composite hardness to 576, with an increase in fibreglass volume to 6%. The total amount of fibreglass volume fraction decreased composite hardness, as observed with a 7% fibre volume fraction, which had a hardness of 504. In contrast, there was a gain in composite hardness with an 8% fibre volume fraction to 661.

The composite has a hardness of 695 because it contains 20% rubber particles and 5% fibreglass. The hardness of the material decreases to 656 as the volume fraction of fibreglass increases to 6%. Furthermore, adding more fibreglass reduced the hardness of the material. This may be shown with 7% fibreglass, which has a strength of 639. However, increasing the fibreglass volume percentage to 8% resulted in a hardness increase to 679.

The graph in Figure 4.24 presents the effects that a hybrid composite consisting of 300 µm rubber particles and glass fibres has on composite hardness.

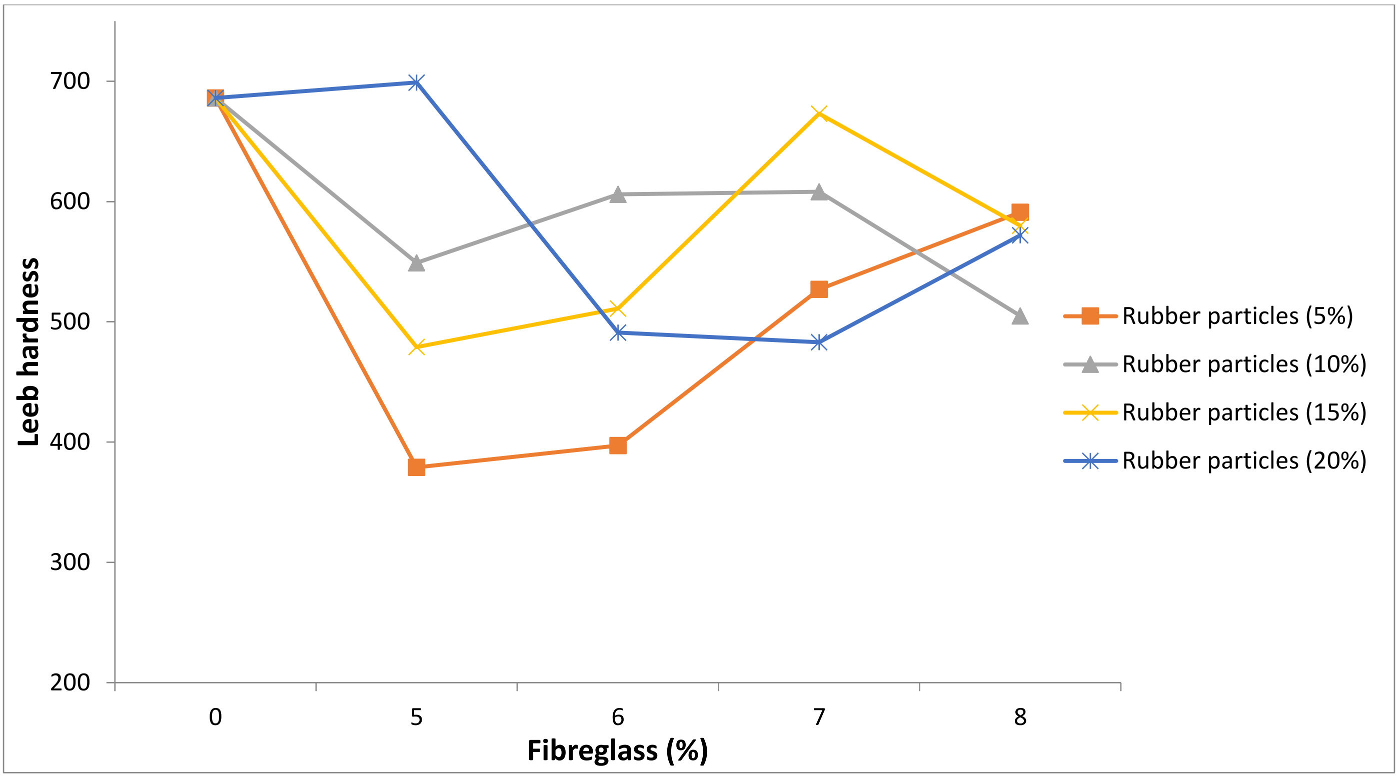

Figure 4.24 - Effects of 300 µm rubber particles and glass fibre on the hardness of composite

The hardness of the composite shown in Figure 4.24, containing 5% rubber particles and 5% fibreglass, had a hardness of 379. As the fibreglass volume fraction increased to 6%, there was a marginal increase in hardness to 397. The addition of fibreglass above 6% gave a general incremental trend in composite hardness. The composite containing an 8% fibreglass volume fraction had the highest hardness for that composite of 591.

The hardness of composite containing 10% rubber particles and 5% fibreglass was recorded as549. As the fibreglass volume fraction increased to 6%, there was an increase in hardness to 606. The incremental increase in fibreglass to 7% fibre gives a composite hardness of 608. However, a further increase in fibreglass volume fraction to 8% reduced hardness to 505.

The hardness of the composite with 15% rubber particles and 5% fibreglass was 479. As the fibreglass volume fraction was increased to 6%, hardness increased to 511. Further addition of fibreglass to 7% resulted in an increase in hardness to 673. Yet, a further increase in fibreglass volume fraction to 8% resulted in a reduction in composite hardness to 580.

The hardness of the composite consisting of 20% rubber particles and 5% fibreglass was 699. As the fibreglass volume fraction increased to 6%, hardness decreased to 491. Adding fibreglass to 7%

fibreglass decreased the composite hardness marginally to 483. However, a further increase in fibreglass volume fraction to 8% resulted in an increase in composite hardness to 572.

The hardness of 150 µm rubber particles with a volume fraction of 5% was 648. Increasing the fibreglass content increased composite hardness. Composite had an initially incremental trend in composite hardness with the addition of fibreglass up to 8% Hardness of 150 µm rubber particles size with volume fraction of 15% was 538. However, composite hardness increased at 8% fibreglass loading to 661. The hardness of 150 µm rubber particle size with a volume fraction of 20% was 659, but after varying fibreglass from 5 to 8%, hardness was increased to 695.

The fabricated composites with fibreglass, polyester resin and rubber particles showed outstanding hardness compared to composites with only rubber particles and polyester resin. The thickness of 300 µm rubber particle size with a volume fraction of 5% was 549. However, after varying fibreglass from 5 to 8 %, hardness was increased to 591. Hardness of 300 µm rubber particle size with a volume fraction of 10% was 501, but after varying fibreglass from 5 to 8 %, hardness increased to 608. Hardness of 300 µm rubber particle size with volume fraction of 15% was 587. However, after varying fibreglass from 5 to 8%, hardness increased to 673. The hardness of 300 µm rubber particle size with a volume fraction of 20% was 536, but after varying fibreglass from 5 to 8%, it was increased to 699.

Figure 4.23 and Figure 4.24 indicates how increasing rubber particle volume fraction regardless of particle size has an adverse effect on the composite hardness. This phenomenon can be attributed to the roughness and hardness of rubber particles to the resin resulting in the composite being hard. The polyester is brittle; adding fibreglass and rubber particles aids the hybrid composite to be hard.

The results observed in this study align to the research by Rachchh et al. (2018) that showed volume fraction of fibreglass increases hardness. Composites with greater than 15% rubber particles were observed to have higher hardness. However, those composites had low mechanical strength due to the presence of voids and pockets due to insufficient resin and poor dispersal of rubber particles and fibreglass.

The current study fabricated composite sleepers with excellent hardness and durability compared with composite sleepers made of thermoplastic materials. The plastic sleeper can be re-hardened when cooled and softened.

4.3 Vibrational properties

This section discusses the vibration and damping properties of the fabricated composites.

4.3.1 Effects of fibreglass on the vibration and damping properties of the composite

Figure 4.25 presents the effects of fibreglass volume fraction on the composite damping properties.

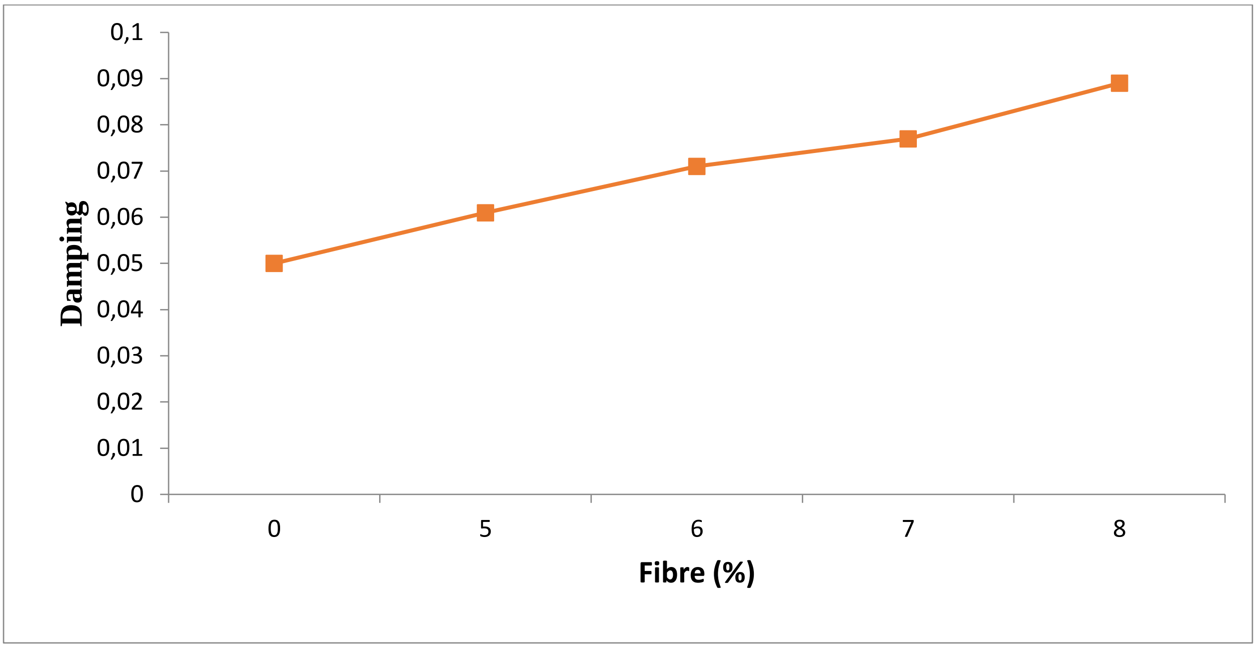

Figure 4.25 - Effect of fibreglass volume fraction on the vibration and damping properties of the composite

Figure 4.25 presents that there is an overall increasing trend in the damping with an increase in the fibreglass volume faction. The graph shows an increase in damping from 0.050 to 0.089 with an increase in fibreglass volume fraction of 5 to 8%, respectively. The overall damping gained from 5 to 8% fibreglass volume fraction is 44 %.

A study by Tang *et al.* (2020) stated that the volume fraction of fibre reinforcement directly influences the energy dissipation within the matrices of composite. The observation made by Tang *et al.* (2020) supports the present study's results that the incremental volume fraction of fibreglass enhances composite vibrational damping properties due to the presence of interpenetrating polymer networks. These networks dissipate the vibrational forces depending on the orientation and stacking sequence of fibres within the composites. This has been observed in the present study, as shown in Figure 4.25, with an increase in fibre loading resulting in an increase in damping.

4.3.2 Effects of rubber particles on the vibration and damping properties of the composite

Figure 4.26 presents the effects on vibrational damping of rubber particles of sizes 150 and 300 µm.

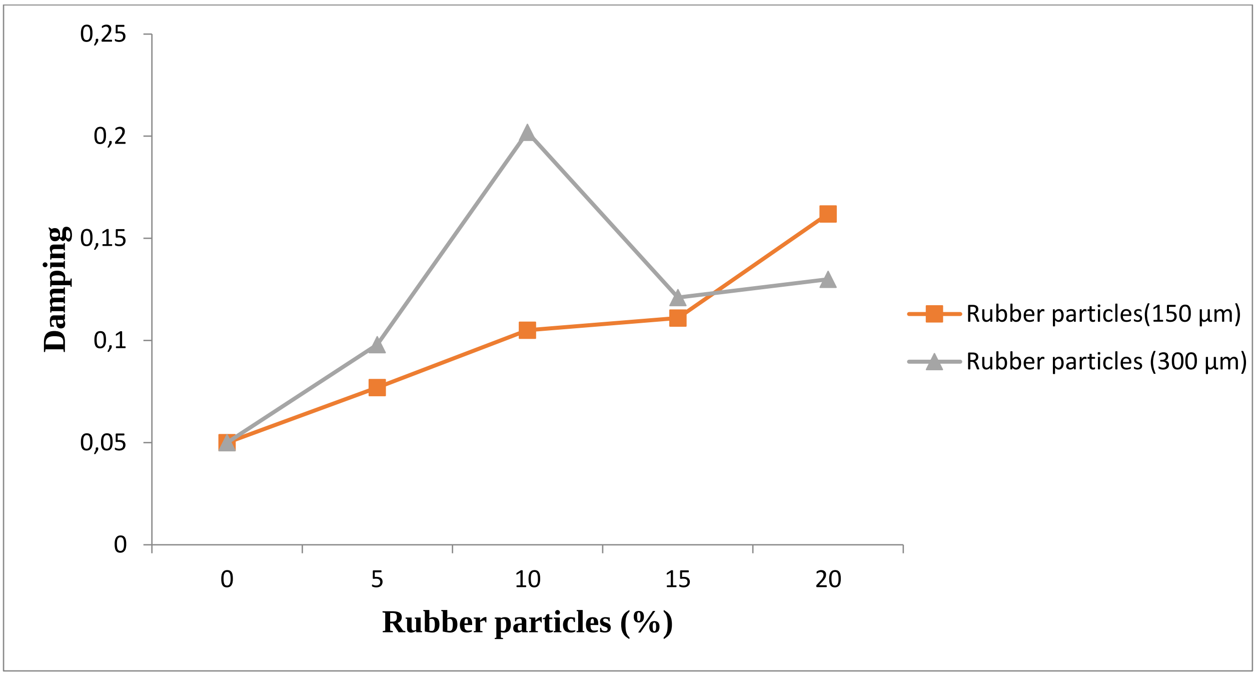

Figure 4.26 – Effect of rubber particles on vibration and damping properties

Figure 4.26 presents that for 150 µm rubber particles, the initial damping at 5% is 0.077. As the rubber particle volume fraction increased to 10%, there was a marginal increase in damping to 0.105. Further addition of rubber particles beyond 10% resulted in a decrease in composite damping as observed with composite containing 15% rubber particles giving a damping of 0.111. Further increase in rubber particle volume fraction to 20% resulted in a slight rise in damping to 0.162.

The composite containing 300 µm rubber particles at a 5% rubber particle volume fraction gave vibrational damping of 0.098. As the rubber particle volume fraction increased to 10%, there was a marginal increase in damping to 0.202. However, further addition of rubber particles to 15% resulted in a sharp decrease in composite damping to 0.121. Further increase in rubber particle volume fraction to 20% gave composite vibrational damping of 0.130.

The fabricated composites from particles size 300 µm have greater damping compared to a composite made with 150 µm rubber particles. A study by Wang et al. (2014) stated that larger rubber particles of sizes greater than 300 µm increase damping, but use of extremely coarse rubber particles tends to lead to a lack of homogeneity in their dispersal. This lack of homogeneity can be attributed to coarse rubber particles having large surface areas, allowing air pockets to ingress into the composite. The particles of sizes less than 150 µm possess lower vibrational damping as they have a larger specific area that enhances the matrix bond with the polyester resin. Rubber particles size of less than 150 µm has less damping compared to rubber particles greater than 300 µm in size. The rubber particles less than 150 µm have better cohesion than coarse particles, which could help enhance composite properties but decrease damping. Thus, when the size of rubber particles increases, voids within rubber particles also increase. This phenomenon can be attributed to damping increases due to voids within rubber particles and decreases in composite material strength.

It was observed in this study that an increase in rubber particle size and volume fraction leads to an increase in damping. However, rubber particle volume fraction greater than 20% tends to have inherent voids and cracks. A study by Hartwig *et* al. (2002) reported that these cracks at high rubber particle loading tend to contribute to the damping of the composite material. As the rubber particles volume fraction was increased beyond 15%, the composite tended to foam surface micro-cracks which reduced the strength of the composite but improved damping. This phenomenon could be attributed to vibration energy dissipation at the location of cracks under load until this energy balance is broken due to further fatigue leading to composite failure.

The formation and growth of micro-cracks in brittle epoxide matrix composites contributes to energy dissipation under fatigue load, improving composites' fatigue behaviour.

4.3.3 Effect of combination of rubber particles and glass fibre on composite vibration and damping properties

The graph in Figure 4.27 presents how a hybrid composite consisting of rubber particles size 150 µm and glass fibres at varying proportions affects composite vibrational damping.

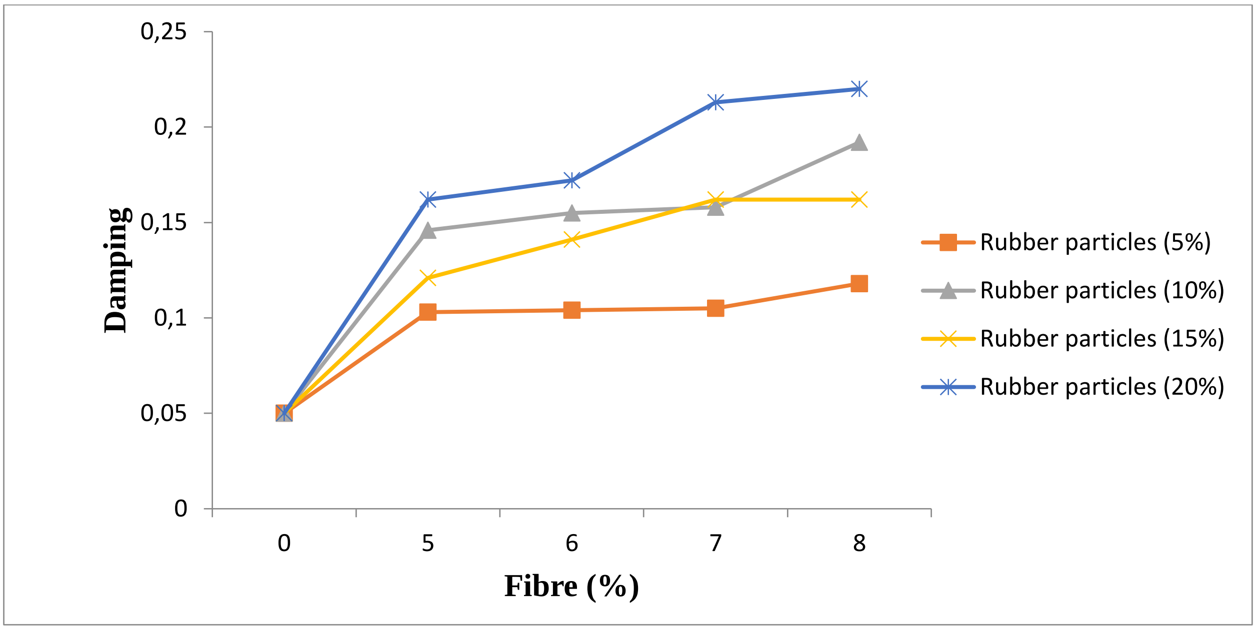

Figure 4.27 - Effect of 150 µm rubber particles and glass fibre on vibration damping properties of composite

Figure 4.27 presents the hybrid composite containing 5% rubber particles and 5% fibreglass damping of 0.103. As the fibreglass volume fraction increased to 6%, there was a minimal increase in damping to 0.104. Further addition of fibreglass above 6% increased composite damping as observed with composite containing 7 % fibreglass giving damping of 0.105. Further increase in fibreglass volume fraction to 8% resulted in an increase in damping to 0.118.

The composite containing 10% rubber particles and 5% fibreglass had damping of 0.146. As the fibreglass volume fraction increased to 6%, there was an increase in the damping to 0.155. Further addition, fibreglass increased the composite damping as observed with 7% fibreglass giving vibrational damping of 0.158. Further increase in fibreglass volume fraction to 8% resulted in a further increase in damping to 0.192.

The composite made up of 15% rubber particles, and 5% fibreglass had a damping of 0.121. There was an increase in composite damping to 0.141, with an increase in fibreglass volume to 6%. The incremental amount of fibreglass volume fraction increased composite damping as observed with a 7% fibre volume fraction, which had a damping of 0.162. Further addition of fibreglass to 8% resulted in constant damping of 0.162.

The composite constituting of 20% rubber particles and 5% fibreglass gave damping of 0.162. The damping of the material increases to 0.172 as the volume fraction of fibreglass increased to 6%. Further addition of fibreglass beyond 5% gave an increase of damping. This is observed with 7% and 8% fibreglass volume fraction giving damping of 0.213 and 0.220 respectively.

The graph in Figure 4.28 presents the effect that a hybrid composite consisting of rubber particles size 300 µm and glass fibres at varying proportions has on composite damping.

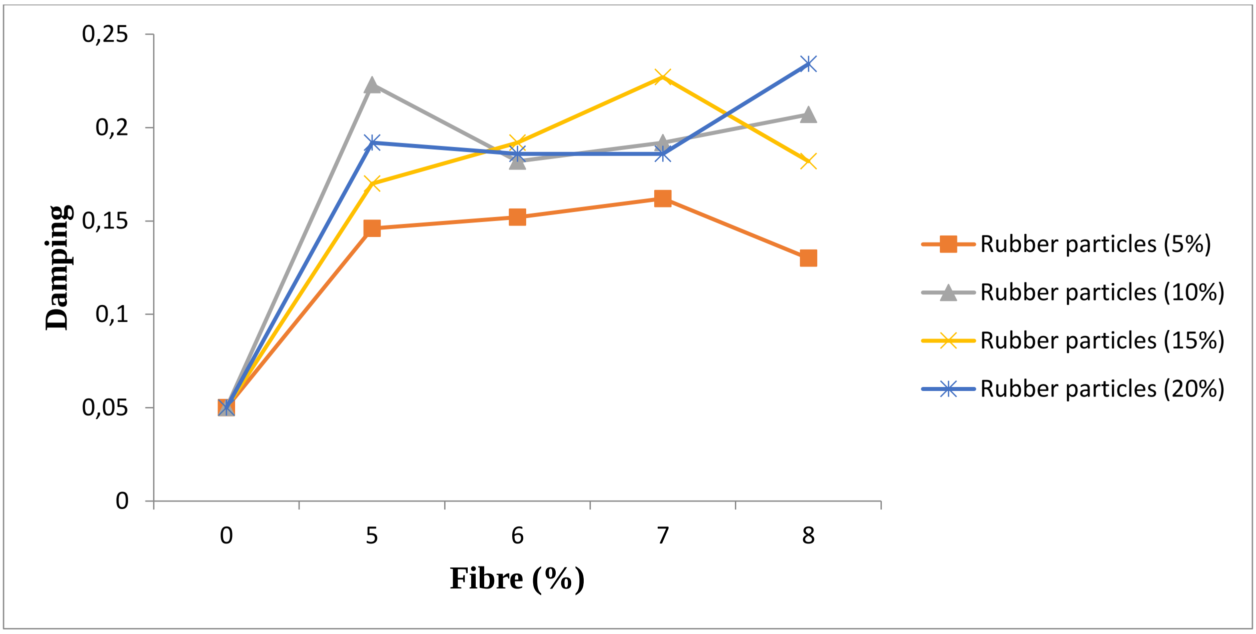

Figure 4.28 – Effects of 300 µm rubber particles and glass fibre on vibration damping properties of composite

Figure 4.28 presents that the hybrid composite containing 5% rubber particles and 5% fibreglass had a damping of 0.146. As the fibreglass volume fraction increased to 6%, there was a minimal increase in damping to 0.152. Further addition of fibreglass above 6% increased composite damping, as observed with the composite containing 7 % fibreglass giving vibrational damping of 0.162. However, a further increase in fibreglass volume fraction to 8% decreased damping to 0.130.

The composite containing 10% rubber particles and 5% fibreglass had vibrational damping of 0.223. As the fibreglass volume fraction increased to 6%, there was a decrease in the damping to 0.182. However, any further addition of fibreglass increased the composite damping as observed with 7% fibreglass, giving a vibration damping of 0.192. Further increase in fibreglass volume fraction to 8% resulted in a further increase in damping to 0.207.

The composite made up of 15% rubber particles and 5% fibreglass damping 0.170. There was an increase in composite damping to 0.192, with an increase in fibreglass volume to 6%. The incremental amount of fibreglass volume fraction increased composite damping, as observed with a 7% fibre volume fraction, which had damping of 0.227. However, there was a reduction in composite damping with the use of 8% fibre volume fraction to 0.182.

The composite containing 20% rubber particles and 5% fibreglass had vibrational damping of 0.192. The damping of the composite material decreased to 0.186 as the fibreglass volume increased to 6%. Adding more fibreglass to 7% did not significantly change the vibrational damping of the composite. However, increasing the fibreglass volume percentage to 8% resulted in a vibrational damping increase to 0.234.

4.3.4. Vibrational Modeling results

Modal analysis bending modes were considered for base vibration perpendicular to the beam (vertical). The vibrational frequencies adopted in the model were between 75 – 1600 Hz, as these are the expected frequencies that the composite will be subjected to.Figure 32 presents that 75 Hz give maximum displacement of 1.21×10^{04} mm, as frequency is increased to 466 Hz displacement decreases to 0.62×10^{5} .Furthermore , the freguency at 1600 Hz give displacement of 0.1×10^{5}mm and beyond 1600Hz displacement became constant.

4.3.4.1 Mode 1 at 75 Hz frequency (1^{st} order bending).

Figure 4.29 presents a modelled specimen that is subjected to a 75Hz frequency mode.

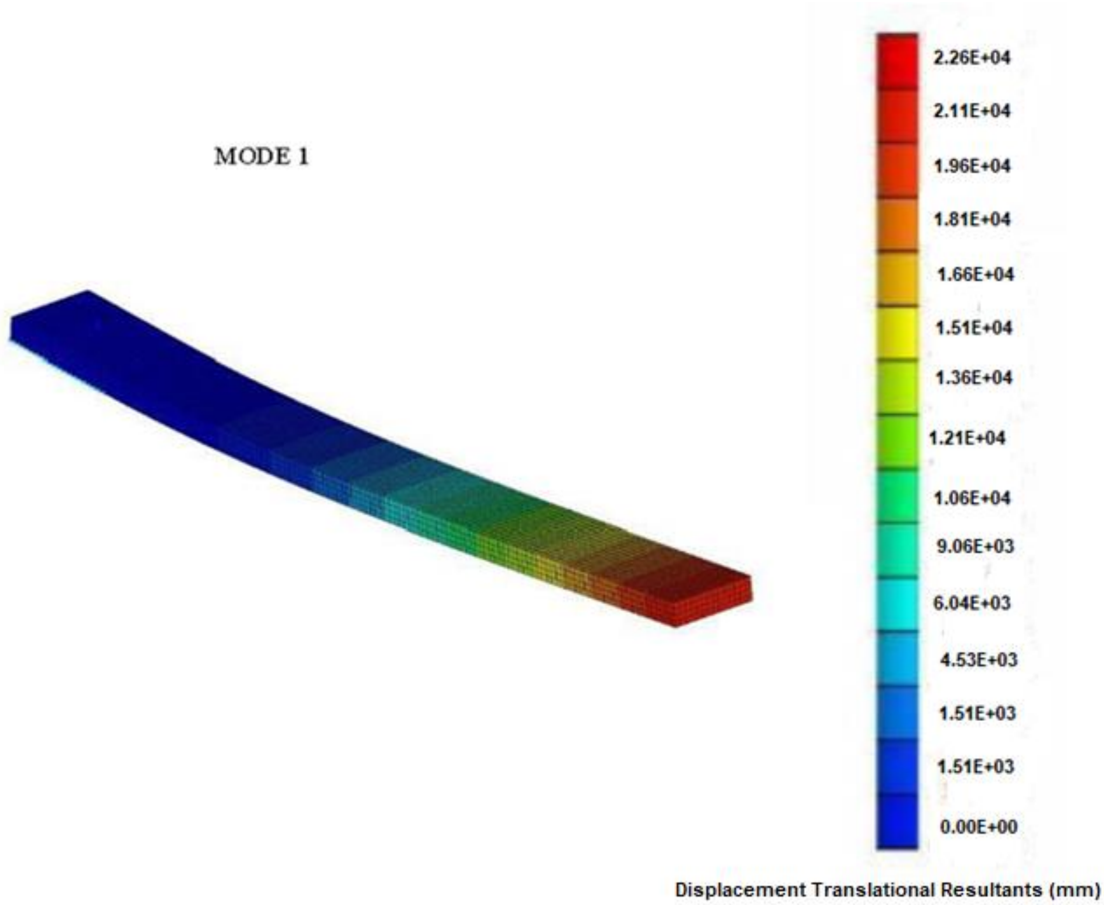

Figure 4.29 – Analysis of bending modes at 75Hz frequency

The colour palate on the specimen represent displacement as the sample flexes under vibration testing. The highest displacement values were at the sample's tip, represented in red in the region of 2.26×10^{04} mm. The medium displacement was obtained in the middle of the sample in light green with a displacement of approximately 1.21×10^{04} mm. The lowest displacement was realised at the clamping point of the sample and is represented by the dark blue colour with a minute displacement of 1.518×10^{3}mm.

4.3.4.2 Mode 3 at 466 Hz

Figure 4.30 presents the bending modes at 466 Hz (2nd order bending). Modal analysis bending modes were considered for base vibration perpendicular to the beam (vertical).

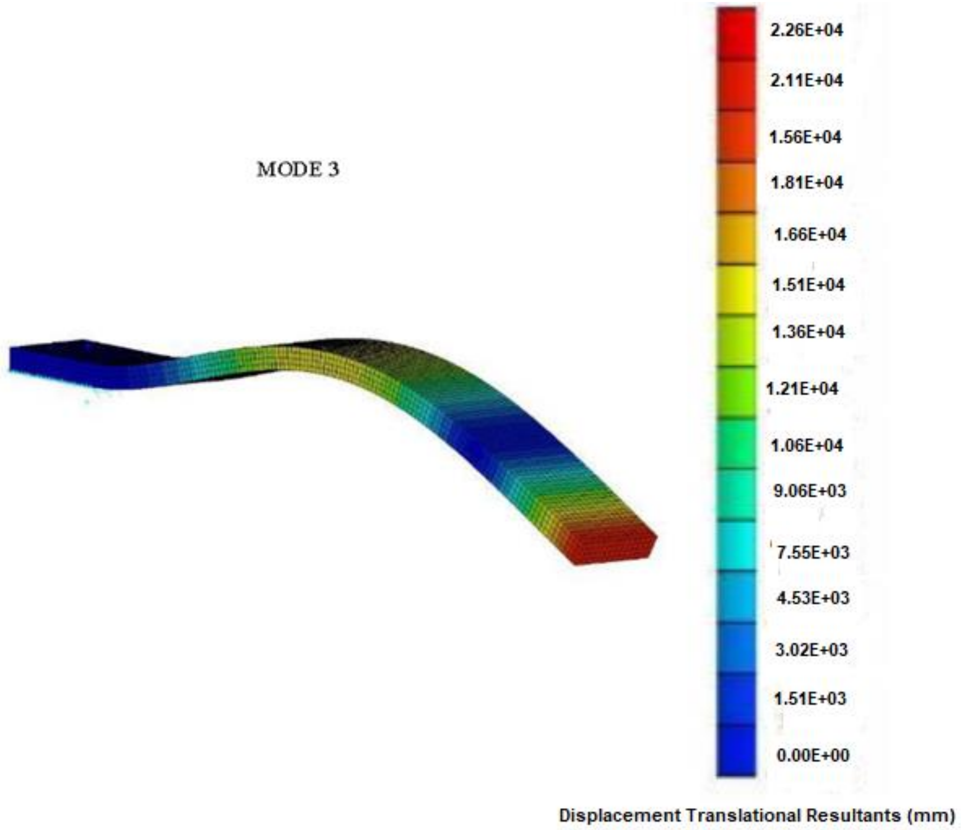

Figure 4.30 - Analysis of bending modes at 466Hz frequency

The highest displacement was realized at the tip of the specimen with a positive displacement of 2.26×10^{04} mm. This was a higher displacement value than the sample subjected to 75 Hz. The medium part of the sample had a positive displacement of 1.216×10^{4} mm, represented in green.

4.4.3.3 Mode 5 at 1300 Hz frequency (3rd order bending)

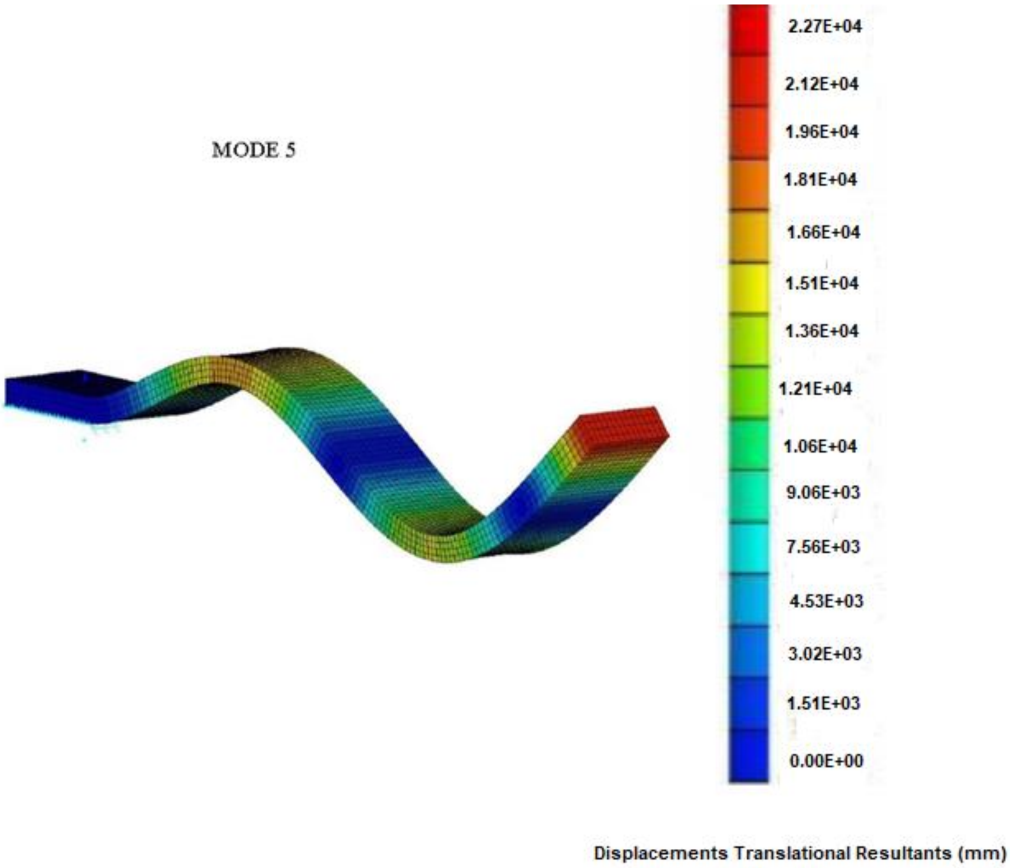

Figure 4.31 – Analysis of bending modes at 1300Hz frequency

The highest displacement of the specimen was realized at the tip, a positive displacement of 2.27×10^{04} mm. This was a higher displacement value compared to the samples subjected to 75 Hz and 466Hz. The medium part of the specimen had a positive displacement of 1.21×10^{04} mm, represented in green. The lowest value of the displacement is found near the clap on the specimen, giving a value of 1.51×10^{03}mm.

4.2.3.1.4 Frequency response chart

Figure 4.32 shows the frequency response against acceleration at the free end of the composite sample.

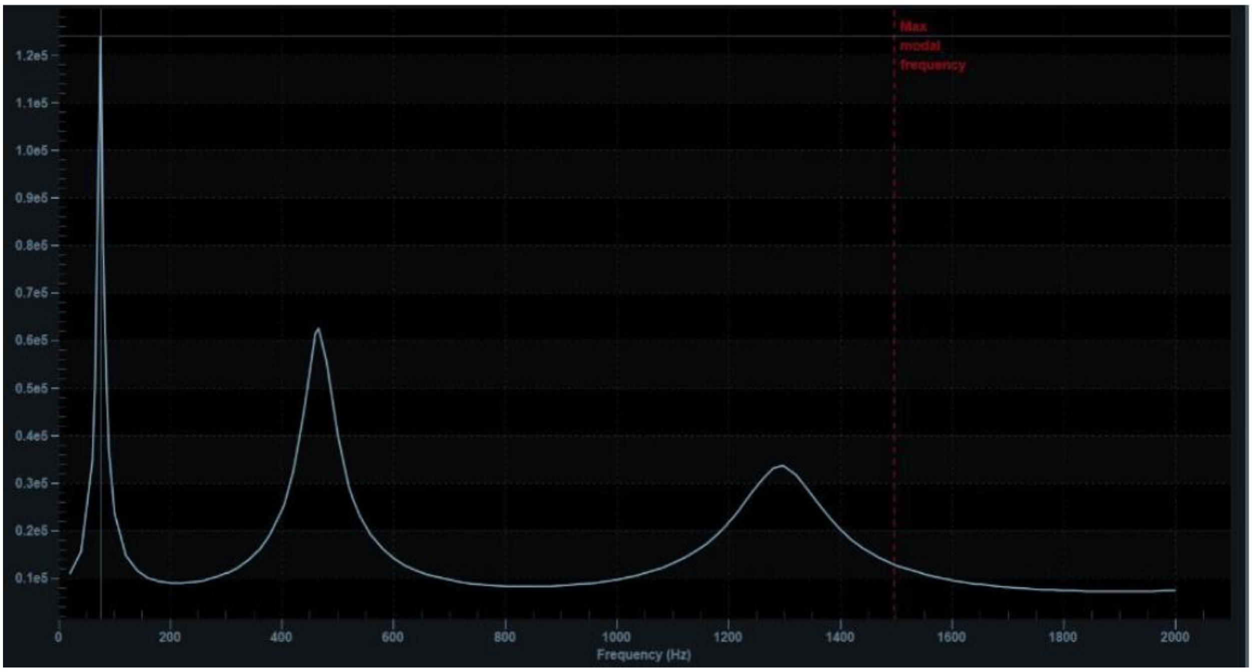

Figure 4.32 – Frequency chart showing acceleration against the frequency of the free end of the sample under vibration test

The graph shows the frequency (Hz) of the vibration on the base axis vs acceleration (mm/s²), at the free end of the beam. There are amplification peaks at the frequency of each mode mentioned above, with the most prominent peak at Mode 1 and then progressively lower for the higher modes. The highest acceleration was recorded at a frequency of 75 Hz and gave acceleration at the free end of the specimen of 1.268×10^5 mm/s^2. The frequency of 466 Hz gave an acceleration of 0.62×10^5 mm/s^2. The frequency of 1300 Hz gave an acceleration of 0.35×10^5 mm/s^2. The general trend observed was that increased frequency resulted in a decrease in acceleration of the free end of the sample. Vibration damping was determined from the value of acceleration for each mode. The test frequency band was selected to cover at least one prominent peak.

4.4 Optimization

The experimental results were analysed using Minitab software, and a model was developed to optimise the results. The developed model was then validated experimentally.

4.4.1 Optimum composite regions

This section discusses the regression analysis of mechanical characterization results for tensile strength, compression strength, flexural strength and vibrational damping properties.

4.4.1.1 Regression analysis

Analysis of Variance (ANOVA) was carried out on Minitab software for the tensile, compression, flexural strength, hardness and vibration responses

4.4.1.2 Tensile Strength

The ANOVA analysis of tensile strength is reported in Table 4.2.

Table 4.2 - ANOVA for composite tensile strength

Source	DF	Adj ss	Adj MS	F-Value	P-Value	Summary
Model	9	207.305	341.601	6.00	0.000	S = 1.95883 R^2 = 60.69% Adj R^2 - 50.58%
Linear	3	74.566	0.0039	6.48	0.001	
A	1	0.004	71.0529	0.00	0.975	
B	1	71.053	13.1527	18.52	0.000	
C	1	13.153	19.3244	3.43	0.073	
Square	3	57.973	38.0280	5.04	0.005	
A*	1	38.028	12.5006	9.91	0.003	
B*B	1	12.501	5.6381	3.26	0.080	
C*C	1	5.638	6.9174	1.47	0.234	
2-Way Interaction	3	20.752	0.1271	c	0.165	
A *B	1	0.127	9.7107	0.03	0.857	
A*C	1	9.711	11.3356	2.53	0.121	
B*C	1	11.336	3.8370	2.95	0.094	
Error	35	134.295				
Total	44	341.601				

A-Rubber particle volume fraction; B – Fibre volume fraction; C – Rubber particle size MS – Mean square; DF – Degree of freedom; SS – the sum of squares; R^2 – Coefficient of determination; Adj R^2 – Adjusted coefficient of determination

From Table 4.2, it was observed that fibre mass fraction was statistically insignificant for the linear terms, according to the t-test having a p-value of less than 0.05. However, the rubber particle fibre fraction was statistically significant, having a p-value of 0.975. The particle size was statistically significant, having a p-value of 0.073. The effects of the interaction between the squares of ABC were statistically significant. The R^2 value shows that the model explains 60.69%, indicating that the model accurately represents fits the data.

By applying multiple regression analysis, the following tensile strength regression equation was obtained

$$\begin{aligned}\text{Tensile strength} &= 7.50 + 0.698\,B + 0.314\,A - 0.0280\,C.A + 0.0895\,.B\,.B \\ &+ 0.000098\,.C.C + 0.0035.A\,.B - 0.001113\,.A.C - 0.00253\,.B\,.C\end{aligned} \qquad \{4.1\}$$

4.4.1.2 Compressive strength

The ANOVA analysis of compressive strength is reported in Table 4.3.

Table 4.3 - ANOVA for composite compression strength

Source	DF	Adj ss	Adj MS	F-Value	P-Value	Summary
Model	8	4949.23	618.654	28.29	0.000	S = 4.67674
Linear	3	1390.30	463.434	21.19	0.000	R^2 = 86.60%
A	1	912.04	912.042	41.70	0.000	Adj R^2 – 83.58%
B	1	184.11	184.114	8.42	0.006	
C	1	6.26	6.263	0.29	0.596	
Square	2	309.81	154.907	7.08	0.003	
A* A	1	79.30	79.298	3.63	0.065	
B*B	1	241.69	241.685	11.05	0.002	
2-Way Interaction	3	580.64	193.548	8.85	0.000	
A *B	1	564.16	564.159	25.79	0.000	
A*C	1	8.37	8.367	0.38	0.540	
B*C	1	0.97	0.967			
Error	35	765.52	21.872			
Total	43	5714.78				

A-Rubber particle volume fraction; B – Fibre volume fraction; C – Rubber particle size MS – Mean square; DF – Degree of freedom; SS – the sum of squares; R^2 – Coefficient of determination; Adj R^2 – Adjusted coefficient of determination

From Table 4.3, it was observed that fibre mass fraction and rubber particle volume were statistically insignificant for the linear terms, according to the t-test having a p-value of less than 0.05. However, rubber particle size was statistically significant, having a p-value of 0.596. The effects of the interaction between the square of ABC were statistically insignificant and significant. Rubber particles volume fraction and rubber particles volume fraction interaction were statistically significant, giving a p value of 0.065. However, fibreglass and fibreglass were statically significant, giving a p-value of less than 0.05. The interaction between the square of adj R^2 was 50.58, and The R^2 value shows that the model explains 86.60%, indicating that the model accurately represents the data.

By applying multiple regression analysis, the following compression strength regression equation was obtained

$$\text{Compression strength} = 22.70 + 0.505\,A + 6.45\,B - 0.0193C - 0.0392\,A.A - 0.394\,B.B - 0.2307\,A.B + 0.2307.A.B + 0.00103\,.A.C + 0.00074.B.C \quad \{4.2\}$$

4.4.1.3 Flexural Strength

The ANOVA analysis of flexural strength is reported in Table 4.4.

Table 4.4 - ANOVA for composite flexural strength

Source	DF	Adj ss	Adj MS	F-Value	P-Value	Summary
Model	8	2884.99	360.624	8.15	0.000	S = 6.65205
Linear	3	1326.63	442.209	9.99	0.000	R^2 = 65.05%
A	1	342.05	342.051	7.73	0.009	Adj R^2 – 57.08%
B	1	577.14	5771.135	13.04	0.001	
C	1	25.23	25.233	0.57	0.455	
Square	2	111.26	55.632	1.26	0.297	
A* A	1	105.59	105.589	2.39	0.131	
B*B	1	7.93	7.925	0.18	0.675	
2-Way Interaction	3	140.01	46.669	1.05	0.381	
A *B	1	126.46	126.461	2.86	0.100	
A*C	1	1.79	1.786	0.04	0.842	
B*C	1	9.98	9.976	0.23	0.638	
Error	35	1548.74	44.250			
Total	44	4433.74				

A-Rubber particle volume fraction; B – Fibre volume fraction; C – Rubber particle size MS – Mean square; DF – Degree of freedom; SS – the sum of squares; R^2 – Coefficient of determination; Adj R^2 – Adjusted coefficient of determination

From Table 4.4, it was observed that fibre mass fraction was statistically insignificant for the linear terms, according to the t-test having a p-value of less than 0.05. Furthermore, rubber particle, fibre fraction and particle size were statistically significant, having a p-value of 0.009, 0.001 and 0.455, respectively. The effects of the interaction between the square of ABC were statistically significant, and insignificant rubber particles and rubber particles gave a value of 0.131, which is statistically significant. Fibreglass gave 0.675, which is statically insignificant, giving a p-value greater than 0.05. However, the interaction between the square of adj R^2 was 50.58, and The R^2 value shows that the model explains 65.05%, indicating that the model accurately represents the data.

By applying multiple regression analysis, the following flexural strength regression equations were obtained

$$\begin{aligned} \text{Flexural strength} \\ &= 15.7 + 0.772A + 3.94\,B + 0.0021\,C - 0.0452.A.A - 0.071\,.B\,.B \\ &- 0.1092A\,.B - 0.1092.A.B - 0.00048\,.A.C - 0.00237\,.B\,.C \end{aligned} \quad \{4.3\}$$

4.4.1.4 Vibrational damping

The ANOVA analysis of vibrational damping is reported in Table 4.5.

Table 4.5 - ANOVA for composite vibrational damping

Source	DF	Adj ss	Adj MS	F-Value	P-Value	Summary
Model	9	0.086457	0.009606	17.03	0.000	S = 0.0237515 R^2 = 81.41% Adj R^2 - 76.63%
Linear	3	0.056340	0.018780	33.29	0.000	
A	1	0.026193	0.026193	46.43	0.000	
B	1	0.007172	0.007172	12.71	0.001	
C	1	0.000001	0.00001	0.00	0.974	
Square	3	0.002584	0.000861	1.53	0.225	
A* A	1	0.001159	0.00159	2.05	0.161	
B*B	1	0.000041	0.000041	0.07	0.789	
C*C	1	0.001479	0.001479	2.62	0.114	
2-Way Interaction	3	0.003581	0.001194	2.12	0.116	
A *B	1	0.000763	0.000763	1.35	0.253	
A*C	1	0.002653	0.000763	4.70	0.037	
B*C	1	0.000042	0.002653	0.07	0.787	
Error	35	0.019745	0.000042			
Total	44	0.106202	0.000564			

A-Rubber particle volume fraction; B – Fibre volume fraction; C – Rubber particle size MS – Mean square; DF – Degree of freedom; SS – the sum of squares; R^2 – Coefficient of determination; Adj R^2 – Adjusted coefficient of determination

From Table 4.5, it was observed that fibre mass fraction and fibreglass were statistically insignificant for the linear terms, according to the t-test having a p-value of less than 0.05. However, the rubber particle size fraction was statistically significant, having a p-value of 0.974. The interaction effects between the square of AB and C were statistically significant. However, the interaction between the square of adj R^2 was 50.58, and The R^2 value shows that the model explains 81.41%, indicating that the model accurately represents fits the data.

By applying multiple regression analysis, the following vibrational damping regression equation was obtained

$$Dampimg = 0.0500 + 0.01029.A + 0.00363.B - 0.000279.C - 0.000150\,.A\,.A + 0.000162\,.B.B + 0.000002.C\,.C + 0.000268\,.A\,.B - 0.000018\,.A.C - 0.000005\,.B\,.C \quad \{4.4\}$$

4.4.1.5 Hardness

The ANOVA analysis of hardness is reported in Table 4.6.

Table 4.6 - ANOVA for composite hardness

Source	DF	Adj ss	Adj MS	F-Value	P-Value	Summary
Model	8	106088	13261.1	2.67	0.021	S = 70.5164 R^2 = 37.87% Adj R^2 – 23.67%
Linear	3	77484	25828.0	5.19	0.004	
A	1	30	30.3	0.01	0.938	
B	1	5687	5686.9	1.14	0.292	
C	1	55773	55773.3	11.22	0.002	
Square	2	9183	4591.6	0.92	0.407	
A* A	1	3003	3003.3	0.60	0.442	
B*B	1	6539	6538.9	1.31	0.259	
2-Way Interaction	3	5039	1679.7	0.34	0.798	
A *B	1	668	667.6	0.13	0.716	
A*C	1	3578	3578.4	0.72	0.402	
B*C	1	513	512.9	0.10	0.750	
Error	35	174040	4972.6			
Total	43	280128				

A-Rubber particle volume fraction; B – Fibre volume fraction; C – Rubber particle size MS – Mean square; DF – Degree of freedom; SS – the sum of squares; R^2 – Coefficient of determination; Adj R^2 – Adjusted coefficient of determination

From Table 4.6, it was observed that particle size was statistically insignificant for the linear terms, according to the t-test having a p-value of less than 0.05. However, rubber particle was statistically significant and gave a value of 0.938, and fibre fraction was statistically significant, with a p-value of 0.292. The effects of the interaction between the square of ABC were statistically significant. However, the 2-way interaction indicates that rubber particles and fibreglass and the particle size were statistically significant. However, the rubber particles' volume fraction and particle size were statically insignificant. The R2 value shows that the model explains 37.87 %, indicating that the model inaccurately represents fits the data.

By applying multiple regression analysis, the following hardness equation was obtained

$$Hardness = 7.15 - 6.83.A - 5.2.B - 0.717.C + 0.241.A.A + 2.05.B.B - 0.251.A.B + 0.0214.A.C - 0.0170.B.C \quad \{4.5\}$$

4.4.2 Overlaid contour plot

This section discusses the optimum regions for the various mechanical properties, which include tensile strength, compression strength, flexural strength and hardness in the form of contour plots. Furthermore, there is a plot for the optimum regions for vibrational damping.

4.4.2.1 Tensile

The contour plot Figure 4.33 shows the tensile strength of a hybrid composite that is fabricated from rubber particles size 150 µm, polyester resin and fibreglass.

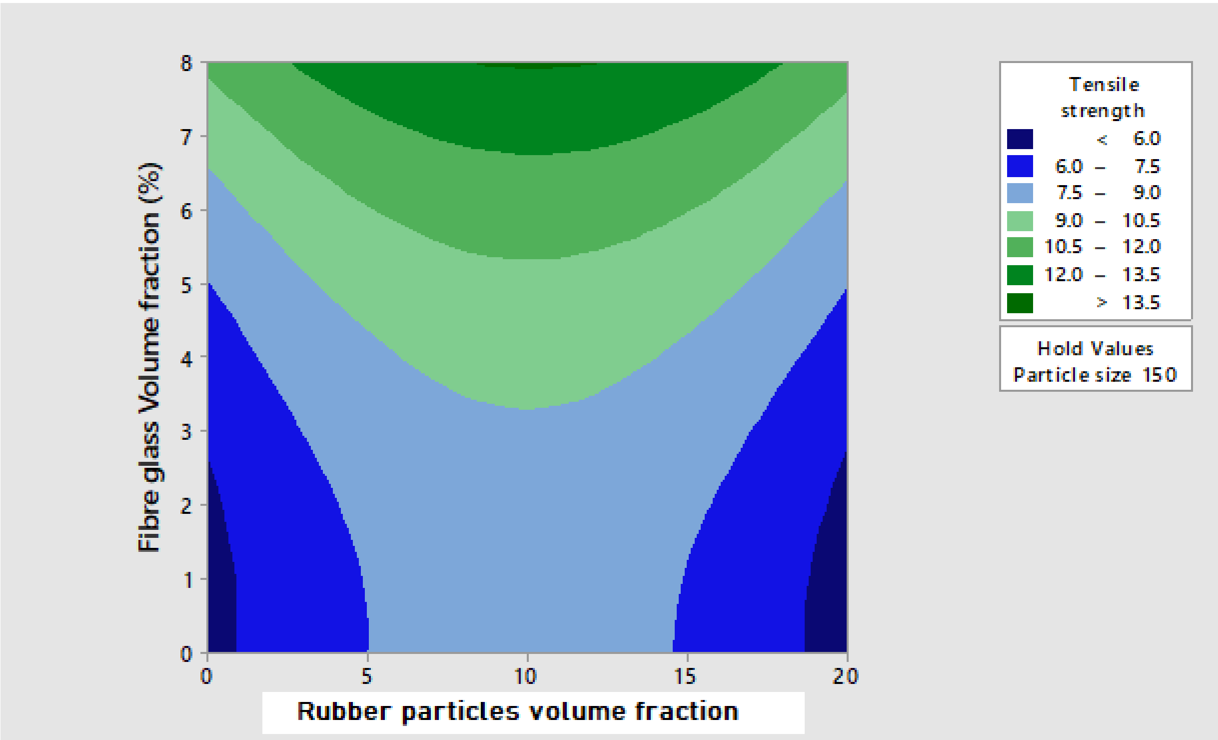

Figure 4.33 - Contour plot of tensile strength against fibreglass volume fraction (%), rubber particles

The highest values of rating for tensile strength, which gave the strength of greater than 13.5 MPa, are in the upper centre of the plot between 5% and 16% rubber particle volume fraction and limited to 6.8 – 8% fibreglass loading. The lowest values of rating tensile strength are in the lowest left and right corners of the plot, which corresponds with low values of both fibreglass (0 – 2.5%) and rubber particles volume fraction of between 0-0.5% and 19 -20%.

4.4.2.2 Compression strength

The contour plot Figure 4.34 shows compression strength of hybrid composite that is fabricated from rubber particles size 150 µm, polyester resin and fibreglass.

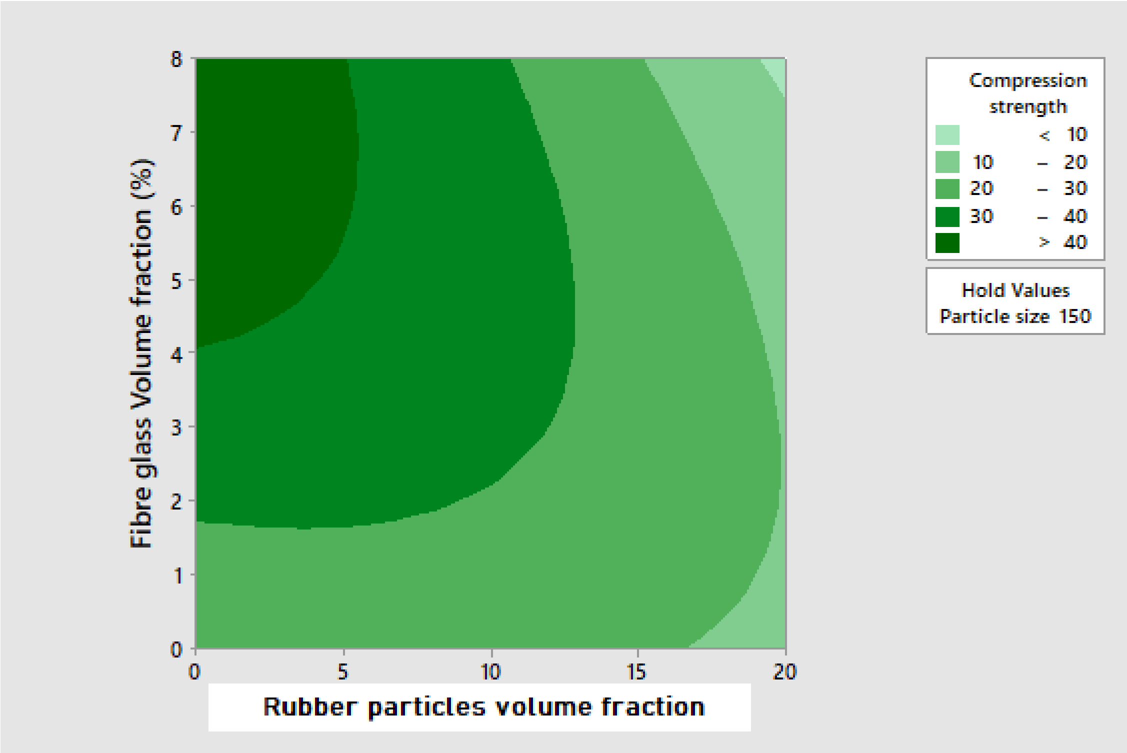

Figure 4.34 - Contour plot of compression strength against fibreglass volume fraction (%), rubber particles

The highest ratings for the hybrid composite's compression strength gave greater than 40 MPa in the plot's upper right corner between 0% and 5% rubber particle volume fraction and limited to 4 – 8% fibreglass loading, which are also the highest percentage values for both fibreglass volume fractions. The low values of both fibreglass between (0 – 8%) and rubber particles volume fraction of between 17 -20%.

4.4.2.3 Flexural strength

The contour plot Figure 4.35 shows a flexural strength of hybrid composite that is fabricated from rubber particles size 150 µm, polyester resin and fibreglass.

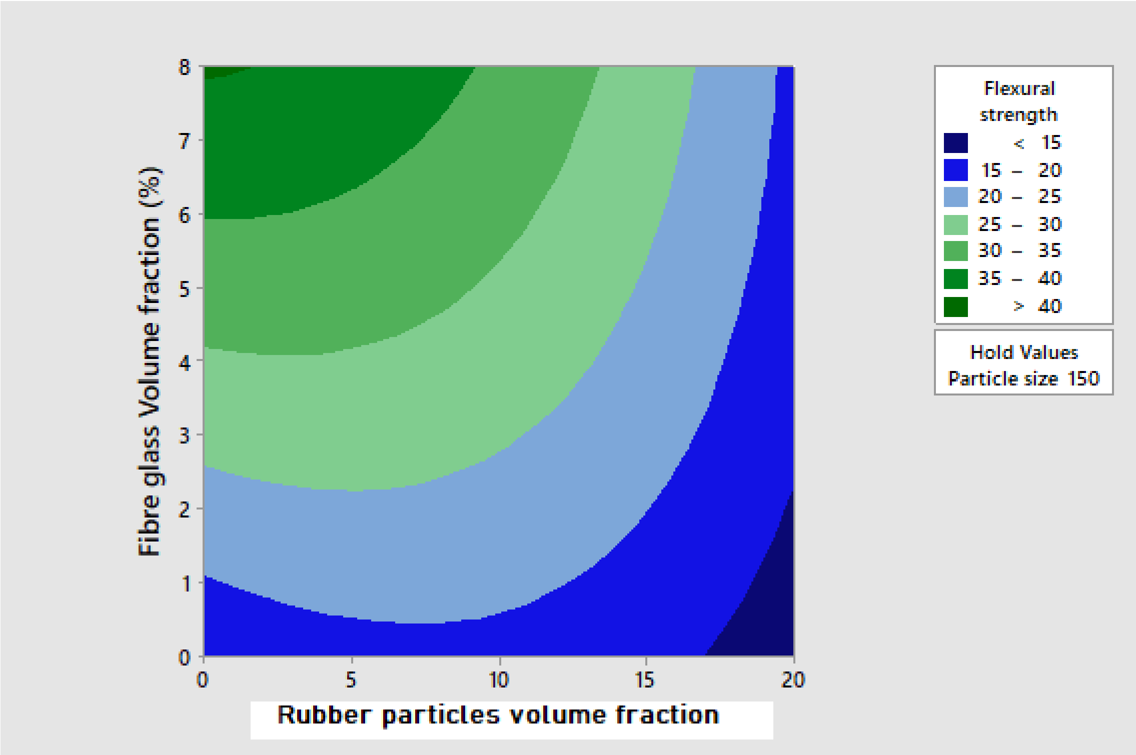

Figure 4.35 - Contour plot of flexural strength against fibreglass volume fraction (%), rubber particles

In the upper left corner of the plot, which corresponds to the high values of both fibreglass volume fractions in %, are the highest ratings for flexural strength of the hybrid composite, giving flexural strength greater than 40 MPa. The lowest rating values are in the lower left corner of the plot, giving flexural strength less than 15 MPa, that is, between 17 - 20% volume fractions of rubber particles at the lowest values of fibreglass of 0 - 2%.

4.4.2.4 Hardness

The contour plot Figure 4.36 shows the hardness of a hybrid composite that is fabricated from rubber particles size 150 µm, polyester resin and fibreglass.

Figure 4.36 - Contour plot of hardness against fibreglass volume fraction (%), rubber particles

The highest values of rating for the hardness of hybrid composite are in the upper right corner of the plot between 0 -4% of volume fraction of rubber particles and between fibreglass volume fraction of 7.2 – 8 %, which correspond with the high values of both fibreglass volume fractions in percentage. The lowest hardness values are in the lowest left corner of the plot and gave hardness of less than600 between volume fraction of 0 - 17%, at a volume fraction of fibreglass between 0 -5.2% which corresponds with low values of both fibreglass and rubber particles volume fraction.

4.4.2.2 Damping

The contour plot Figure 4.37 shows the damping of hybrid composite fabricated from rubber particles size 150 µm, polyester resin and fibreglass.

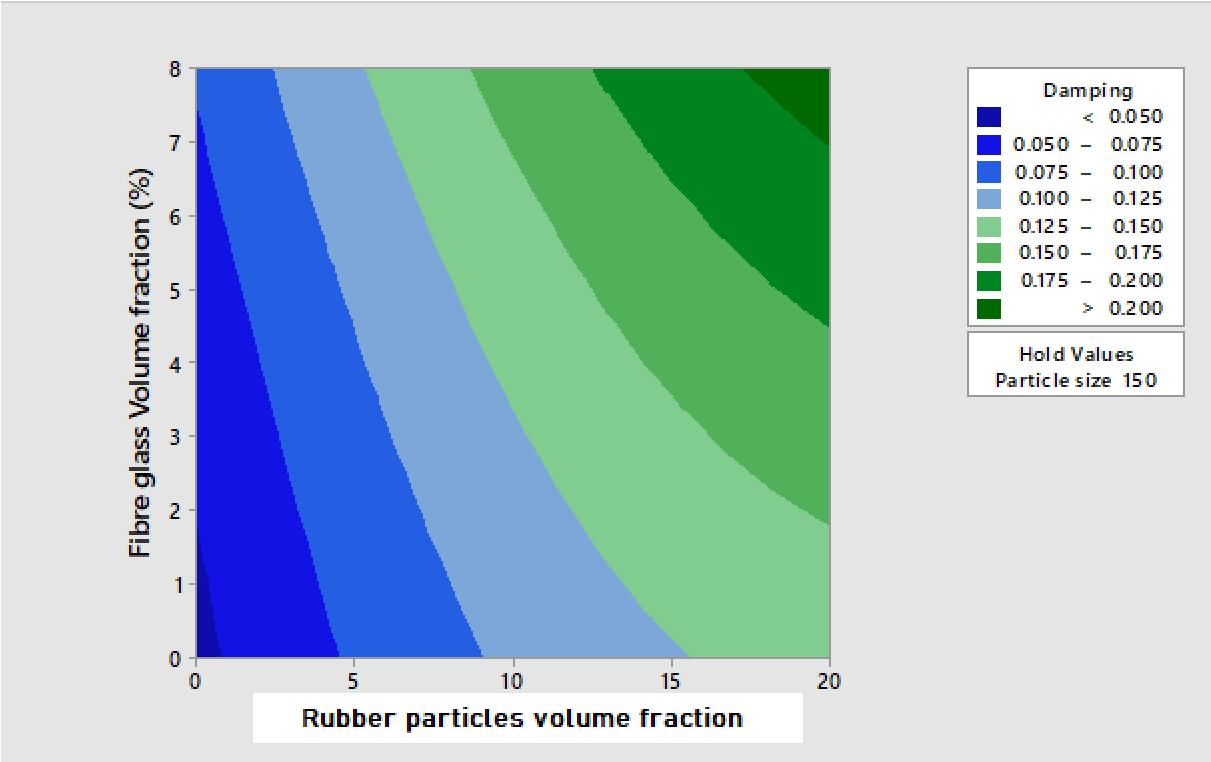

Figure 4.37 - Contour plot of damping against fibreglass volume fraction (%), rubber particles

The highest values of rating in the plot gave damping of greater than 0.2 in the upper right corner of the plot in between 17% and 20% rubber particle volume fraction and limited to 7 – 8% fibreglass loading. The lowest values of rating damping are in the lowest right corners of the plot, which corresponds with low values of both fibreglass (0 – 1.7%) and rubber particles volume fraction of between 0 - 1%.

4.4.3 Numerical Optimization

The optimization plot, as shown in Figure 4.38, displays the fitted values for the predictor settings

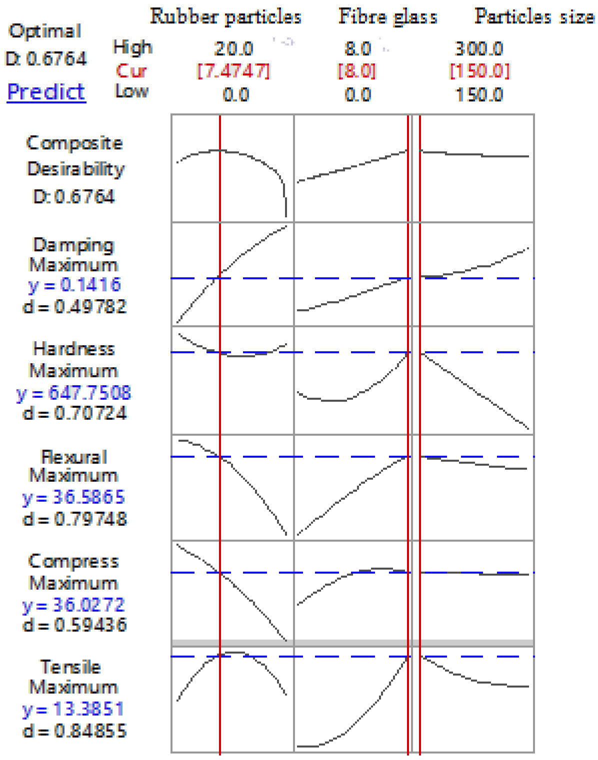

Figure 4.38 - Optimization plot for mechanical and damping properties

The composite desirability in the model was recorded as 0.6764, which was greater than 0.5, indicating that the model accurately optimises the overall responses. The optimum mix design from the model is 7.4747% of 150 um rubber particles at an 8% fibreglass volume fraction. From Figure 4.39, increasing the rubber particle content steadily increases vibrational damping. However, an increase in rubber particles lowers the composite's hardness, flexural strength and compressive strength. An incremental amount of rubber particles increases the tensile strength to an optimum point, and beyond that, the tensile strength is reduced.

The addition of fibres to the composite increased all the mechanical strength properties and vibrational properties, as shown in Figure 4.39. Increasing rubber particle size has different responses. Increasing rubber particle size increases damping value but decreases hardness, compression flexural and tensile strength. Therefore, the optimal setting is in the range of (150.0), which is a compromise between conflicting goals. This result suggests that rubber particles less than 150 should be considered to maximize mechanical strength while marinating composite damping.

The graphs show that when particle size is crease, damping increases. However, strength would decrease.

4.4.3.1 Response prediction

The standard error of fit estimates the variation in the estimated mean responses for the specified variable settings. Vibrational damping, flexural strength, compressive strength and tensile strength had a low standard error of fit, indicating that with 95% confidence, the mean is within range, as shown in Table 4.7. However, hardness had a high standard error due to the unpredictability of its results.

Table 4.7 - Multiple response prediction

Response	Fit	SE Fit	95% CI	95% PI
Vibrational Damping	0.14160	0.00983	(0.12164, 0.16156)	(0.08941, 0.19378)
Hardness	647.80	29.20	(588.5, 707.0)	(492.8, 802.7)
Flexural strength	36.59	2.75	(31.00, 42.18)	(21.97, 51.20)
Compression strength	36.03	1.94	(32.10, 39.96)	(25.75, 46.30)
Tensile strength	13.39	0.81	(11.739, 15.031)	(9.081, 17.689)

The 95% confidence interval for all the responses is within range for all the experimental data. The confidence intervals for all responses are relatively narrow, implying strong confidence in the mean of future values.

The 95% prediction interval assesses the prediction precision. The prediction intervals are all within acceptable boundaries for the responses except for hardness. The low prediction interval for hardness could be attributed to the lack of composite homogeneity giving variable results due to the nature of random laying. The prediction interval has a wider range than the confidence interval due to uncertainty in predicting a single response compared to a mean response. The mean damping is 0.14160, and the range of likely values for a single future value is 0.08941 to 0.19378. The mean hardness is 647.8, and the range of likely values for a single future value is 492.8 to 802.7.

4.4.4 Model validation

The model validation was done by fabricating the composite using optimum values obtained from the model. The rubber particles of size 150 µm at a volume fraction of 7.476% reinforced with 8% fibreglass was used to fabricate the composite. Table 4.8 shows the deviation of experimental results from the model.

Table 4.8 - Model validation

Properties	**Units**	**Optimum results**	**Experimental results**	**Absolute relative error**
Tensile strength	MPa	13.385	13.106	2.0%
Compression strength	MPa	36.027	36.152	0.4%
Flexural strength	MPa	36.587	37.001	1.1%
Hardness	Leeb	647.751	800.00	19 .0%
Damping		0.142	0.146	2.7%

The standard deviation of the results was low for all the parameters except hardness. This low standard deviation showed a good fit between the experimental and predicted optimum results. The higher standard deviation for hardness was of concern; however, it was within acceptable limits.The standard devation for hardness should be between 4% and 95%.

Chapter 5: Conclusion and recommendations

5.1 Introduction

The current study aimed to fabricate a composite railway sleeper material from waste tyre rubber particles, fibreglass and polyester resin with enhanced vibrational damping and increased structural strength. The major conclusions reached and recommendations are outlined in this chapter.

5.2 Conclusions

- The maximum rubber particle moisture absorption of 0.575% was recorded after 2 hours at a temperature of 135 ^{0}C. Railway sleeper composites are exposed to harsh operating conditions, including frequently being in contact with or submerged in water. Low moisture absorption in composites is desirable to minimize swelling of the composites, inadvertently altering their dimensional stability. The low moisture absorption of the rubber particles was desirable, preventing ingress of ground that could contain heavy metals such as magnesium, calcium, and potassium, which can aide in the environmental degradation of the composite.
- When observed under SEM, the rubber particles showed a heterogeneous appearance, with the surface of the particles being rough, elongated, and porous. The rubber particles were observed to consist of particles having varying sizes making it difficult to approximate the specific size of the particles
- A hybrid composite was fabricated from fibreglass, rubber particles and polyester resin according to a 3-factor and 2-level full factorial experimental design. The fibreglass volume fraction was varied in five levels between 5% and 8%, and the rubber particle volume fraction was varied between 5 and 20% for two rubber particle sizes of 150 µm and 300 µm. The composite fabrication method used in the study was hand lay-up.
- The composite consisting of fibreglass only had a maximum tensile at 8 % fibre content giving tensile strength of 12.13 MPa. The composite consisting of rubber particles only had a maximum tensile strength of 8.86 MPa at 10% of 150 µm rubber particle loading. The composite consisting of a combination of rubber particles and fibreglass gave full tensile strength of 15.31 MPa at 8% fibre content and at 300 µm and 10% rubber particle content. The hybrid composite fabricated increased the structural tensile strength while growing damping for composite to eliminate aggressive forces that are applied on composite railway sleepers by heavily loaded trains.
- The highest compression strength with fibreglass only was 55.164 MPa at 8% fibre loading. The maximum tensile strength recorded on rubber particles only was 36.515 MPa at a 5%

rubber particle volume fraction. The combination of rubber particles of size 150 µm and fibreglass gave maximum compression strength of 44.35 MPa at 5 % rubber content and 6 % fibreglass.

- The composite consisting of fibreglass only had a maximum flexural at 8% fibre content giving a strength value of 42.658 MPa. The composite consisting of rubber particles only had a maximum flexural strength of 20.369 MPa at 5% of 150 µm rubber particles. The composite consisting of a combination of rubber particles and fibreglass gave maximum flexural strength of 44.45 MPa at 7% fibre content and at 5% rubber particles. The flexural strength of the composite sleeper was increased while increasing the structural damping of the composite to rebound forces that are exerted on the railway composite.
- The maximum hardness measured on composite containing fibreglass only was 745 Leeb, and on rubber particles, only composite was 659 Leeb. The hybrid composite consisting of fibreglass and rubber particles gave a maximum hardness value of 759 Leeb at 8% fibre and 20% 150 µm rubber particle content.
- It was observed that the incorporation of 150 µm rubber particles increased vibrational damping of the composite to a maximum of 0.162 at a 20% rubber particle volume fraction. Furthermore, using bigger rubber particles such as the 300 µm further positively affected vibrational damping. Maximum vibrational damping of 0.202 was realized at 10% 300 µm rubber particle volume fractions. However, the increase in vibrational damping negatively affected the composite's mechanical strength properties. This decrease necessitated a compromise on the optimum properties of the composite.
- The ANOVA test showed the model's accuracy in predicting tensile strength, compression strength, flexural strength, and vibrational damping, as shown by R^2 values of 60.69%, 86.60%, 60.05% and 81.41 %, respectively. However, the model was not reliable for hardness which had an R^2 value of 37.87%.
- The optimum composite mix design obtained from the developed model was 7.4747% of 150 um rubber particles and 8% fibreglass volume fraction. These factors correspond to responses 13.385 MPa, 36.027 MPa, 36.587 MPa, 647.751 Leeb and 0.142 for tensile, compressive, flexural strength, hardness and vibrational damping.

5.3 Recommendation for future work

There is a need for further research into the use of a wide range of rubber particle sizes 75 µm and its effects on the vibrational damping and mechanical properties of the composite railway sleeper. Furthermore, there is a need to study the effects of various synthetic and natural rubber types on composite properties.

References

A, Suresh Kumar, and M Muthukannan. 2019. “An Examination on Performance of Railway Sleepers,” no. 4: 37–44. https://doi.org/10.35940/ijrte.D1010.1284S219.

Ab, Sicomp. n.d. “High Quality Flax Fibre Composites Manufactured by the Resin Transfer Moulding Process” 20 (07). https://doi.org/10.1106/CA5A-6FAX-VJRB-80P0.

Abu-jdayil, Basim, Abdel-hamid I Mourad, and Atif Hussain. 2016. “Investigation on the Mechanical Behavior of Polyester-Scrap Tire Composites.” *Construction and Building Materials* 127: 896–903. https://doi.org/10.1016/j.conbuildmat.2016.09.138.

Acoustics, Environmental. 2009. “Standard Test Method for Measuring Vibration-Damping Properties of Materials 1.” *Annual Book of ASTM Standards* 05 (Reapproved 2017): 1–14. https://doi.org/10.1520/E0756-05R17.2.

Allan, Manalo, and Aravinthan Thiru. 2012. “Behavior of Full-Scale Railway Turnout Sleepers from Glue-Laminated Fiber Composite Sandwich Structures.” *Journal of Composites for Construction* 16 (6): 724–36. https://doi.org/10.1061/(ASCE)CC.1943-5614.0000307.

Andersons, J, and R Joffe. 2011. “Composites : Part A Estimation of the Tensile Strength of an Oriented Flax Fiber-Reinforced Polymer Composite.” *Composites Part A* 42 (9): 1229–35. https://doi.org/10.1016/j.compositesa.2011.05.005.

Araújo, Edcleide M., Kasselyne D. Araújo, Osanildo D. Pereira, Pollyana C. Ribeiro, and Tornás J.A. De Melo. 2006. “Fiberglass Wastes/Polyester Resin Composites: Mechanical Properties and Water Sorption.” *Polimeros* 16 (4): 332–35. https://doi.org/10.1590/S0104-14282006000400014.

Reiff R, Walker R ,Schreiber P, wilson, and Thompson H“Assessment of Rail Seat Abrasion Patterns and Environment.” 2012, no. May.

ASTM. 1998. “Standard Test Method for Equotip Hardness Testing of Steel Products 1.” *Current* 03 (September): 1–5. https://doi.org/10.1520/A0956-12.2.

ASTM 2014. “D6641: Standard Test Method for Compressive Properties of Polymer Matrix Composite Materials Using a Combined Loading Compression (CLC) Test Fixture” i: 1–13.

https://doi.org/10.1520/D6641.

ASTM 2019. "Standard Test Method for Determining the Flexural Strength of a Geosynthetic Cementitious Composite Mat (GCCM) Using the Three-Point Bending Test 1," 1–6. https://doi.org/10.1520/D8058-19.2.

Awuchi, Chinaza Godswill, Erick Nyakundi Ondari, Chukwuka U Ogbonna, Anjani K Upadhyay, Katarzyna Baran, Charles Odilichukwu R Okpala, Małgorzata Korzeniowska, and Raquel P F Guiné. 2021. "Mycotoxins Affecting Animals, Foods, Humans, and Plants: Types, Occurrence, Toxicities, Action Mechanisms, Prevention, and Detoxification Strategies—A Revisit." *Foods* 10 (6): 1279.

B, Ridout. 2013. "Timber Decay in Buildings: The Conservation Approach to Treatment.," no. Taylor & Francis.

Bakhareu T, Struble LJ. 1997. "Microstructural Features of Railseat Deterioration in Concrete Ties.J Master Civil Eng" 9: 146–53.

Bakri, A. M. M., Liyana, J., Norazian, M. N., Kamarudin Al, and C. M H., & Ruzaidi. 2013. "Mechanical Properties of Polymer Composites with Sugarcane Bagasse Filler." *Advanced Materials Research*, 740, 739–744.

Bala, Anu, and Supratic Gupta. 2021. "Thermal Resistivity, Sound Absorption and Vibration Damping of Concrete Composite Doped with Waste Tire Rubber: A Review." *Construction and Building Materials* 299: 123939.

Benazzouk A, Douzane O, Mezreb K, Laidoudi B, and Quéneudec M. 2008. "Thermal Conductivity of Cement Composites Containing Rubber Waste Particles." *Experimental Study and Modelling Constr Build Mater*, no. 22: 573–79.

Carpenter, F.G., and V.R. Deitz. 1950. "Methods of Sieve Analysis with Particular Reference to Bone Char." *Journal of Research of the National Bureau of Standards* 45 (4): 328. https://doi.org/10.6028/jres.045.036.

Carrascal, I A, J A Casado, J A Polanco, and F Gutie. 2007. "Dynamic Behaviour of Railway Fastening Setting Pads ´" 14: 364–73. https://doi.org/10.1016/j.engfailanal.2006.02.003.

Carter, G B, and V T J Schenk. 1975. "ULTRA-HIGH MODULUS ORGANIC FIBRES," 454–55.

Chin JW, Aouadi K, Nguyen T. 1997. "Effects of Environmental Exposure on Fibre- Reinforced Plastic (FRP) Materials Used in Construction.," no. J Compos Tech Res: 9:205–13No.

Connolly, D P, G Kouroussis, O Laghrouche, C L Ho, and M C Forde. 2015. "Benchmarking Railway Vibrations – Track , Vehicle , Ground and Building Effects" 92: 64–81. https://doi.org/10.1016/j.conbuildmat.2014.07.042.

Control, Constrained, Linear Quadratic Regulator, Model Predictive Controller, and Delay Recovery. 2017. "Railway Research" 4 (1).

D 3518. 2007. "Standard Test Method for In-Plane Shear Response of Polymer Matrix Composite Materials by Tensile Test of a 645 ° Laminate 1." *Annual Book of ASTM Standards* 94 (Reapproved): 1–7. https://doi.org/10.1520/D3518.

Das, Saswat Kumar, Tribhuwan Singh, Amit Kumar Gupta, Amit Kumar, Amit Kumar Singh, and Anil Kumar. 2018. "Composite Railway Sleeper." *Invertis Journal of Renewable Energy* 8 (4): 197–201.

Dechojarassri, D. 2005. "Natural Rubber Composites for Railway Sleepers." *A Feasibility Study. Faculty of Engineering, Thammasat University.*

Deng, Yelin, Dimos Paraskevas, Yajun Tian, Karel Van Acker, Wim Dewulf, and Joost R Du. 2016. "Life Cycle Assessment of Fl Ax- Fi Bre Reinforced Epoxidized Linseed Oil Composite with a Fl Ame Retardant for Electronic Applications" 133. https://doi.org/10.1016/j.jclepro.2016.05.172.

Design, Life-cycle, J Sadeghi, and P Barati. 2012. "Comparisons of the Mechanical Properties of Timber , Steel and Concrete Sleepers" 2479. https://doi.org/10.1080/15732479.2010.507706.

Dhanasekar, G, and P Prema. 2020. "Mechanical Behaviour of Aramid and Glass Fibre Reinforced Polyester Resin Composite" 5 (4): 1469–72.

Dyk, B. J., Dersch, M. S., and Edwards, J. R. Van. 2012. "International Concrete Crosstie and Fastening System Survey – F." *Final Results", Technical Report, RailTEC, University of Illinois at Urbana-Champaign, Illinois, USA.*, 347.

El-wazery, M S, M I El-elamy, and S H Zoalfakar. 2017. "Mechanical Properties of Glass Fiber Reinforced Polyester Composites," no. November 2016: 121–31.

https://doi.org/10.6703/IJASE.2017.14(3).121.

Ellis, D.C. 2001. “Track Terminology. British Railway Track. England: The Permanent Way, Institution.” *The Permanent Way, Institution.*.

Esveld, C. 2001. “Modern Railway.” *MRT Production*, 2001.

Ferdous, Wahid, Allan Manalo. 2014. “Failures of Mainline Railway Sleepers and Suggest Remedies-R Eview of Current Practice,” no. 6 February 2014.

Ferdous, W, A Manalo, M Muttashar, P Yu, R Kakarla, C Salih, and P Schubel. 2021. “Composites for Alternative Railway Sleepers BT - EASEC16.” In , edited by Chien Ming Wang, Vinh Dao, and Sritawat Kitipornchai, 267–76. Singapore: Springer Singapore.

Ferdous, Wahid, Allan Manalo, Gerard Van Erp, Thiru Aravinthan, and Sakdirat Kaewunruen. 2015. “Composite Railway Sleepers – Recent Developments , Challenges and Future Prospects Composite Railway Sleepers – Recent Developments , Challenges and Future Prospects.” *Composite Structures* 134 (August): 158–68. https://doi.org/10.1016/j.compstruct.2015.08.058.

Gajapriya, M., Jayalakshmi Somasundaram, and R. V. Geetha. 2020. “Fillers in Composite Resins-Recent Advances.” *European Journal of Molecular and Clinical Medicine* 7 (1): 971–77.

Gerhards, CC. 1982. “Effect of Moisture Content and Temperature on the Mechanical Properties of Wood.” *An Analysis of Immediate Effects. Wood Fiber Sci* 14: 4–36.

Ghorban, Amir. 2013. “Polymeric Composite Railway Sleepers,” 9–11.

Gourley, J. T., and G. B. Johnson. 2005. “Developments in Geopolymer Precast Concrete." World Congress Geopolymer.” *Geopolymer Institute Saint-Quentin, France,*.

Graebe, Gudrun, Joerg Woidasky, and J V Fraunhofer. 2010. “Railway Sleepers from Mixed Plastic Waste-Railwaste Project Status Information.” *Fraunhofer ICT*.

Gupta, Ankit, Rajeev Sharma, and Rajnish Katarne. 2021. “Experimental Investigation on Influence of Damping Response of Composite Material by Natural Fibers-a Review.” *Materials Today: Proceedings* 47: 3035–42.

Hagaman, B. R., and R. J.A. McAlpine. 1991. “ROA Timber Sleeper Development Project.” In *National Conference Publication - Institution of Engineers, Australia*.

Hamzah, Siti Hawa, and Khafilah Din. 2008. “APPRAISAL OF USED WOODEN RAILWAY SLEEPER” 3 (3): 224–33.

Herbandez FCR, kock. k, Barrera Gp. 2007. “Transit Cooperative Research Program.Transportation Research Board.Final Report for TCRP Project D-7.Task 14 Rail Base Corrosion Detection and Prevection.”

Horwood M Eldridge R. 2005. “Termites in New South Wales:Part 2.Termite Infestations:Inspection Detection and Treatment.For Resour Res,” 22.

Imbernon, S and Norvez, L. 2016. “Landfilling to Vitrimer Chemistry in Rubber Life Cycle EUR Polym J” 82: 347–76.

Inagaki, Michio. 2009. “Pores in Carbon Materials-Importance of Their Control.” *New Carbon Materials* 24 (3): 193–232. https://doi.org/10.1016/S1872-5805(08)60048-7.

Indraratna, Buddhima, Yujie Qi, Miriam Tawk, and Cholachat Rujikiatkamjorn. 2022. “Mining Waste Materials and Recycled Rubber Matrix for Rail Tracks under Cyclic Loading,” 239–48. https://doi.org/10.1061/9780784484067.025.

J Singh. 1999. “Dry Rot and Other Wood-Destroying Fungi:Their Occurenece,Biology ,Pathology and Control.Indoor Build Enviroment,” 8:3-20.

Jabu, Mbatha Abednigo, A. A. Alugongo, O. Maube, and N. Z. Nkomo. 2021. “A Review of the Effectiveness of Different Types of Railway Sleepers.” *International Journal of Engineering Trends and Technology* 69 (10): 193–99. https://doi.org/10.14445/22315381/IJETT-V69I10P224.

Jacob, Amanda. 2004. “Indian Composites Industry Set to Take Off.” *Reinforced Plastics* 48 (3): 34–39. https://doi.org/https://doi.org/10.1016/S0034-3617(04)00231-0.

Jain, Chirag, Shubham Khandelwal, Shivi Mehrotra, and Ritika Gupta. 2016. “A Review Paper on Use of Composite Material for Railway Sleepers in Railway Track” 3 (5): 104–8.

Jani, S P, A Senthil Kumar, M Adam Khan, and M Uthaya Kumar. 2016. “Machinablity of Hybrid Natural Fiber Composite with and without Filler as Reinforcement.” *Materials and Manufacturing Processes* 31 (10): 1393–99. https://doi.org/10.1080/10426914.2015.1117633.

Kaewunruen, S., L. M.Cortes Lopes, and M. P. Papaelias. 2018. “Georisks in Railway Systems under Climate Uncertainties by Different Types of Sleeper/Crosstie Materials.” *Lowland Technology International*.

Kaewunruen, S. 2013. “Acoustic and Dynamic Characteristics of a Complex Urban Turnout Using Fibre-Reinforced Foamed Urethane (FFU) Bearers.” *International Workshop on Railway Noise*.

Kaewunruen, Sakdirat, and Alex M. Remennikov. 2006. “Sensitivity Analysis of Free Vibration Characteristics of an in Situ Railway Concrete Sleeper to Variations of Rail Pad Parameters.” *Journal of Sound and Vibration*. https://doi.org/10.1016/j.jsv.2006.05.034.

Kaewunruen, Sakdirat, and Alexander Remennikov. 2011. “A Numerical Study to Evaluate Dynamic Responses of Voided Concrete Railway Sleepers to Impact Loading,” no. November: 1–8.

Kernes, Ryan G, J Riley Edwards, Marcus S Dersch, David A Lange, and Christopher P L Barkan. 2011. “Investigation of the Dynamic Frictional Properties of a Concrete Crosstie Rail Seat and Pad and Its Effect on Rail Seat Deterioration (RSD),” no. 217.

Khennane, Amar, Australian Defence, Force Academy, and Obada Kayali. 2013. “Advanced Composites in Construction 2013, ACIC 2013 - Conference Proceedings.” *Advanced Composites in Construction 2013, ACIC 2013 - Conference Proceedings*, no. January 2013.

Koh, Taehoon, and Seonkeun Hwang. 2015. “Field Evaluation and Durability Analysis of an Eco-Friendly Prestressed Concrete Sleeper.” *Journal of Materials in Civil Engineering* 27 (7): B4014009.

Kondrashchenko, Valerii I, Guo Qing Jing, and Chuang Wang. 2019. “Wood-Polymer Composite for the Manufacture of Sleepers.” In *Materials Science Forum*, 945:509–14. Trans Tech Publ.

Lampo, Richard, Thomas Nosker, and Henry Sullivan. 2003. “Development, Testing and Applications of Recycled Plastic Composite Cross Ties.” *US Army Engineer R&D Centre*.

Langman WF. 1983. “Steel Railroad Sleeper:US Onmark Industries Inc.”

Li, M. 2014. “Preparation and Damping Properties of (Waste Rubber Powder)/ Hindered Phenol Composites, J. Vinyl Add. Technol” 20 (4): 225–229.

Li, Xue, Lope G Tabil, and Satyanarayan Panigrahi. 2007. “Chemical Treatments of Natural Fiber for Use in Natural Fiber-Reinforced Composites: A Review.” *Journal of Polymers and the Environment* 15 (1): 25–33. https://doi.org/10.1007/s10924-006-0042-3.

Li, Zongjun, Amar Khennane, Paul J. Hazell, and Alex M. Remennikov. 2018. “Performance of a Hybrid GFRP-Concrete Beam Subject to Low-Velocity Impacts.” *Composite Structures* 206 (December): 425–38. https://doi.org/10.1016/J.COMPSTRUCT.2018.08.036.

Lichtberger, Bernhard. 2005. “Track Compendium.” *Hamburg, Eurailpress Tetzlaff-Hestra GmbH & Co. Publ*, 1–192.

Lim, Chie Hong, Sakdirat Kaewunruen, Nhlanganiso Mlilo, Prestressed Concrete Sleepers, Dan Li, Chayut Ngamkhanong, and Sakdirat Kaewunruen. 2021. “A Comparative Study on Recycled Plastic Railway Sleeper with Concrete Sleeper A Comparative Study on Recycled Plastic Railway Sleeper with Concrete Sleeper.” https://doi.org/10.1088/1757-899X/1145/1/012006.

Liu, An-Shuang, Delan Yin, and Guoxiang Liu. 2012. “A Study on the Application of Resin Composite Sleeper in the Design of Long-Span Rail Bridges.” In *Sustainable Transportation Systems: Plan, Design, Build, Manage, and Maintain*, 523–31.

Louie, ML. 2013. “Editor Sustainable Solutions for Railroad Trackwork. Urban Public Transportation System.” *American Society of Civil Engineers (ASCE).*

Lutch, Russell H. 2009. “Capacity Optimization of a Prestressed Concrete Railroad Tie,” 230.

M.Sakthive, S.Ramesh. 2013. “Mechanical Properties of Natural Fiber (Banana, Coir, Sisal) Polymer Composites”, Science Park” Vol-1 (Issue-1).

Manalo, A., T. Aravinthan, W. Karunasena, and A. Ticoalu. 2010. “A Review of Alternative Materials for Replacing Existing Timber Sleepers.” *Composite Structures* 92 (3): 603–11. https://doi.org/10.1016/J.COMPSTRUCT.2009.08.046.

McIntyre, J Eric. 2005. *Synthetic Fibres: Nylon, Polyester, Acrylic, Polyolefin*. Taylor & Francis US.

Meesit, Ratthaphong, Sakdirat Kaewunru Hq, Ratthaphong Meesit, and Sakdirat Kaewunruen. 2017. “Vibration Characteristic of Micro-Engineered Crumb Rubber Concrete for Railway Sleeper Applications Vibration Characteristics of Micro-Engineered Crumb Rubber Concrete for Railway Sleeper Applications” 15: 65–76. https://doi.org/10.3151/jact.15.55.

Ministry of Railways, Government of India. 2021. “INDIAN RAILWAY STANDARD SPECIFICATION FOR Serial No. IRS: T 59-2021.” *RESEARCH DESIGNS AND STANDARDS ORGANISATION (Ministry of Railways)*, 17.

Miura, Shigeru, Hideyuki Takai, Masao Uchida, and Yasuto Fukada. 1998. “The Mechanism of Railway Tracks.” *Japan Railway & Transport Review* 3 (March): 38–45.

Mohajerani, Abbas, Lucas Burnett, John V. Smith, Stefan Markovski, Glen Rodwell, Md Tareq Rahman, Halenur Kurmus, et al. 2020. “Recycling Waste Rubber Tyres in Construction Materials and Associated Environmental Considerations: A Review.” *Resources, Conservation and Recycling* 155 (April): 104679. https://doi.org/10.1016/J.RESCONREC.2020.104679.

Nadal M., Rovira J., Díaz-Ferrero J., Schuhmacher M., Domingo L. J. 2016. “Human Exposure to Environmental Pollutants after a Tire Landfill Firein Spain.” *Health Risks. Environment International* 97: 37–44.

Nagavally, Rahul Reddy. 2016. “Composite Materials - History, Types, Fabrication Techniques, Advantages, and Applications.” *International Journal of Mechanical And Production Engineering*, 25–30.

Najim, Khalid B, and Matthew R Hall. 2012. “Mechanical and Dynamic Properties of Self-Compacting Crumb Rubber Modified Concrete.” *Construction and Building Materials* 27 (1): 521–30.

Nosker, Thomas, Richard Renfree, Jennifer Lynch, Mark Lutz, Barry Gillespie, Richard Lampo, and Kenneth E Van Ness. 1998. “A Performance-Based Approach to the Development of a Recycled Plastic/Composite Crosstie.” In *TECHNICAL PAPERS OF THE ANNUAL TECHNICAL CONFERENCE-SOCIETY OF PLASTICS ENGINEERS INCORPORATED*, 3:2912–15. SOCIETY OF PLASTICS ENGINEERS INC.

Oladele, Isiaka Oluwole. n.d. “Effect of Bagasse Fiber Reinforcement on the Mechanical Properties of Polyester Composites”, JAPETT.” *2014* Vol.42 (No.1): pp.12-15.

OPTIMAT, L. and MERL, L. 2003. “Wood Plastic Composite Study: Technologies and UK Market Opportunities.” *The Waste and Resources Action Programme, Oxon.*

Parvez, Ahsan, and Stephen James. 2017. “Fatigue of Steel-Fibre-Reinforced Concrete Prestressed

Railway Sleepers.” *Engineering Structures* 141: 241–50. https://doi.org/10.1016/j.engstruct.2017.03.025.

Pattamaprom, Cattaleeya, Duangkamol Dechojarassri, Chakrit Sirisinha, and Worsak Kanok-Nukulchai. 2005. “Natural Rubber Composites for Railway Sleepers: A Feasibility Study.” *Thailand: Thammasat University*.

Poddaeva, Olga, and Anastasia Fedosova. 2021. “Damping Capacity of Materials and Its Effect on the Dynamic Behavior of Structures. Review.” *Energy Reports* 7: 299–307.

Polgar, L M, F Picchioni, S G Tikhomirov, Y V Pyatakov, C A Bekakos, and G Papazafeiropoulos. 2018. “Recycling of Waste Rubber as Fillers : A Review Recycling of Waste Rubber as Fillers : A Review.” https://doi.org/10.1088/1757-899X/368/1/012016.

Qiao, Pizhong, Julio F. Davalos, and Michael G. Zipfel. 1998. “Modeling and Optimal Design of Composite-Reinforced Wood Railroad Crosstie.” *Composite Structures* 41 (1): 87–96. https://doi.org/10.1016/S0263-8223(98)00051-8.

Quan, Enmao, Hongke Xu, and Zhongyang Sun. 2022. “Composition Optimization and Damping Performance Evaluation of Porous Asphalt Mixture Containing Recycled Crumb Rubber.” *Sustainability (Switzerland)* 14 (5). https://doi.org/10.3390/su14052696.

Rachchh, N V, and D N Trivedi. 2018. “ScienceDirect Mechanical Characterization and Vibration Analysis of Hybrid E-Glass / Bagasse Fiber Polyester Composites.” *Materials Today: Proceedings* 5 (2): 7692–7700. https://doi.org/10.1016/j.matpr.2017.11.445.

Ramnath, B Vijaya, C Elanchezhian, M Jaivignesh, S Rajesh, C Parswajinan, and A Siddique Ahmed. 2014. “Evaluation of Mechanical Properties of Aluminium Alloy – Alumina – Boron Carbide Metal Matrix Composites.” *JOURNAL OF MATERIALS&DESIGN* 58: 332–38. https://doi.org/10.1016/j.matdes.2014.01.068.

Razumakov, A. A., N. V. Stepanova, I. A. Bataev, O. G. Lenivtseva, Iu Iu Riapolova, and K. I. Emurlaev. 2016. “The Structure and Properties of Cast Iron Alloyed with Copper.” *IOP Conference Series: Materials Science and Engineering* 124 (1): 1–5. https://doi.org/10.1088/1757-899X/124/1/012136.

Remennikov, A. M., M. H. Murray, and S. Kaewunruen. 2012. “Reliability-Based Conversion of a

Structural Design Code for Railway Prestressed Concrete Sleepers.” *Proceedings of the Institution of Mechanical Engineers, Part F: Journal of Rail and Rapid Transit*. https://doi.org/10.1177/0954409711418754.

Remennikov, Alex M, and Sakdirat Kaewunruen. 2008. “Progress in Structural Engineering and Materials : Structural Safety and Reliability A Review of Loading Conditions for Railway Track Structures Due to Train and Track Vertical Interaction,” no. July 2007: 207–34. https://doi.org/10.1002/stc.

Samsuri, Bin A. 2010. “A Degradation of Natural Rubber and Synthetic Elastomers.”

Sanjay, M. R., P. Madhu, Mohammad Jawaid, P. Senthamaraikannan, S. Senthil, and S. Pradeep. 2018a. “Characterization and Properties of Natural Fiber Polymer Composites: A Comprehensive Review.” *Journal of Cleaner Production* 172: 566–81. https://doi.org/10.1016/j.jclepro.2017.10.101.

Sanjay, M R, G R Arpitha, and B Yogesha. 2015. “Study on Mechanical Properties of Natural - Glass Fibre Reinforced Polymer Hybrid Composites : A Review.” *Materials Today: Proceedings* 2 (4–5): 2959–67. https://doi.org/10.1016/j.matpr.2015.07.264.

Sanjay, M R, P Madhu, Mohammad Jawaid, P Senthamaraikannan, S Senthil, and S Pradeep. 2018b. “Characterization and Properties of Natural Fi Ber Polymer Composites : A Comprehensive Review.” *Journal of Cleaner Production* 172: 566–81. https://doi.org/10.1016/j.jclepro.2017.10.101.

Sathishkumar, T P, J Naveen, and S Satheeshkumar. 2014. “Hybrid Fiber Reinforced Polymer Composites – a Review,” no. September. https://doi.org/10.1177/0731684413516393.

Series, Conference. 2019. “The Effect of Fibre Loading on the Physical and Mechanical Properties of Pineapple Leaf Fibre-Reinforced Biodegradable Composites The Effect of Fibre Loading on the Physical and Mechanical Properties of Pineapple Leaf Fibre-Reinforced Biodegradable Compos.” https://doi.org/10.1088/1742-6596/1349/1/012148.

Sharma, Rakesh Chandmal, Srihari Palli, Sunil Kumar Sharma, and Mritunjoy Roy. 2017. “Modernization of Railway Track with Composite Sleepers.” *International Journal of Vehicle Structures and Systems* 9 (5): 321–29. https://doi.org/10.4273/ijvss.9.5.10.

Shohag, Md Abu S, Emily C Hammel, David O Olawale, and Okenwa I Okoli. 2017. "Damage Mitigation Techniques in Wind Turbine Blades: A Review." *Wind Engineering* 41 (3): 185–210.

Siahkouhi, M., X. Li, V. Markine, and G. Jing. 2021. "An Experimental and Numerical Study on the Mechanical Behavior of Kunststof Lankhorst Product (KLP) Sleepers." *Scientia Iranica* 28 (5 A): 2568–81. https://doi.org/10.24200/sci.2021.57165.5096.

Skripkiūnas, Gintautas, Audrius Grinys, and Kęstutis Miškinis. 2009. "Damping Properties of Concrete with Rubber Waste Additives." *Materials Science (Medžiagotyra)* 15 (3): 266–72.

Srivastava, V. K., and S. Lal. 1991. "Mechanical Properties of E-Glass Fibre Reinforced Nylon 6/6 Resin Composites." *Journal of Materials Science* 26 (24): 6693–98. https://doi.org/10.1007/bf00553694.

Statements, Bias, and Testing Size. 2007. "Standard Test Method for Sieve Analysis of Fine and Coarse Aggregates 1" i (200): 1–5.

Taherinezhad, J., M. Sofi, P. A. Mendis, and T. Ngo. 2013. "A Review of Behaviour of Prestressed Concrete Sleepers." *Electronic Journal of Structural Engineering* 13 (1): 1–16.

Tang, Xiaoning, and Xiong Yan. 2020. "A Review on the Damping Properties of Fiber Reinforced Polymer Composites." *Journal of Industrial Textiles* 49 (6): 693–721. https://doi.org/10.1177/1528083718795914.

The use of sleepers made of FFU synthetic wood in EuropeKoller, Gunther. 2009. "The Use of Sleepers Made of FFU Synthetic Wood in Europe." *Railway Technical Review* 2 (September 2008): 28–32.

Tikish, Tekalign Aregu, and Nefisa Abdulkadir Ali. 2021. "Study on Bagasse Reinforced Waste Thermoplastic Composite : Compressive Strength and Water Absorption" 5 (1): 5–10. https://doi.org/10.11648/j.ajmme.20210501.12.

Uehara, Motoki. 2010. "New Concrete with Low Environmental Load Using the Geopolymer Method." *Quarterly Report of RTRI* 51 (1): 1–7.

Urbans, Mihails, Inese Vilcane, and Jelena Malahova. 2019. "ASSESSMENT OF TECHNOGENIC RISKS," 1616–22. https://doi.org/10.22616/ERDev2019.18.N347.

Vantuono, W. 2010. “TieTek LLC Is up for Grabs, Bids Are Due.” *Railway Age*.

Wang, Jianfeng, Xiaohong Zhang, Lei Jiang, and Jinliang Qiao. 2019. “Advances in Toughened Polymer Materials by Structured Rubber Particles.” *Progress in Polymer Science* 98 (November): 101160. https://doi.org/10.1016/J.PROGPOLYMSCI.2019.101160.

Weyenberg, I Van De, T Chi Truong, B Vangrimde, and I Verpoest. 2006. “Improving the Properties of UD Flax Fibre Reinforced Composites by Applying an Alkaline Fibre Treatment” 37: 1368–76. https://doi.org/10.1016/j.compositesa.2005.08.016.

Wolf, H., Mattson, S., Edwards, J., Dersch, M. and, and C. Barkan. 2014. “Flexural Analysis of Prestressed Concrete Monoblock Crossties.” *Comparison of Current Methodologies and Sensitivity to Support Conditions. Proc. Transportation Research Board 94th Annual Meeting, USA*.

X.LU,W.Wang,L.yu. 2014. “Waste Ground Rubber Powder.” *Waste Ground Rubber Tire Powder/Thermoplastic Vulcanizate Blends:Preparation ,Characterazation and Compatibility,J Apple Polym SCI* 3: 131–39.

Xu, Y, Chung, D.D. 2000. “Improving Silica Fume Cement by Using Silane.” *Cement and Concrete Research* 8: 1305–11.

Yu, Eric. 2011. “Modeling Strategic Relationships for Process Reengineering.” *Social Modeling for Requirements Engineering* 11 (2011): 66–87.

Yun, Won Young, and Luis Ferreira. 2003. “Prediction of the Demand of the Railway Sleepers: A Simulation Model for Replacement Strategies.” *International Journal of Production Economics* 81–82: 589–95. https://doi.org/https://doi.org/10.1016/S0925-5273(02)00299-2.

Zaaba, Nor Fasihah, and Hanafi Ismail. 2019. “Thermoplastic/Natural Filler Composites: A Short Review.” *Journal of Physical Science* 30: 81–99. https://doi.org/10.21315/jps2019.30.s1.5.

Zarembski, Allan M. 1993. “Concrete vs . Wood Ties: Making the Economic Choice.” *Conference on Maintaining Railway Track; Determining Cost and Allocating Resources*, 1–5.

Zhang, S. P., & Zong, L. 2014. “Evaluation of the Relationship between Water Absorption and Durability of Concrete Materials.” *Advances in Materials Science and Engineering*, 1–8.

Zhang, Zhong, and G Hartwig. 2002. "Relation of Damping and Fatigue Damage of Unidirectional Fibre Composites." *International Journal of Fatigue* 24 (7): 713–18.

Zhao, J., A. H.C. Chan, and M. P.N. Burrow. 2007. "Reliability Analysis and Maintenance Decision for Railway Sleepers Using Track Condition Information." *Journal of the Operational Research Society*. https://doi.org/10.1057/palgrave.jors.2602251.

Zheng, Lei, X Sharon Huo, and Yong Yuan. 2008. "Experimental Investigation on Dynamic Properties of Rubberized Concrete." *Construction and Building Materials* 22 (5): 939–47.

Zhou, Weilie, Robert Apkarian, Zhong Lin Wang, and David Joy. 2007. "Fundamentals of Scanning Electron Microscopy (SEM)." *Scanning Microscopy for Nanotechnology: Techniques and Applications,* 1–40. https://doi.org/10.1007/978-0-387-39620-0_1.

Zhu, Yi, Wenjian Wang, Roger Lewis, Wenyi Yan, Stephen R Lewis, and Haohao Ding. 2019. "A Review on Wear Between Railway Wheels and Rails Under Environmental Conditions." *Journal of Tribology* 141 (12). https://doi.org/10.1115/1.4044464.

Appendix A - Sieve certificate

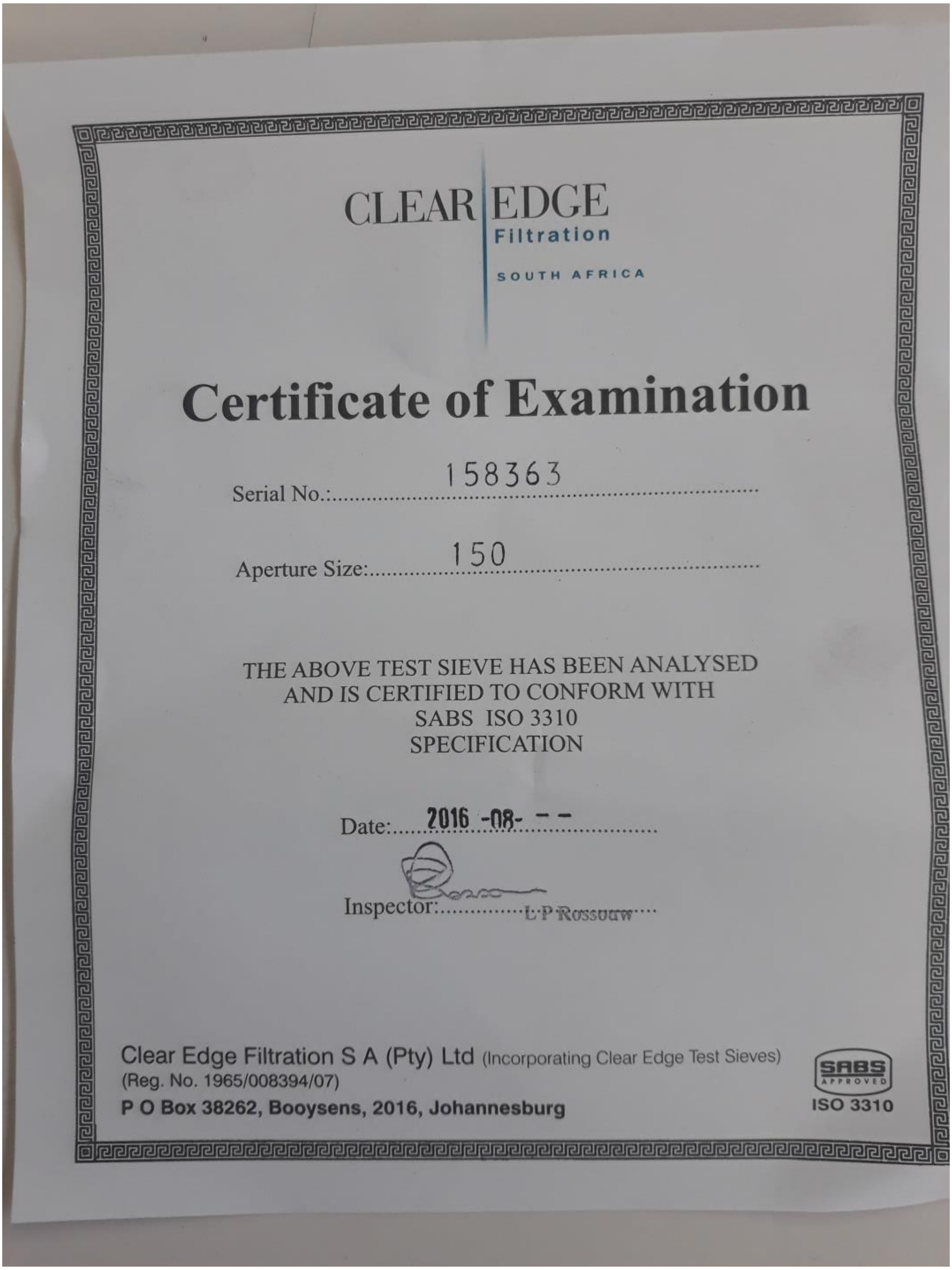

CLEAR EDGE
Filtration
SOUTH AFRICA

Certificate of Examination

Serial No.: 158363

Aperture Size: 150

THE ABOVE TEST SIEVE HAS BEEN ANALYSED
AND IS CERTIFIED TO CONFORM WITH
SABS ISO 3310
SPECIFICATION

Date: 2016 -08- - -

Inspector: L P Rossouw

Clear Edge Filtration S A (Pty) Ltd (Incorporating Clear Edge Test Sieves)
(Reg. No. 1965/008394/07)
P O Box 38262, Booysens, 2016, Johannesburg

SABS APPROVED
ISO 3310

CLEAR EDGE
Filtration
SOUTH AFRICA

Certificate of Examination

Serial No.: 158603

Aperture Size: 75

THE ABOVE TEST SIEVE HAS BEEN ANALYSED
AND IS CERTIFIED TO CONFORM WITH
SABS ISO 3310
SPECIFICATION

Date: 2016 -09- - -

Inspector: L P Rossouw

Clear Edge Filtration S A (Pty) Ltd (Incorporating Clear Edge Test Sieves)
(Reg. No. 1965/008394/07)
P O Box 38262, Booysens, 2016, Johannesburg

SABS APPROVED
ISO 3310

Appendix B - Fibreglass properties

Fibreglass	
Electrical conductivity	Very low
Specific gravity	2.68g/cm^2
Material Alkali Resistant Glass	
Softening point	860 ^{0}C
Chemical resistance	Very high
Modulus of elasticity	72 GPa
Fibre length	18 mm
Filament diameter	14 µm
Loss of ignition%	0.60
Moisture %	0.50 max
Tensile Strength	1.700 Mpa

Benefits and advantages of fibreglass

- Excellent workability
- High Dispersion:200 filaments per kg in fibre length 12 mm
- Does not corrode
- Control and prevention of cracking in fresh concrete
- Overall enhancement of durability and mechanical properties of concrete
- Effective at a very low dosage
- Homogeneous mix
- Safe and easy to handle

Appendix C - Polyester resin properties

FEATURES	BENEFITS
Low viscosity	Excellent glassfibre wet-out
Thixotropic	Minimal drainage
Non air-inhibited	Cures to a tack-free finish
Specially promoted	Predictable geltime and cure rate
Lloyds approved	Meets international quality standards
Heat Distortion Temperature above 80°C	Good heat resistance
Good colour	Readily pigmentable

PROPERTY	SPECIFICATION	NCS TEST METHOD
Relative density 25°/25°C	1,09 - 1,11	14
Viscosity @ 25°C, mPa.s	390 - 600	5.2
Thixotropic index, ratio	1.8 – 3.0	
Acid value, mg KOH/g	< 27	13
Volatile content, %	43 - 46	7
Geltime @ 25°C, using 2 phr* BUTANOX M50, minutes	10 - 13	8
Liquid appearance	Opaque pink	2
Stability in the dark @ 25°C, months	6 minimum	4.1

***phr = parts per hundred resin, by mass.**

NCS 901 PA needs only the addition of catalyst to start the curing reaction. The resin must be allowed to attain workshop temperature (23°C) before being formulated for use. The correct amount of catalyst is therefore added and thoroughly stirred into the resin shortly before use.

The ambient temperature and the amount of catalyst control the geltime of the resin formulation. This can be approximately determined from the table below which shows the geltime of 100 parts by mass of NCS 901 PA, containing 1 to 2 phr BUTANOX M50.

Appendix D - SEM properties of rubber particles

Items	Value
measurement conditions	
Acceleration voltage	10.00 kV
Probe current	-
Magnification	x 350
Process time	T3
Measurement detector	First
Live time	30.00 seconds
Real time	30.16 seconds
Dead time	1.00 %
Count rate	196.00 CPS

Display name	Standard data	Quantification method	Result Type
Spc_001	Standardless	ZAF	Metal

Element	Line	Mass%	Atom%
C	K	82.49±0.83	86.26±0.87
O	K	17.51±1.16	13.74±0.91
Total		100.00	100.00
Spc_001			Fitting ratio 0.1593

Ac

Items	**value**
Measurement conditions	
Acceleration voltage	10.00kV
Probe current	-
Magnification	X350
Process time	T3
Measurement detector	First
Live time	30.00 seconds
Real time	30.16 seconds
Dead time	1.00%
Count rate	196.00CPS

Smp_001

20 mm

Sem_SED_002

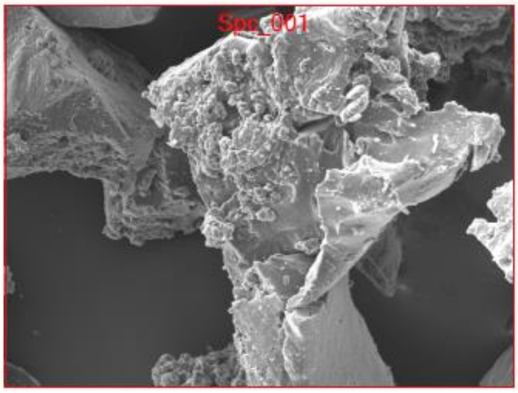

Signal SED
Landing Voltage 10.0 kV
WD 10.0 mm
Magnification x350
Vacuum Mode HighVacuum

50 µm

Smp_001

20 mm

Sem_SED_004

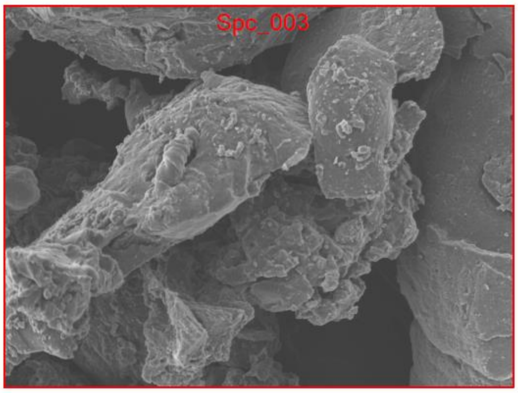

Signal SED
Landing Voltage 10.0 kV
WD 9.9 mm
Magnification x350
Vacuum Mode HighVacuum

50 µm